Formation of Physiologically Relevant Liposomes

by

Kim Soon Horger

A dissertation submitted in partial fulfillment
of the requirements for the degree of
Doctor of Philosophy
(Chemical Engineering)
in the University of Michigan
2013

Doctoral Committee:

Associate Professor Michael Mayer, Chair
Professor Jennifer J. Linderman
Associate Professor David S. Sept
Professor Michael J. Solomon

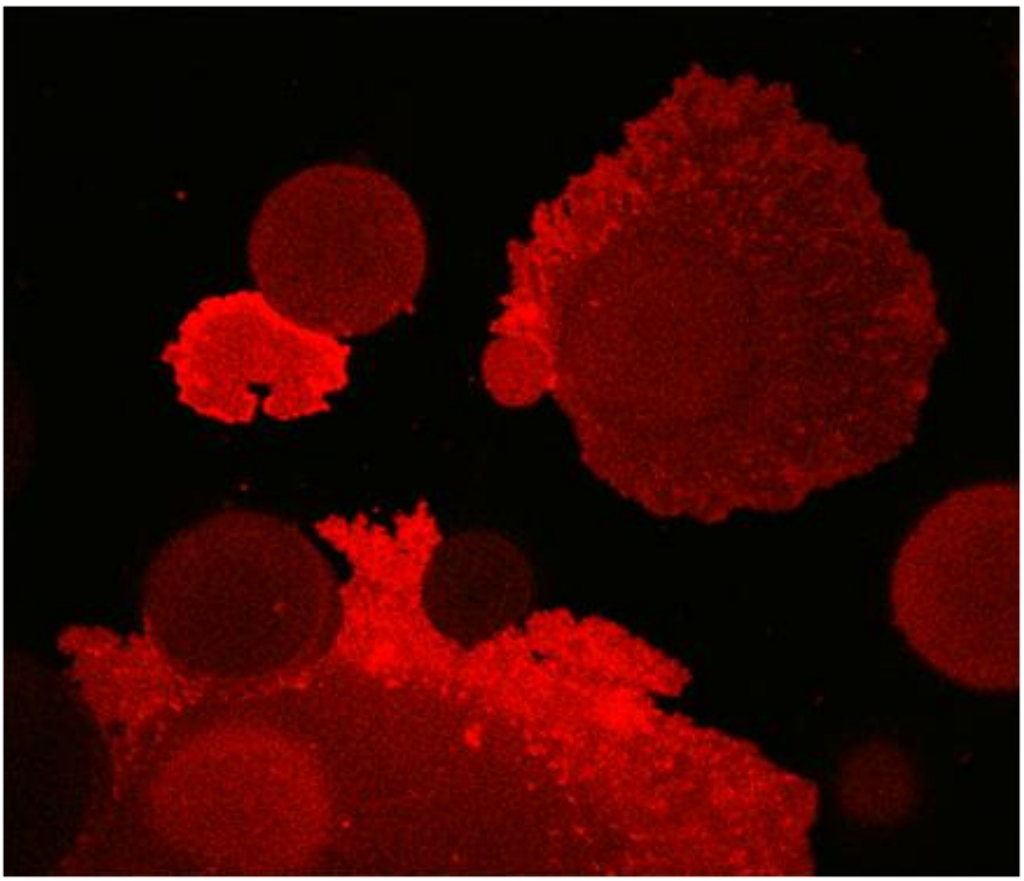

2013

DEDICATION

This thesis is dedicated to my family.
They have uplifted me
through their love and support
to become the person I want to be.

ACKNOWLEDGEMENTS

I am grateful to the many people who have helped me throughout my education. I give special thanks to:

My research advisor, Michael Mayer, for his guidance and support throughout my graduate studies. He has helped me over the stumbling blocks encountered during experiments and developed my technical writing skills. I am grateful for his wisdom and insight.

My dissertation committee, Professor Linderman, Professor Solomon, and Professor Sept. They have challenged me, questioned me, and told me when I was aiming for unrealistic goals. I appreciate their advice and support.

My lab mates, both past and present, for sharing a part of their lives with me. We laughed together, cried together, and groaned in frustration together. I am thankful for their support and discussions.

My parents, who taught me the value of hard work and dedication. They raised me to be a conscientious, free-thinking being who can achieve anything. Without the values they instilled in me, I wouldn't be the person I am today.

My husband, for his unwavering support and understanding. He stood by me when I chose to pursue higher education, tolerated my late nights of studying, brought me dinner when I might have otherwise missed out, and filled in the gaps at home when I was too busy to help. I could not have come this far without him.

My son, for his patience and love. He was a child when I returned to school and grew into a man before I finished. Because of him, I worked hard to get an education and to be the best possible role model for him.

TABLE OF CONTENTS

LIST OF FIGURES

LIST OF APPENDICES

ABSTRACT

In the first part of this work, we addressed the challenge of producing giant unilamellar vesicles (GUV) in solutions of physiologic ionic strength. Methods of producing GUVs were limited previously to low salt concentrations with a few exceptions that typically required specific lipid compositions, specialized equipment, or complex protocols. In this work, a dried film of agarose was coated with lipids and subsequently hydrated. GUVs were formed in solutions of physiologic ionic strength from a variety of lipid compositions. Solubilized agarose associated with the membranes of GUVs, but the membranes remained fluid. Water retention and increased surface area provided by the agarose molecules possibly contributed to orientation of lipid lamellae prior to hydration. Hyperosmotic conditions provided by solubilized agarose between lamellae generated forces that led to swelling of the lipid film similar to electroosmotic forces produced during electroformation. Fusion of adjacent liposomes occurred frequently in the first few minutes of formation.

In the second part of this work, we extended the technique to reconstitute a complex transporter, P-glycoprotein (P-gp), into giant proteoliposomes. P-gp is important due to its role in the blood-brain barrier and because its (over)expression can cause multidrug resistance in cancer cells. Most methods of reconstituting proteins yield proteoliposomes that are too small to discern individually, and so direct effects of potential P-gp modulators can be difficult to evaluate. With P-gp reconstituted in giant

liposomes, the fluorescence of the solution inside liposomes was easily discernible from membrane or background fluorescence and enabled artifacts to be excluded. We found that the presence of P-gp in the membrane increased membrane permeability and a higher rate of passive diffusion compared to liposomes that lacked P-gp. Transport functionality of P-gp was confirmed by a significantly higher transport rate in the presence of ATP than without ATP or with a known inhibitor. An ATPase assay verified ATP hydrolysis functionality of P-gp after reconstitution into giant proteoliposomes. Furthermore, patch clamp experiments revealed the presence of a chloride ion channel protein that co-purified from the host insect cells. These assays demonstrate the usefulness of giant proteoliposomes for transport and patch clamp studies.

CHAPTER I

Introduction and Background

Biological cells are surrounded by a membrane that define the boundaries of the cells and separate their interiors from their environment.[1-3] Cellular membranes are complex structures composed of phospholipids, proteins, and sterols.[1-3] Additionally, carbohydrate groups may be covalently attached to membrane proteins and phospholipids.[1-3]

1.1 Structure of Biological Membranes

The phospholipids of cellular membranes are arranged into a bilayer (shown schematically in Figure 1.1), with their hydrophobic hydrocarbon chains ("tails") aligned toward each other to minimize their energetically unfavorable interaction with water molecules.[1-3] The polar phosphate headgroups of phospholipids point outward to interface with the aqueous intra- and extracellular environs to form the inner and outer leaflets, respectively.[1, 3] The headgroups of phospholipids may be zwitterionic (i.e., contains an equal ratio of positive and negative charges, such that the molecule is net-neutral) or charged either negatively or positively.[1] Charged phospholipids that occur

most commonly in biological cells, however, are negatively charged.[1, 4] The chemical structures of phospholipids that commonly exist in cellular membranes are shown in Figure 1.2.

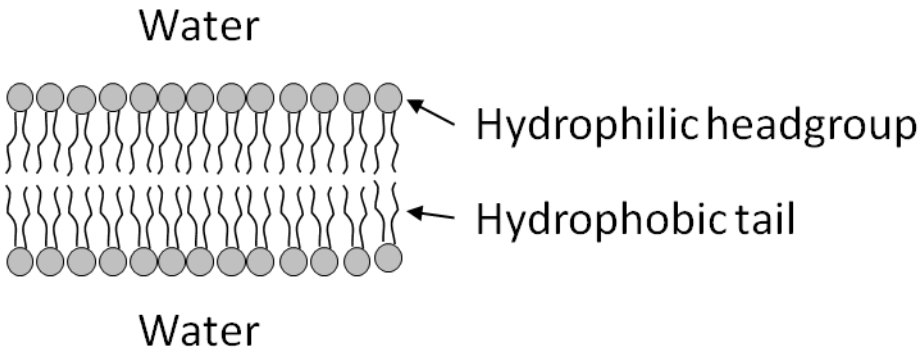

Figure 1.1. Schematic image of phospholipid bilayer. Components are not to scale. Figure is adopted from Bordi and Cametti 2005.[3]

Cholesterol molecules are smaller than phosphoslipids and also are amphipathic (i.e., have both polar and hydrophobic sections).[1, 5] Cholesterol has a hydrophobic body that is comprised of four hydrocarbon rings and a very small headgroup consisting of only a hydroxyl group (see Figure 1.2).[1, 5] The amphipathic nature of cholesterol influences its orientation in the lipid bilayer in the same manner as phospholipids.[5] Cholesterol molecules are interspersed among the phospholipids in both leaflets of the bilayer and help to laterally fill the space that can occur between phospholipids.[5]

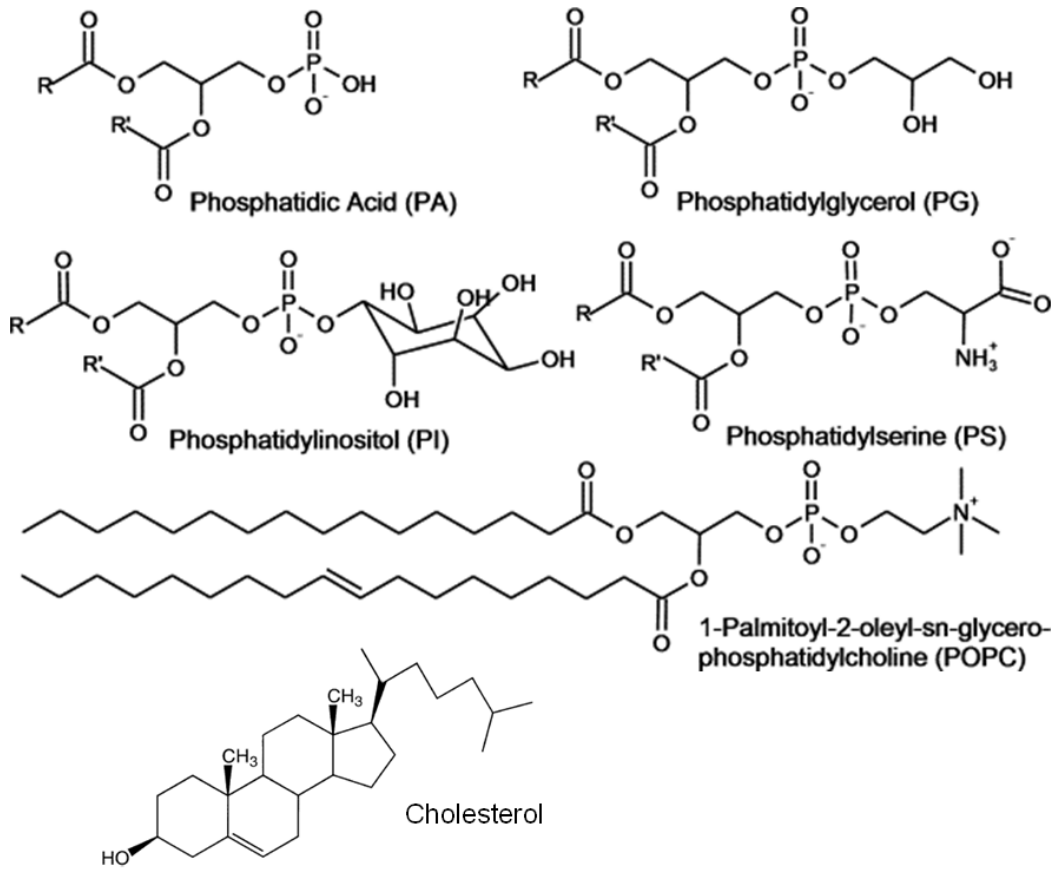

Figure 1.2. Chemical structures of common phospholipids and cholesterol.[5, 6] R and R' denote hydrocarbon chains, typically 12-18 carbons in length, that may be saturated or contain 1-2 double bonds, as shown for POPC.

Membrane proteins belong to one of two classes, integral or peripheral, as determined by their physical relationship to the membrane.[1] Integral proteins are strongly bound to the membrane and cannot be removed except with the use of detergents or nonpolar solvents because a portion of the protein is embedded in the hydrophobic region of the bilayer.[1] Integral proteins may be embedded in one leaflet, sometimes by a lipid anchor, or may span both leaflets of the bilayer with one or more transmembrane segments.[1] Peripheral proteins, on the other hand, are water-soluble and associate at the surface the membrane, often through electrostatic interactions.[1]

Since the membrane components are held together only by relatively weak hydrostatic interactions (as compared to strong chemical bonds), the components diffuse laterally within each leaflet of the bilayer in a fluid-like manner.[1, 3, 7] Thus, the biological membrane is commonly depicted by variations of a fluid-mosaic model,[7] similar to the one shown in Figure 1.3. The rate of diffusion of the components within each leaflet is affected by the structure of the components (e.g., length and saturation of hydrocarbon tails of phospholipids, presence of cholesterol, and structure and concentration of membrane proteins), temperature, presence of certain chemicals (e.g., large alcohols or dimethyl sulfoxide), and by interactions with adjacent surfaces.[1, 5, 8, 9]

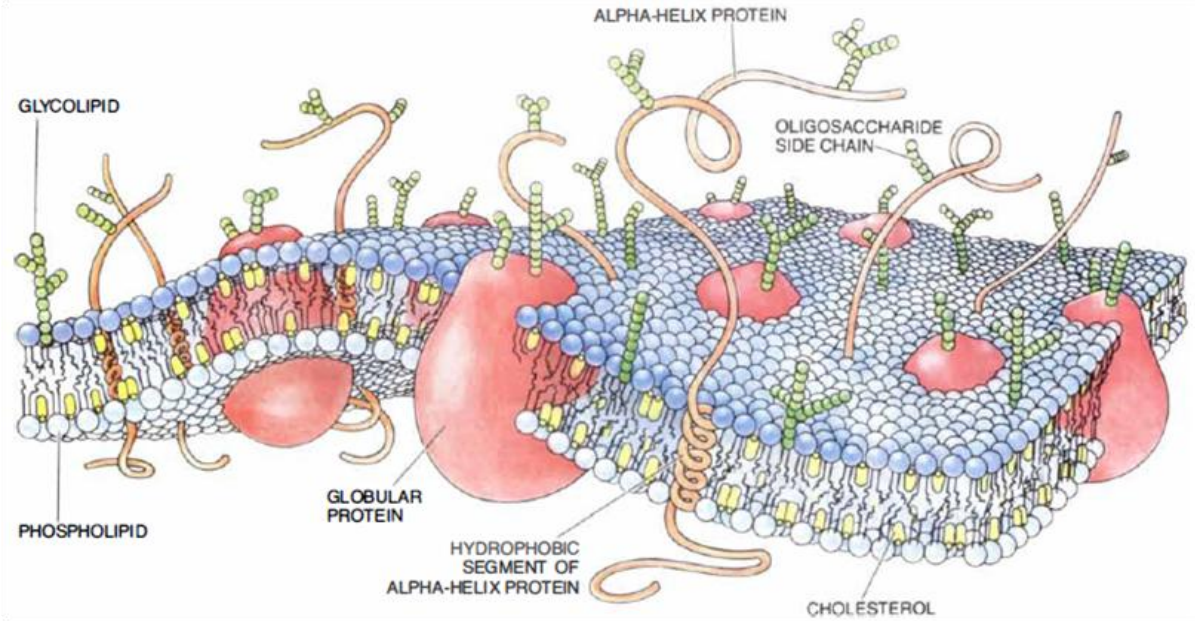

Figure 1.3. Fluid mosaic model of a biological membrane. Reproduced from Bretscher 1985.[10]

Cellular membranes regulate the passage of materials in and out of the cell. The membrane is only 4–6 nm thick, but forms an effective barrier between the cellular contents and the external environment.[3, 11] Water molecules pass somewhat freely

through the membrane, but charged particles and larger hydrophilic molecules, such as sugar, are not able to pass easily through the hydrophobic region of the bilayer.[1, 2] These particles traverse the membrane through channel proteins that enable their passage in a regulated and often highly selective manner.[12-14]

1.2 Planar Membrane Models

The biological membranes of cells are complex structures that can be altered by the cell in response to stimuli.[3, 5, 15] Therefore, to study the properties of cellular membranes and their components, different models may be employed to mimic specific aspects of the membrane and provide a means to study the effects of environmental factors on the properties of membrane components.[16, 17] Planar models are flat and may be supported on a surface or span a pore that separates two small chambers. Alternatively, model membranes may be self-enclosed, spherical shells (a “liposome”) that are suspended in an aqueous solution.

1.2.1 Supported lipid bilayer

A supported lipid bilayer is a planar membrane that lies adjacent to a substrate with a thin film of water between the substrate and the membrane.[8, 18, 19] Common materials for the substrate include glass, quartz, silica, and mica.[18, 20] Chemical modifications of these and other substrate materials have been employed as well.[19] To form a supported lipid bilayer, a solution of liposomes may be applied to a clean glass surface; as liposomes contact the glass, they rupture spontaneously.[19, 21, 22] Another method of forming a supported lipid bilayer, called the Langmuir-Blodgett method, involves dipping the glass twice past a single layer of phospholipids floating on top of an aqueous solution.[19] In the first pass, a single layer of phospholipids (i.e., a monolayer)

associate to the glass with the polar headgroups toward the glass and the hydrophobic tails oriented outward toward the air.[23] The second pass yields a bilayer by formation of another monolayer on top of the first one, with the hydrophobic tails of both monolayers facing toward each other.[23]

Supported lipid bilayers are useful for studying lateral diffusion of membrane components and interactions of molecules with membrane components.[19, 21] The supportive surface helps to prevent rupture of the membrane, and so supported lipid bilayers can be stable for days, or even weeks.[11, 12] This model is limited, however, by the potential interaction of the membrane with the supportive surface.[8, 11, 12, 19] For this reason, the membrane may not be able to include large integral proteins because the protein may adhere to the surface and may even denature due to interactions with the surface.[12]

1.2.2 Pore-spanning lipid bilayer

For a pore-spanning bilayer, a lipid bilayer is suspended over a small hole in a thin sheet separating two chambers.[12, 17] The sheet is most commonly made of Teflon, glass, or silica and is perforated with a small hole, or pore.[12, 17] The pore is typically tens of nanometers to a hundred microns in diameter.[12] To cover the pore with a lipid membrane, a bilayer may be formed on one side of the pore, or alternatively, a monolayer may be formed on each side of a thin sheet with the tails of the phospholipids facing the surface of the sheet.[12, 17, 24] The phospholipid tails of the monolayers on each side of the sheet meet and form a lipid bilayer at the pore.[12, 17, 24] The thin sheet and the lipid bilayer separate two chambers containing aqueous solution.[12, 17, 24]

Three techniques may commonly be used to form a pore-spanning bilayer – painted, folded, or liposome rupture.[11, 12, 24, 25] In the painted technique, phospholipids suspended in an organic solvent, such as decane, are applied to the orifice in the membrane.[11, 12] Lipids self-orient so that their hydrophilic headgroups orient toward the aqueous solution and their hydrophobic tails orient inward at the membrane.[11, 12] The organic solvent spontaneously spreads over the hydrophobic surface surrounding the pore and causes the droplet to thin until the phospholipid tails meet and exclude the solvent from this portion of the membrane.[11, 12] In the folded technique, also referred to as the Montal-Mueller technique, the chambers on both sides of the pore contain aqueous solution at a level below the pore.[11, 24] Phospholipids in organic solvent, such as hexane, are deposited onto the surface of the solution where the lipids spread out and self-orient with their hydrophilic headgroups toward the aqueous solution and hydrophobic tails toward the air above the chambers.[11, 24] The organic solvent evaporates from the open chambers and leaves the lipids floating as a film on top of the aqueous solution.[11] Additional aqueous solution is then added at the bottom of the chamber to raise the solution level without disturbing the lipid film.[11] As the lipids reach the pore, they cover the aperture with their hydrophilic headroups still oriented to the aqueous solution and their hydrophobic tails facing inward toward each other to form a bilayer membrane.[11, 24] In the liposome rupture technique, the pore is oriented horizontally.[24] A solution containing liposomes is deposited above the pore.[24] The liposomes settle downward and rupture when they reach the surface, where they spread outward to form a planar bilayer.[11, 24] If a sufficiently large liposome ruptures near the pore, the membrane may spread over the pore and cover it completely.[17, 24]

Pore-spanning bilayers are useful models to study ionic flux through a bilayer (e.g., through ion channel proteins or channel-forming peptides).[12, 17, 24] Pore-spanning bilayers can be stable for several hours.[12, 25] This stability is sufficient for many ion channel experiments since channel events can last for less than one second.[11, 12] To study ionic flux through channel proteins or peptides, however, the channel of interest needs to be incorporated in the membrane.[12, 17] Many peptides are small and, therefore, will self-insert into the membrane.[11, 17] Integral proteins, on the other hand, often require constant association with phospholipids or detergent molecules to prevent denaturing.[11, 17] Therefore, fusion of small proteoliposomes may be necessary to incorporate channel proteins into a pore-spanning bilayer.[11, 12, 17] This fusion is difficult to control and frequently requires the use specific lipids in the liposome preparation or inclusion of fusogenic molecules or peptides in the aqueous solution.[11, 12, 17]

1.3 Liposomal Membrane Models

Liposomes are self-enclosed, spherical shells of phospholipids.[26, 27] These 3-dimensional models of biological membranes can be formed in a variety of sizes, ranging from tens of nanometers to a couple hundred microns in diameter.[28] Much of the effort in forming liposomes focuses on the yield of vesicles within a narrow size distribution and having a single bilayer (a “unilamellar” liposome), as opposed to having multiple bilayers, or lamellae.[28, 29]

1.3.1 Small liposomes

Liposomes that are less than 100 nm in diameter are called small unilamellar vesicles (SUV).[26] Due to their tiny size, they cannot be resolved individually by optical

microscopy, but fluorescence techniques can be performed to evaluate specific biomarkers.[30] For example, the binding kinetics between two molecules can be measure when one molecule is bonded to a surface and the other is linked to fluorescently-labeled SUVs.[30] This method depends on the concentration of SUVs and so must be performed in comparison to experiment controls, or standards.[30] SUVs have also been of considerable interest for their potential in drug delivery.[26, 29, 31] The drug(s) of interest can be encapsulated within SUVs to increase circulation time.[26, 29] Specific biological molecules may be added to the exterior surface of SUVs to aid in targeting specific cells in the body.[26]

Formation of SUVs is generally straightforward and reliable. One commonly employed technique is by sonication.[27, 28, 32, 33] Lipids in organic solvent are dried into a thin film onto the inner surface of a vessel, and remaining traces of solvent are removed under vacuum.[28] The lipid film is then covered with aqueous solution and the solution is ultra-sonicated to disrupt the film and form SUVs.[28] Alternatively, after covering the lipid film with aqueous solution, the vessel may be incubated in a warm water bath to allow formation of liposomes of diverse sizes.[28, 32] The mixture would then be passed multiple times across a filter ("extrusion") to force the liposomes into a homogenous population, with the size dependent on the filter pore size.[27, 28, 32]

1.3.2 Large liposomes

Liposomes with a single bilayer and in the size range of approximately 100-500 nm are typically classified as large unilamellar liposomes (LUV).[26] LUVs are useful for studying interactions between membrane components, assessing diffusion or transport characteristics of molecules using fluorescence techniques, and determining osmotic effects of different solutions on membrane stability.[34-36] Individual LUVs are difficult to

distinguish clearly with an optical microscope, and so attributes are generally based on average measurements from the population.[33]

Formation of LUVs can be difficult to control and often results in a heterogeneous population of liposomes.[33] Two methods typically used include the extrusion method and freeze-thaw.[28, 33] The freeze-thaw method involves subjecting a solution containing liposomes (often initially a heterogeneous and multilamellar population) to repeated cycles of rapid temperature changes.[37] This process leads to fusion with adjacent membranes, possibly due to the formation of ice crystals disrupting the membrane.[37]

1.3.3 Giant liposomes

Liposomes that are greater than 1 μm in diameter and consist of a single bilayer are giant unilamellar vesicles (GUV).[33] GUVs are large enough to be observed on an optical microscope using phase contrast or fluorescence.[38] This trait makes GUVs useful for studying membrane properties, including phase separations,[39] vesicle formation or rupture,[40] and effects of external stimuli on vesicle shape,[41-43] membrane diffusivity,[44] or permeability.[42, 45] The size of GUVs can vary from diameters in the single micron range to over a hundred microns.[33] In many studies of GUVs, however, a homogeneous population is desirable to reduce the number of factors affecting the results of the experiment.[44, 46]

GUVs are the most difficult type of liposome to generate reliably due to the fragility of the membrane at such large sizes.[47] The first method of forming GUVs was a “gentle hydration” method, in which lipids in organic solvent are dried into a thin film and then rehydrated with aqueous solution.[48] Gentle hydration yielded a diverse population of liposomes including sub-micron sized and multilamellar vesicles. Isolation

of only the GUVs from a diverse population is tedious and may yield only a few GUVs. Later, Angelova and Dimivtrov discovered that an electric field applied transverse to the dried lipid film ("electroformation") greatly increased the yield of GUVs.[49] A variety of techniques have been developed that are based on the original protocols of gentle hydration and electroformation to help increase the ratio of GUVs over less desired structures.[42, 50-53] Many of these techniques focus on lipid orientation and separation of lamellae so that the bilayers peel from the lipid film in large sheets before spontaneously closing into vesicles.

A pre-hydration step is frequently included as part of the protocol, in which the dried lipid film is incubated in a humid environment prior to adding aqueous solution.[42, 50] Water molecules of the humid air purportedly help the phospholipids to self-orient into lamellae, beginning with the phospholipids exposed directly to the moist environment.[48, 50] These phospholipids orient their hydrophobic hydrocarbon chains away from the water molecules to minimize their energetically unfavorable interactions. Phospholipids directly adjacent to these self-oriented phospholipids then also self-orient to minimize their energetically unfavorable interactions of hydrophilic headgroups with hydrophobic tails. This manner of self-orientation continues through a number of layers of phospholipids, but their organization decreases with each layer due to defects disrupting their orderly arrangement.[49]

In addition to arranging the phospholipids into lamellae, generation of liposomes is influenced by the number of layers detaching simultaneously from the lipid film.[49] To reduce the occurrence of multiple bilayers peeling together, some protocols employ techniques to separate lamellae. Lamellae may repel each other by inclusion of lipids

with negatively charged headgroups[42] or headgroups containing a long chain of polyethylene glycol (PEG).[50] Other molecules, such as sugar or ethylene glycol, may be dried with the lipids to maintain space between lamellae.[54-56]

1.3.4 Proteoliposomes

Liposomes that contain integral membrane proteins (proteoliposomes) are increasing in importance in medical research because many of these proteins are targets for drug delivery.[27, 57, 58] Small proteoliposomes can be generated by a detergent-dialysis method.[57] First the protein of interest needs to be expressed in native cells or suitable host cells, removed from the native membrane components by solubilization with detergent (to prevent denaturing), and purified.[58-61] These solubilized proteins then are incubated with small liposomes to allow the proteins to self-insert into membranes.[61] The detergent is removed by dilution and filtration through a size-selective filter that allows the detergent molecules to pass but not the liposomes.[59] The dialysis process can be hastened by the addition of hydrophobic beads in the dialysis buffer to adsorb the detergent and lower the concentration in solution.[62] The detergent-dialysis method generally yields only small liposomes because the presence of detergents compromises the integrity of larger liposomes.[63] The size of the small liposomes may be refined after formation by extrusion, fusion, or by using other specialized protocols.[60, 64, 65]

1.4 Summary of Dissertation

Giant unilamellar vesicles (GUVs) are particularly useful models of biological membranes because they can be observed individually on an optical microscope.[66, 67]

Due to the sensitive and fragile nature of GUVs, however, methods of their formation can be challenging, especially in solutions containing ions or when incorporating integral proteins into the membrane.[17, 33] This work focuses on the development of a new method to form GUVs and giant proteoliposomes.

Chapter II presents a simple and reliable technique that we developed for generating GUVs in solutions of physiologic ionic strength (~150 mM monovalent salt) using a variety of different lipid compositions. Results were compared to three stages of the mechanism of liposome formation as described in literature and also compared to a previously established protocol.

In Chapter III, an extension of the technique presented in Chapter II is described and applied to the formation of giant proteoliposomes that incorporated the large transmembrane protein, P-glycoprotein (P-gp). We used several independent assays to test protein functionality. The suitability of this technique to generate giant proteoliposomes for transport studies was compared to a previously established protocol.

Lastly, Chapter IV discusses the overall conclusions from this work and additional experiments that would complement the results in each chapter.

References

1. Lodish, H., Baltimore, D., Berk, A., Zipursky, S. L., Matsudaira, P., and Darnell, J. (1995) *Molecular cell biology; Third edition*, Scientific American Books Inc. {a}, 41 Madison Avenue, New York, New York 10010, USA.

2. McIntosh, T. J. (1999) Structure and physical properties of the lipid membrane, In *Membrane Permeability*, pp 23-47.

3. Bordi, F., and Cametti, C. (2005) Biomembranes, In *Encyclopedia of Condensed Matter Physics* (Editors-in-Chief: Franco, B., Gerald, L. L., and Peter, W., Eds.), pp 116-122, Elsevier, Oxford.

4. Cevc, G. (1990) MEMBRANE ELECTROSTATICS, *Biochimica Et Biophysica Acta 1031*, 311-382.

5. Ohvo-Rekila, H., Ramstedt, B., Leppimaki, P., and Slotte, J. P. (2002) Cholesterol interactions with phospholipids in membranes, *Progress in Lipid Research 41*, 66-97.

6. Hautala, J. T., Riekkola, M. L., and Wiedmer, S. K. (2007) Anionic phospholipid coatings in capillary electrochrornatography binding of Ca2+ to phospholipid phosphate group, *J. Chromatogr. A 1150*, 339-347.

7. Singer, S. J., and Nicolson, G. L. (1972) FLUID MOSAIC MODEL OF STRUCTURE OF CELL-MEMBRANES, *Science 175*, 720-731.

8. Fenz, S. F., Merkel, R., and Sengupta, K. (2009) Diffusion and Intermembrane Distance: Case Study of Avidin and E-Cadherin Mediated Adhesion, *Langmuir 25*, 1074-1085.

9. Doeven, M. K., Folgering, J. H. A., Krasnikov, V., Geertsma, E. R., van den Bogaart, G., and Poolman, B. (2005) Distribution, lateral mobility and function of membrane proteins incorporated into giant unilamellar vesicles, *Biophysical Journal 88*, 1134-1142.

10. Bretscher, M. S. (1985) THE MOLECULES OF THE CELL-MEMBRANE, *Sci.Am. 253*, 100-&.

11. Zagnoni, M. (2012) Miniaturised technologies for the development of artificial lipid bilayer systems, *Lab on a Chip 12*, 1026-1039.

12. Demarche, S., Sugihara, K., Zambelli, T., Tiefenauer, L., and Voros, J. (2011) Techniques for recording reconstituted ion channels, *Analyst 136*, 1077-1089.

13. Grassl, S. M. (2012) Chapter 11 - Mechanisms of Carrier-Mediated Transport: Facilitated Diffusion, Cotransport and Countertransport, In *Cell Physiology Source Book (Fourth Edition)* (Nicholas, S., Ed.), pp 153-165, Academic Press, San Diego.

14. Massaldi, H. A., and Borzi, C. H. (1984) THE PHYSICOCHEMICAL MECHANISM OF MEDIATED TRANSPORT .1. FACILITATED DIFFUSION, *J. Theor. Biol. 106*, 537-557.

15. Edidin, M. (2003) Timeline - Lipids on the frontier: a century of cell-membrane bilayers, *Nat. Rev. Mol. Cell Biol. 4*, 414-418.

16. Suzuki, H., and Takeuchi, S. (2008) Microtechnologies for membrane protein studies, *Analytical and Bioanalytical Chemistry 391*, 2695-2702.

17. Tiefenauer, L., and Demarche, S. (2012) Challenges in the Development of Functional Assays of Membrane Proteins, *Materials 5*, 2205-2242.

18. Dimitrievski, K. (2010) Influence of Lipid-Bilayer-Associated Molecules on Lipid-Vesicle Adsorption, *Langmuir 26*, 5706-5714.

19. Sackmann, E. (1996) Supported membranes: Scientific and practical applications, *Science 271*, 43-48.

20. Weirich, K. L., Israelachvili, J. N., and Fygenson, D. K. (2010) Bilayer Edges Catalyze Supported Lipid Bilayer Formation, *Biophysical Journal 98*, 85-92.

21. Majd, S., and Mayer, M. (2005) Hydrogel stamping of arrays of supported lipid bilayers with various lipid compositions for the screening of drug-membrane and protein-membrane interactions, *Angewandte Chemie-International Edition 44*, 6697-6700.

22. Horger, K. S., Estes, D. J., Capone, R., and Mayer, M. (2009) Films of Agarose Enable Rapid Formation of Giant Liposomes in Solutions of Physiologic Ionic Strength, *Journal of the American Chemical Society 131*, 1810-1819.

23. Blodgett, K. B. (1935) Films built by depositing successive monomolecular layers on a solid surface, *Journal of the American Chemical Society 57*, 1007-1022.

24. Steller, L., Kreir, M., and Salzer, R. (2012) Natural and artificial ion channels for biosensing platforms, *Analytical and Bioanalytical Chemistry 402*, 209-230.

25. Hirano-Iwata, A., Aoto, K., Oshima, A., Taira, T., Yamaguchi, R. T., Kimura, Y., and Niwano, M. (2010) Free-Standing Lipid Bilayers in Silicon Chips-Membrane Stabilization Based on Microfabricated Apertures with a Nanometer-Scale Smoothness, *Langmuir 26*, 1949-1952.

26. Maherani, B., Arab-Tehrany, E., Mozafari, M. R., Gaiani, C., and Linder, M. (2011) Liposomes: A Review of Manufacturing Techniques and Targeting Strategies, *Curr. Nanosci. 7*, 436-452.

27. Watwe, R. M., and Bellare, J. R. (1995) MANUFACTURE OF LIPOSOMES - A REVIEW, *Curr. Sci. 68*, 715-724.

28. Jesorka, A., and Orwar, O. (2008) Liposomes: Technologies and Analytical Applications, In *Annual Review of Analytical Chemistry*, pp 801-832, Annual Reviews, Palo Alto.

29. Meure, L. A., Foster, N. R., and Dehghani, F. (2008) Conventional and Dense Gas Techniques for the Production of Liposomes: A Review, *AAPS PharmSciTech 9*, 798-809.

30. Edwards, K. A., and Baeumner, A. J. (2006) Liposomes in analyses, *Talanta 68*, 1421-1431.

31. Monfardini, C., and Veronese, F. M. (1998) Stabilization of substances in circulation, *Bioconjugate Chemistry 9*, 418-450.

32. Segota, S., and Tezak, D. (2006) Spontaneous formation of vesicles, *Advances in Colloid and Interface Science 121*, 51-75.

33. Walde, P., Cosentino, K., Engel, H., and Stano, P. (2010) Giant Vesicles: Preparations and Applications, *Chembiochem 11*, 848-865.

34. Ohlsson, G., Tabaei, S. R., Beech, J., Kvassman, J., Johanson, U., Kjellbom, P., Tegenfeldt, J. O., and Hook, F. (2012) Solute transport on the sub 100 ms scale across the lipid bilayer membrane of individual proteoliposomes, *Lab on a Chip 12*, 4635-4643.

35. Mui, B. L. S., Cullis, P. R., Evans, E. A., and Madden, T. D. (1993) OSMOTIC PROPERTIES OF LARGE UNILAMELLAR VESICLES PREPARED BY EXTRUSION, *Biophysical Journal 64*, 443-453.

36. Sabin, J., Prieto, G., Ruso, J. M., and Sarmiento, F. (2007) Fractal aggregates induced by liposome-liposome interaction in the presence of Ca2+, *European Physical Journal E 24*, 201-210.

37. Castile, J. D., and Taylor, K. M. G. (1999) Factors affecting the size distribution of liposomes produced by freeze-thaw extrusion, *International Journal of Pharmaceutics 188*, 87-95.

38. Menger, F. M., and Angelova, M. I. (1998) Giant vesicles: Imitating the cytological processes of cell membranes, *Accounts of Chemical Research 31*, 789-797.

39. Veatch, S. L. (2007) Electro-formation and fluorescence microscopy of giant vesicles with coexisting liquid phases, In *Methods in Molecular Biology* (McIntosh, T. J., Ed.), pp 59-72, Humana Press Inc, 999 Riverview Dr, Ste 208, Totowa, Nj 07512-1165 USA.

40. Menger, F. M., and Gabrielson, K. D. (1995) Cytomimetic Organic-Chemistry - Early Developments, *Angewandte Chemie-International Edition in English 34*, 2091-2106.

41. Hotani, H., Nomura, F., and Suzuki, Y. (1999) Giant liposomes: from membrane dynamics to cell morphogenesis, *Current Opinion in Colloid & Interface Science 4*, 358-368.

42. Akashi, K., Miyata, H., Itoh, H., and Kinosita, K. (1996) Preparation of giant liposomes in physiological conditions and their characterization under an optical microscope, *Biophysical Journal 71*, 3242-3250.

43. Farge, E., and Devaux, P. F. (1992) Shape changes of giant liposomes induced by an asymmetric transmembrane distribution of phospholipids, *Biophysical Journal 61*, 347-357.

44. Mathivet, L., Cribier, S., and Devaux, P. F. (1996) Shape change and physical properties of giant phospholipid vesicles prepared in the presence of an AC electric field, *Biophysical Journal 70*, 1112-1121.

45. Estes, D. J., and Mayer, M. (2005) Giant liposomes in physiological buffer using electroformation in a flow chamber, *Biochimica Et Biophysica Acta-Biomembranes 1712*, 152-160.

46. Taylor, P., Xu, C., Fletcher, P. D. I., and Paunov, V. N. (2003) A novel technique for preparation of monodisperse giant liposomes, *Chemical Communications*, 1732-1733.

47. Sabin, J., Prieto, G., Ruso, J. M., Hidalgo-Alvarez, R., and Sarmiento, F. (2006) Size and stability of liposomes: A possible role of hydration and osmotic forces, *European Physical Journal E 20*, 401-408.

48. Reeves, J. P., and Dowben, R. M. (1969) Formation and Properties of Thin-Walled Phospholipid Vesicles, *Journal of Cellular Physiology 73*, 49-60.

49. Angelova, M. I., and Dimitrov, D. S. (1986) Liposome Electroformation, *Faraday Discussions 81*, 303-311.

50. Yamashita, Y., Oka, M., Tanaka, T., and Yamazaki, M. (2002) A new method for the preparation of giant liposomes in high salt concentrations and growth of protein microcrystals in them, *Biochimica Et Biophysica Acta-Biomembranes 1561*, 129-134.

51. D'Onofrio, T. G., Hatzor, A., Counterman, A. E., Heetderks, J. J., Sandel, M. J., and Weiss, P. S. (2003) Controlling and measuring the interdependence of local properties in biomembranes, *Langmuir 19*, 1618-1623.

52. Montes, L. R., Alonso, A., Goni, F. M., and Bagatolli, L. A. (2007) Giant Unilamellar Vesicles Electroformed from Native Membranes and Organic Lipid Mixtures under Physiological Conditions, *Biophys. J. %R 10.1529/biophysj.107.116228 93*, 3548-3554.

53. Dimova, R., Aranda, S., Bezlyepkina, N., Nikolov, V., Riske, K. A., and Lipowsky, R. (2006) A practical guide to giant vesicles. Probing the membrane nanoregime via optical microscopy, *Journal of Physics: Condensed Matter 18*, S1151-S1176.

54. Tsumoto, K., Matsuo, H., Tomita, M., and Yoshimura, T. (2009) Efficient formation of giant liposomes through the gentle hydration of phosphatidylcholine films doped with sugar, *Colloids and Surfaces B-Biointerfaces 68*, 98-105.

55. Keller, B. U., Hedrich, R., Vaz, W. L., and Criado, M. (1988) Single channel recordings of reconstituted ion channel proteins: an improved technique, *Pflugers Arch 411*, 94-100.

56. Crowe, J. H., Crowe, L. M., Carpenter, J. F., and Wistrom, C. A. (1987) STABILIZATION OF DRY PHOSPHOLIPID-BILAYERS AND PROTEINS BY SUGARS, *Biochem. J. 242*, 1-10.

57. Overington, J. P., Al-Lazikani, B., and Hopkins, A. L. (2006) Opinion - How many drug targets are there?, *Nature Reviews Drug Discovery 5*, 993-996.

58. Seddon, A. M., Curnow, P., and Booth, P. J. (2004) Membrane proteins, lipids and detergents: not just a soap opera, *Biochimica Et Biophysica Acta-Biomembranes 1666*, 105-117.

59. Franzusoff, A. J., and Cirillo, V. P. (1983) SOLUBILIZATION AND RECONSTITUTION OF THE GLUCOSE-TRANSPORT SYSTEM FROM SACCHAROMYCES-CEREVISIAE, *Biochimica Et Biophysica Acta 734*, 153-159.

60. Rigaud, J.-L., and Lévy, D. (2003) Reconstitution of Membrane Proteins into Liposomes, In *Methods in Enzymology* (Nejat, D., Ed.), pp 65-86, Academic Press.

61. Naito, M., and Tsuruo, T. (1995) RECONSTITUTION OF PURIFIED P-GLYCOPROTEIN INTO LIPOSOMES, *J. Cancer Res. Clin. Oncol. 121*, 582-586.

62. Rigaud, J. L., Levy, D., Mosser, G., and Lambert, O. (1998) Detergent removal by non-polar polystyrene beads - Applications to membrane protein reconstitution and two-dimensional crystallization, *European Biophysics Journal with Biophysics Letters 27*, 305-319.

63. Wrigglesworth, J. M., Wooster, M. S., Elsden, J., and Danneel, H. J. (1987) DYNAMICS OF PROTEOLIPOSOME FORMATION - INTERMEDIATE STATES DURING DETERGENT DIALYSIS, *Biochem. J. 246*, 737-744.

64. Girard, P., Pecreaux, J., Lenoir, G., Falson, P., Rigaud, J. L., and Bassereau, P. (2004) A new method for the reconstitution of membrane proteins into giant unilamellar vesicles, *Biophysical Journal 87*, 419-429.

65. Varnier, A., Kermarrec, F., Blesneac, I., Moreau, C., Liguori, L., Lenormand, J. L., and Picollet-D'hahan, N. (2010) A Simple Method for the Reconstitution of Membrane Proteins into Giant Unilamellar Vesicles, *Journal of Membrane Biology 233*, 85-92.

66. Menger, F. M., and Keiper, J. S. (1998) Chemistry and physics of giant vesicles as biomembrane models, *Current Opinion in Chemical Biology 2*, 726-732.

67. Rodriguez, N., Pincet, F., and Cribier, S. (2005) Giant vesicles formed by gentle hydration and electroformation: A comparison by fluorescence microscopy, *Colloids and Surfaces B-Biointerfaces 42*, 125-130.

CHAPTER II

Formation of Giant Liposomes in Solutions of Physiologic Ionic Strength

Abstract

This chapter describes a method to form giant liposomes in solutions of physiologic ionic strength, such as phosphate buffered saline (PBS) or 150 mM KCl. Formation of these cell-sized liposomes proceeded from hybrid films of partially dried agarose and lipids. Hydrating the films of agarose and lipids in aqueous salt solutions resulted in swelling and partial dissolution of the hybrid films and in concomitant rapid formation of giant liposomes in high yield. This method did not require the presence of an electric field or specialized lipids; it generated giant liposomes from pure phosphatidylcholine lipids or from lipid mixtures that contained cholesterol or negatively charged lipids. Hybrid films of agarose and lipids even enabled the formation of giant liposomes in PBS from lipid compositions that are typically problematic for liposome formation, such as pure phosphatidylserine, pure phosphatidylglycerol, and asolectin. This chapter discusses biophysical aspects of the formation of giant liposomes from hybrid films of agarose and lipids in comparison to established methods and shows that

gentle hydration of hybrid films of agarose and lipids is a simple, rapid, and reproducible procedure to generate giant liposomes of various lipid compositions in solutions of physiologic ionic strength without the need for specialized equipment.

2.1 Introduction

Giant liposomes are useful models to study cellular membranes since they approximate the size and membrane curvature of live cells[1-6] and since they can be observed individually by optical microscopy.[2, 3, 5-7] Several methods produce giant liposomes; these methods include "gentle hydration",[7-11] "freeze-and-thaw",[12, 13] "solid hydration",[14] "solvent evaporation",[15, 16] emulsion-based methods,[17] and "electroformation".[1, 2, 9, 18-21] These methods generate giant liposomes of high quality and yield, but they are typically limited to solutions of low ionic strength (≤50 mM monovalent salt)[1, 3, 7-10, 16, 22] unless specialized lipid formulations[8-10] or specific electroformation protocols[22, 23] are used.

Due to this limitation, most biophysical and biochemical studies on giant liposomes so far have been carried out in aqueous solutions with an ionic strength significantly below the physiologic range.[22, 23] At least six important properties of giant liposomes can, however, be affected by ionic strength; these include: i) electrostatic interactions of lipid membranes with proteins,[24-26] with adjacent lipid membranes,[22, 27] or with other molecules or ions in solution;[27-30] ii) osmotic properties;[5, 7, 31, 32] iii) packing of lipid headgroups in the membrane;[5, 33] iv) curvature,[7] bending elasticity,[34] and mechanical stability of lipid bilayers;[5, 35] v) activity of membrane proteins;[36] and vi) ion channel conductance.[35-37] Consequently, it would be desirable to prepare giant

liposomes in solutions that make it possible to extend these studies to physiologically relevant salt concentrations.[22]

In order to comprehend why it is difficult to form giant liposomes in solutions of physiologic ionic strength, a detailed understanding of the molecular mechanisms of formation of giant liposomes would be helpful. While the exact mechanisms of formation of giant liposomes still present questions,[23, 33, 38-40] the process can be separated into three stages as illustrated in Figure 2.1.[1, 3, 10, 41, 42] In the first stage of the formation of giant liposomes, lipids in a solid lipid film are hydrated, leading to the self-assembly and separation of lipid lamellae in the film.[1, 10, 11] This process can be promoted by electrostatic repulsion of negatively charged lipids,[8, 22, 32, 43] steric effects from bulky headgroups,[10, 44] and by pre-hydrating the lipid film[8, 10, 11] to orient lamellae of lipids and to separate the bilayers. Solutions of high ionic strength hinder this first step of separation of lamellae due to electrostatic screening of repulsive charges.[22, 27] The second stage in the formation of giant liposomes involves swelling of liposomes due to forces normal to the bilayers[3, 42] and recruitment of lipids from the lipid film.[1, 22] Osmotic pressure,[11, 42] line tension,[42] and electric fields[42, 45] can provide this force, but can also be affected by solutions of high ionic strength. The third and final stage involves fusion of adjacent liposomes due to mechanical stresses.[33, 41]

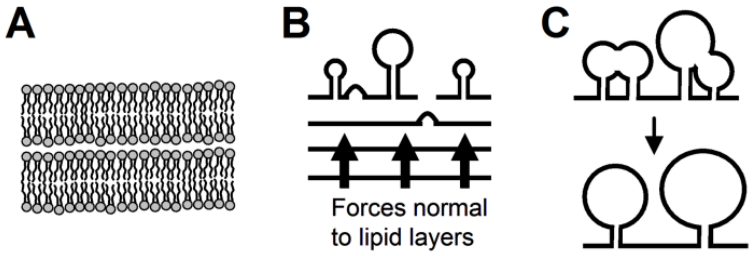

Figure 2.1. Cartoon illustrating three important stages during the formation of giant liposomes. A) Orientation and self-assembly of lipids into bilayers, leading to the

formation of lipid lamellae.[1, 10, 11] B) Growth of liposomes promoted by forces normal to the bilayers.[3, 42] C) Fusion of adjacent liposomes into giant liposomes due to crowding and associated mechanical forces.[2, 41, 46] The black lines in B and C represent lipid bilayers.

Here we intended to promote all three stages of liposome formation in order to develop a method for the formation of giant liposomes in solutions of physiologic ionic strength, such as phosphate buffered saline (PBS), without the requirement for specialized lipids,[8-10] specialized equipment,[23] or a separate pre-hydration step.[8-11] We hypothesized that forming giant liposomes from a hybrid film of hydrogel and lipids may (i) promote the separation of lipid lamellae by providing pre-hydration and pre-orientation of lipids; (ii) promote growth of liposomes by generating forces normal to the lipid lamellae during the swelling of the agarose film; and (iii) promote fusion of adjacent liposomes due to crowding of growing liposomes that are attached to the swelling, porous film of agarose.

2.2 Results and Discussion

2.2.1 Formation of giant liposomes in physiologic solutions

Figure 2.2 illustrates the procedure of forming giant liposomes from hybrid films of agarose and lipids. This method proceeded in three simple steps and formed giant liposomes in physiological buffers within minutes after hydrating the hybrid films.

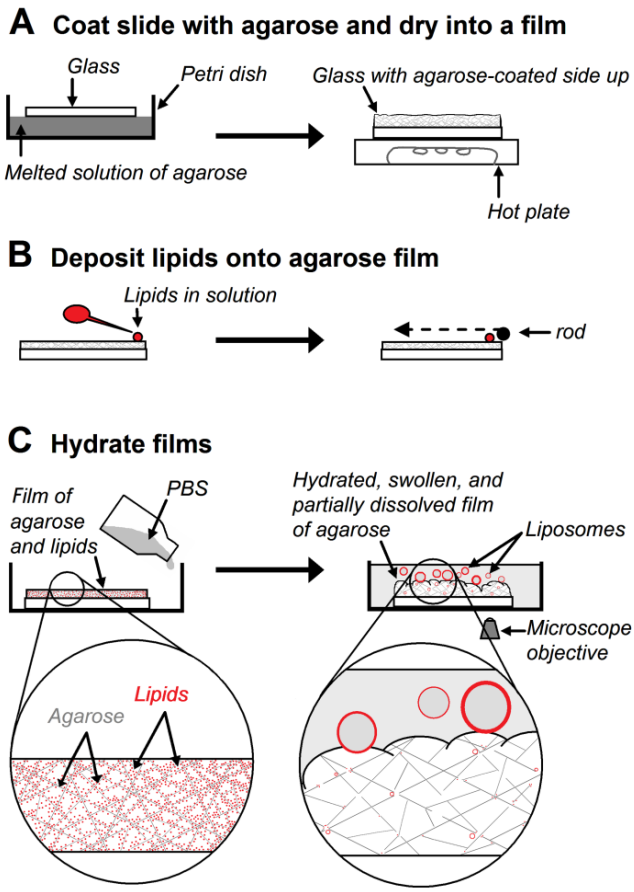

Figure 2.2. Procedure of forming giant liposomes from hybrid films of agarose and lipids. A) The procedure started by dipping one side of a clean glass slide in an aqueous solution of 1% (w/w) agarose with ultra-low melting temperature (Type IX-A). After dripping off excess solution, the slide was turned and dried on a hot plate at a temperature of ~40 °C while keeping the agarose solution spread evenly over the glass slide (if necessary by moving a straight glass or metal rod tangentially over the surface during the drying process). This procedure generated a film of agarose with fairly uniform thickness on one side of the glass slide. B) In the next step, a total volume of 30 µL of 3.75 mg mL^{-1} lipid in 90% (v/v) chloroform and 10% (v/v) methanol was spread evenly over (and into) the film of agarose by using a glass or metal rod while the solvents evaporated (see Experimental Section, Figure 2.8). To remove traces of solvent, the glass slide with the resulting hybrid film of agarose and lipids was placed in a vacuum chamber (approx. -730 mTorr) for at least 20 min. C) To generate liposomes, this slide was placed into a Petri dish such that the hybrid film of agarose and lipids faced upwards and an aqueous solution containing 150 mM KCl, PBS, or deionized water was poured into the dish until it covered the slide.

In order to illustrate the benefit of forming giant liposomes from hybrid films of agarose and lipids in ionic solutions, we compared this method to the established method of “gentle hydration,” i.e. the formation of liposomes from lipid films formed directly on bare glass substrates without agarose. Figure 2.3 shows that giant liposomes formed from films of agarose within a few minutes in remarkable yield in PBS solutions. Since we used optical phase-contrast and fluorescence microscopy to observe the formation of liposomes, we could only resolve liposomes with diameters ≥ 1 μm. We observed the formation of such giant liposomes only on the surface of the hybrid film of agarose and lipids. Figure 2.4 shows, however, that lipids penetrated the entire agarose film, and therefore small liposomes (<< 1 μm) likely formed within the agarose network.

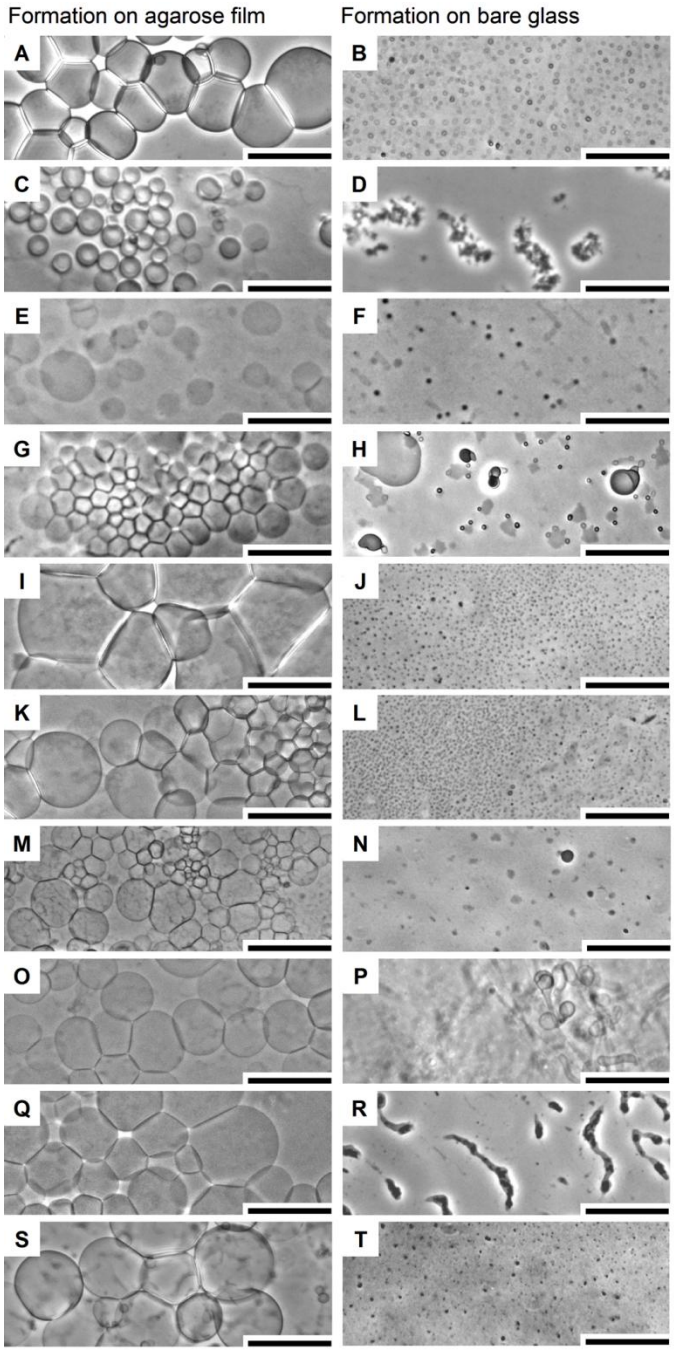

Figure 2.3. Phase contrast images of giant liposomes formed within 1 h in phosphate buffered saline (PBS). The column of images on the left shows liposomes that formed from hybrid films of agarose and lipids; the column on the right shows the control experiments of liposomes that formed from lipid films on bare glass. The following lipid compositions were used (in mol%): A, B) Pure 1-palmitoyl-2-oleoyl-*sn*-glycero-3-phosphatidylcholine (POPC). C, D) Pure 1,2-dioleoyl-*sn*-glycero-3-[phospho-L-serine] (DOPS). E, F) Pure 1-palmitoyl-2-oleoyl-*sn*-glycero-3-[phosphor-*rac*-(1-glycerol)]

(POPG). G, H) Asolectin from soybean. I, J) Mixture of 90% POPC with 10% cholesterol. K, L) Mixture of 80% POPC with 20% cholesterol. M, N) Mixture of 90% POPC with 10% of the negatively charged lipid POPG[47]. O, P) Mixture of 50% POPC with 50% POPG. Q, R) Mixture of 90% POPC with 10% of the negatively charged lipid DOPS. S, T) Mixture of 95% POPC with 5% 1,2-dipalmitoyl-sn-glycero-3-phosphatidylethanol-amine-N-[methoxy (polyethylene glycol)-2000] (also referred to as PEG-PE or PEGylated lipid). Scale bars = 100 µm.

The giant liposomes that we could resolve on the surface of the hybrid film were typically surface-attached, appeared spherical (or polygonal when aggregated), and were often arranged in several layers above the surface. As new liposomes developed and swelled, previously formed liposomes were often pushed away from the surface. The liposomes in the resulting layers may be tethered to the surface or to other liposomes (some tethers were visible when viewed by phase contrast microscopy). A few liposomes appeared to have detached completely but this occurrence was not common within any given population of liposomes. We procured free-floating liposomes by prying apart the chamber and allowing the contents to drip into a collection vessel or by applying gentle suction using a pipette or needle and syringe to remove the solution from the chamber (see Appendix A, Figure A.1). Remarkably, giant liposomes formed over 30-80% of the surface of the chamber from a range of lipid compositions that included pure zwitterionic lipids (Figure 2.3A), lipids that typically pose difficulties for the formation of giant liposomes (such as pure DOPS, pure POPG, or asolectin; for full names of lipids, see figure caption of Figure 2.3)[19] (Figure 2.3C,E,G), as well as mixtures of zwitterionic lipids with 10 or 20 mol% cholesterol (Figure 2.3I,K), with 10 or 50 mol% negatively charged lipids (Figure 2.3M,O,Q), or with 5 mol% PEGylated lipids (Figure 2.3S). All these lipid mixtures formed hundreds of giant liposomes with

diameters above 10 μm in solutions of physiologic ionic strength as well as in deionized water when grown from hybrid films of agarose and lipids. As expected,[8, 10] we obtained the best liposomes with respect to their number, size, and surface coverage from lipid mixtures containing up to 50% negatively charged lipids or PEGylated lipids. The repulsive forces generated by these lipids also reduced the aggregation of liposomes that is typical in salt solutions.[1, 8-10, 45, 48] With respect to the effect of the ions present in solution on the formation of giant liposomes, we found that giant liposomes formed best in deionized water, followed by 150 mM KCl (see Appendix A, Figure A.2) and PBS. In summary, formation of giant liposomes in PBS proceeded in high yield from all lipid compositions that we tried, as shown in Figure 2.3.

Figure 2.3 illustrates that the presence of a film of agarose was essential for the formation of giant liposomes in solutions of physiologic ionic strength. Control experiments with lipid films deposited directly on glass or on surfaces of indium tin oxide (ITO), showed either no formation or only sporadic formation of giant liposomes (Figure 2.3B,D,F,H,J,L,N,P,R,T). The few giant liposomes that did form from lipid films on bare glass (or bare ITO) surfaces were typically smaller than 5 μm. Interestingly, even lipid mixtures containing up to 50% negatively charged lipids or PEGylated lipids generated a very low yield of giant liposomes in PBS when formed from lipid films on bare glass surfaces (Figure 2.3N,P,R,T).[49]

To investigate if pre-hydration of the lipid film would improve the yield of giant liposomes from bare glass surfaces in PBS, we performed the protocol described by Akashi *et al*. using a lipid mixture containing 90% POPC and 10% POPG.[8] Using Akashi's method on bare glass surfaces with pre-hydration, we observed the formation

of only a few giant liposomes in PBS; these liposomes were typically smaller than 10 μm. These results are consistent with those by Akashi *et al.* who reported no formation of giant liposomes in solutions with KCl or NaCl concentrations greater than 100 mM.[8] Figure 2.3 hence illustrates that formation of giant liposomes from hybrid films of agarose and lipids provides a significant and important benefit over currently existing methods of formation of giant liposomes in solutions of physiologic ionic strength.

2.2.2 Characterization of hybrid films of agarose and lipids

Before discussing the role of films of agarose in promoting the formation of giant liposomes in ionic solutions, it is necessary to understand the location of the lipids relative to the agarose molecules in the hybrid films of agarose and lipids prior to adding aqueous solution (i.e., at the end of step B in Figure 2.2). This aspect is important because the effect of interactions between lipid and agarose molecules on the formation of liposomes likely depends on the contact area between agarose molecules and lipid molecules. If lipids penetrated into the agarose film, then surface interactions between lipids and agarose molecules in a porous agarose film would be increased due to the larger surface area compared to a flat surface (such as bare glass or the surface of a non-porous film). To test if lipids penetrated the film of agarose, we compared micrographs of particularly thick (~16 μm), hybrid films of agarose and fluorescently-labeled lipids. Cross-sectional views of these films revealed that the fluorescently-labeled lipids penetrated the entire thickness of the film of agarose (Figure 2.4).[50] Hence, the resulting hybrid film of agarose and lipids inevitably generated a large contact area between agarose and lipid molecules, and this extended interface area influenced the formation of lipid lamellae and giant liposomes as discussed below.

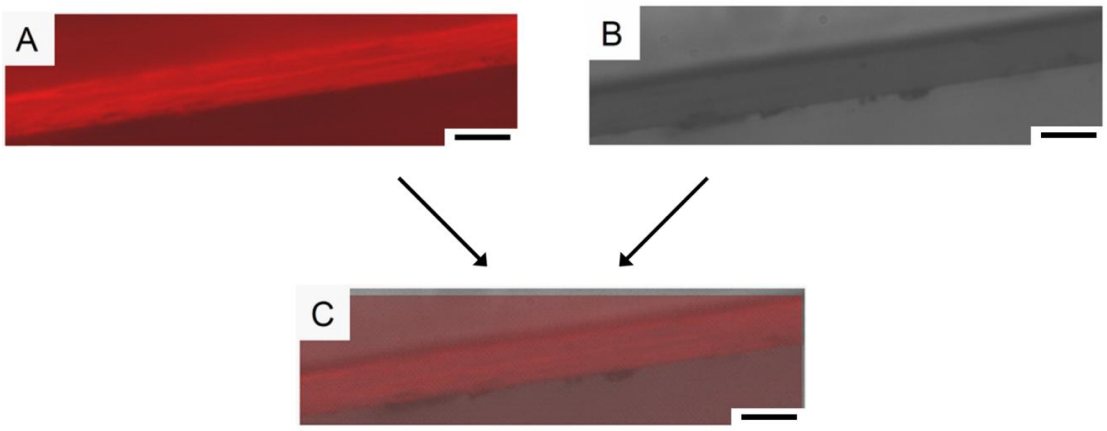

Figure 2.4. Cross-section through a thick film of agarose that was coated with fluorescently-labeled lipids. A) Epifluorescence image of a cross-section of the film. B) Phase contrast image of the cross-section of the film. C) Overlap of images A and B with A at 50% transparency, indicating that the fluorescently-labeled lipids penetrated completely through the film of agarose. Scale bars = 20 µm.

Another important factor for understanding how the hybrid film of agarose and lipids promotes the formation of giant liposomes is whether or not the film of agarose dissolves to some extent to form agarose molecules in solution. Agarose is a polysaccharide consisting of alternating residues of β-1,3-linked D-galactose and α-1,4-linked 3,6-anhydro-α-L-galactopyranose (see Figure 2.5A).[51-57] This linear polymer adopts a structure of left-handed helices[51, 52, 56] that are stabilized by weak hydrogen bonds and intramolecular hydrophobic interactions.[55, 57, 58] As solutions transition into a gel, agarose helices aggregate to form long fibers containing 10 to 10^4 molecules.[51, 52, 57] Figure 2.5C illustrates that SEM imaging of a film of agarose that formed a gel before drying the film (e.g. standard melting temperature agarose) displayed surface features that appeared to contain fibrillar structures. In contrast, SEM images of films of agarose that dried without noticeably forming a gel (e.g. ultra-low melting agarose) did not show these structures (Figure 2.5D). We characterized the surface of films

prepared from four types of agarose by AFM and SEM (see Figure A.3 in Appendix A) and found that films from ultra-low melting agarose appeared to display the smoothest (i.e., the least fibrous-looking) surface. We attribute this observation to two reasons: 1) the average molecular weight of ultra-low melting agarose was the lowest of the four types of agarose,[53] and 2) ultra-low melting temperature agarose did not gel to a noticeable extent during the formation of the agarose film at 40°C; it remained dissolved in solution.

In the experiments presented here, we formed films of ultra-low melting temperature agarose by partially drying agarose solution on a glass surface. Foord and Atkins demonstrated by x-ray diffraction that drying a solution of agarose at elevated temperature resulted in a film that contained agarose molecules in the form of extended helices, which were not interlinked.[52] We therefore expected the agarose molecules in the films of ultra-low melting agarose to be present in the form of extended helices that lay loosely over each other in random directions to form an unbound mesh of agarose molecules. Since the molecules were not tightly associated in a gel structure, it is likely that they can dissolve into solution. We demonstrate below that films of ultra-low melting temperature agarose did, indeed, partially dissolve during liposome formation, and we discuss the possible importance of this characteristic for the formation of giant liposomes in solutions of physiologic ionic strength. We also show that agarose films that did not dissolve noticeable did not promote the formation of giant liposomes in PBS.

Since ultra-low melting temperature agarose dissolves in solution, one important question is if agarose molecules associate with the membranes during the formation of liposomes. This question is relevant because binding of agarose molecules to

liposomes may influence their formation in ionic solutions. To answer this question, we formed giant liposomes from a hybrid film of fluorescently-labeled, ultra-low melting temperature agarose and POPC lipids. Confocal microscopy revealed an increase in fluorescence intensity of giant liposomes formed from films of fluorescently-labeled agarose compared to the fluorescence intensity of liposomes formed from non-labeled agarose (see Appendix A, Figure A.4). These results suggest that the fluorescently-labeled agarose molecules associated with the liposome membranes. This association of macromolecular agarose molecules with lipid membranes may hence provide a similar benefit to the formation of giant liposomes as provided by PEGylated lipids.[(10)]

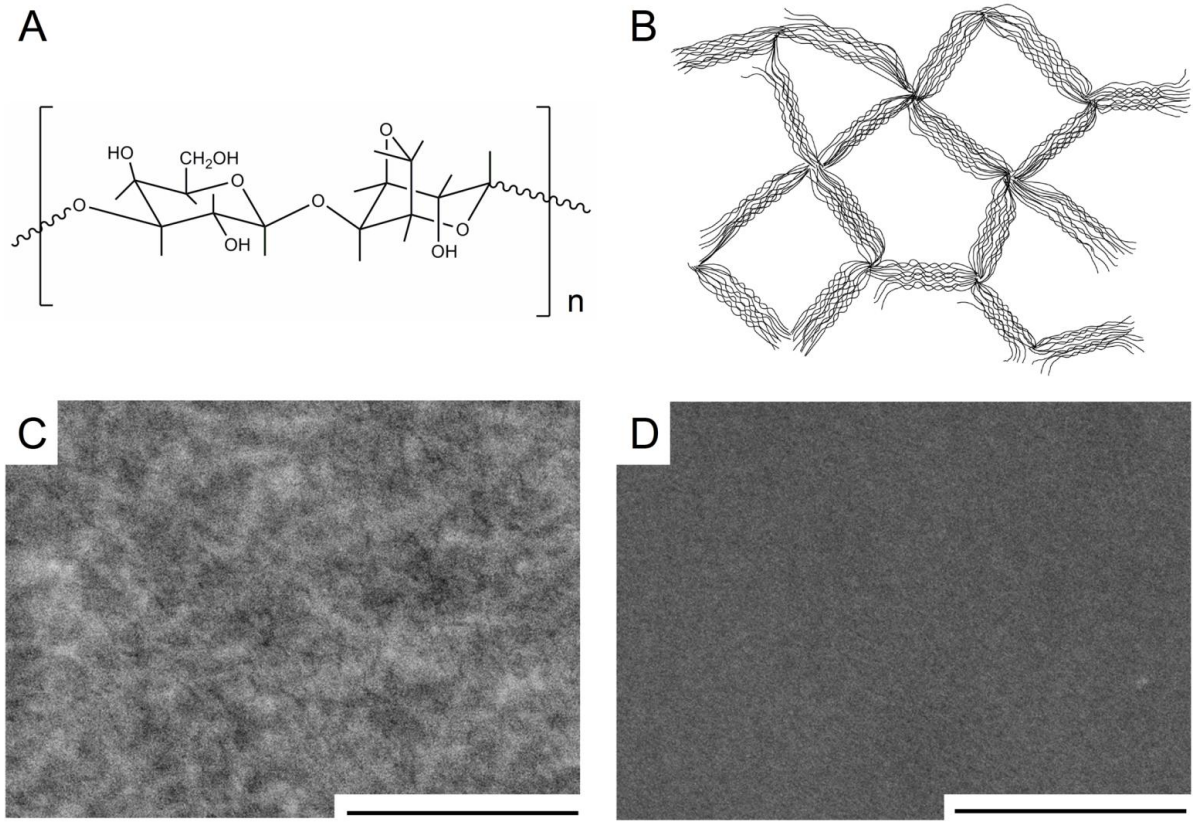

Figure 2.5. Chemical and physical structure of agarose. A) Chemical structure of the fundamental unit of agarose.[(51-53)] Agarose is a polysaccharide consisting of alternating residues of β-1,3-linked D-galactose and α-1,4-linked 3,6-anhydro-α-L-galactopyranose,

and the linear polymer forms left-handed helices.[51, 52, 56] B) During formation of an agarose gel, 10 to 10^4 helices aggregate into long fibers,[51, 52, 57] which in turn associate in three dimensions to form a gel network.[51, 53-55] Artwork adapted from Arnott, S.; Fulmer, A.; Scott, W.E., *J. Mol. Biol.* **1974**, *90*, 269-284.[51] C) SEM micrograph of a film of standard melting temperature agarose. Note the appearance of fiber-like structures. D) SEM micrograph of a film of ultra-low melting agarose. No fiber-like structures could be resolved. Scale bars = 400 nm.

In order to determine the effect of membrane-associated agarose on the diffusivity of lipids in the membranes of liposomes formed from hybrid films of agarose and lipids, we performed fluorescence recovery after photobleaching (FRAP) experiments.[29, 59] We found that the lipids in the resulting giant liposomes were mobile (see Appendix A, Figure A.5), indicating that the presence of (and interaction with) agarose did not result in immobilization of lipids in the liposome membranes.

After determining that agarose molecules associate with the membranes of giant liposomes during formation, we assessed the importance of the hybrid *film of agarose* and lipids for the formation of liposomes, in comparison to formation of liposomes from bare glass but in the presence of a solution that contained *soluble agarose* molecules. We explored two different approaches for using agarose in solution for the formation of giant liposomes. In the first approach, we exposed a lipid solution to agarose molecules before coating the lipids onto a glass slide to determine if this approach would lead to formation of giant liposomes. To carry out this experiment, we agitated a two phase system containing a 1% solution of ultra-low melting agarose dissolved in deionized water and a solution of POPC lipids in chloroform and methanol. After vigorous shaking and allowing the immiscible fluids to separate, we extracted the chloroform/lipid solution and used it to coat plain glass slides with a film of lipids according to Figure 2.2B. We

immersed the resulting lipid-coated slides in PBS and carried out formation of liposomes for 3 h. This method did not lead to significant formation of giant liposomes, indicating that, in order to form giant liposomes, agarose molecules had to be present either in the form of a film or in the aqueous solution during liposome formation. In order to distinguish between these remaining two possibilities, we carried out a second experiment that determined if association of agarose molecules dissolved in aqueous phase with lipid molecules during hydration would lead to formation of giant liposomes. We tested this possibility by coating plain glass slides with a solution of POPC lipids in chloroform and methanol according to Figure 2.2B. Subsequently, we immersed the coated slides in a PBS solution that contained dissolved ultra-low melting temperature agarose at a concentration of 0.06% (w/w). This concentration was similar to the final concentration attainable if the slide had been coated with a film of agarose (as described in Figure 2.2) and if all of the agarose had dissolved; this concentration was also sufficiently low that ultra-low melting agarose did not gel at room temperature. This method did not lead to significant formation of giant liposomes within 3 h. These experiments thus demonstrated that the formation of giant liposomes in PBS depended on the presence of agarose as a film prior to generating the hybrid film of agarose and lipids.

2.2.3 Possible role of hybrid film on three stages of liposome formation

Based on the findings that (i) lipids infiltrate the films of agarose (Figure 2.4) during the coating procedure (Figure 2.2), (ii) agarose initially must be present as a film, and (iii) agarose molecules associate with lipid membranes after formation (Figure A.4 of Appendix A), we examined the possible benefits of agarose on each of the three

stages of formation that are outlined in Figure 2.1. Due to the limited understanding of the molecular mechanisms of the formation of giant liposomes,[23, 33, 38-40] we cannot provide a definitive explanation of the role of films of agarose in the formation of giant liposomes. The work presented here does, however, examine several possible roles of agarose in promoting the formation of these liposomes, and it provides evidence in support of these roles.

With regard to stage 1, i.e. the proposed pre-orientation of lipids and formation of lamellae,[1, 10, 11] we hypothesized that the porous film of agarose with its large surface area may promote the formation of lamellae. Previous work indicated that the formation of lamellae may be influenced by interactions of the lipids with the solid surface on which they are supported.[1, 60] For instance, Angelova and Dimitrov reported that the lipid layers closest to a surface are structured differently than lipid layers located further away from the surface.[1] In the case of the hybrid film of agarose and lipids, Figure 2.4 shows that lipids infiltrate the porous film of agarose. It is reasonable to assume that the resulting large contact area between agarose molecules and lipid molecules affects the formation of lipid lamellae, especially when considering that the agarose film contained residual water.[51, 54, 61],[62],[63] Although the method described in Figure 2.2 involved partially drying the film of agarose for 1-3 h (until the film no longer appeared wet), we found that the film of agarose still contained ~15 wt% of water and ~85% agarose (see Appendix A).

The residual water in the hybrid films of partially dried agarose and lipids may hence serve a similar function as the traditional pre-hydration step that is required by the protocols developed by Akashi *et al.*[8] and Yamashita *et al.*[10] Pre-hydration

purportedly affects the orientation of lipids and the formation of lipid lamellae.[8, 10, 11] The residual water content in the partially dried film of agarose could thus provide this function during the formation of the lipid film from chloroform solutions and thereby eliminate the need for a separate pre-hydration step. To test this hypothesis, we varied the residual water content in films of agarose and compared the extent of formation of giant liposomes from the resulting hybrid films of agarose and lipids. First, we prepared particularly dry agarose films (water content <1 wt%, agarose content >99%) by keeping the agarose films overnight in an oven above 100 °C. Second, we prepared agarose films in the usual way (Figure 2.2) of drying at 40 °C for approximately 2 h (water content ~15 wt%, agarose content ~85%). And third, we prepared films of agarose in the usual manner (Figure 2.2) and then provided a separate pre-hydration step by exposing the hybrid film of agarose and lipids to water vapor in an enclosed chamber for 30 min. This pre-hydration procedure resulted in a water content of ~15-20 wt%. We found that the extent of formation of giant liposomes was reduced when the film of agarose was dried overnight at a temperature above the boiling point of water compared to the standard procedure as described in Figure 2.2. The liposomes that we did observe were typically smaller than 5 µm. Interestingly, vapor-based pre-hydration of hybrid films of agarose and lipids that had been prepared in the usual manner (2 h drying at 40°C) did not yield an increase in formation of giant liposomes. These results suggest that films of agarose, when dried partially at 40°C for ~2 h, provided a similar effect as pre-hydration and that additional pre-hydration did not increase the benefit provided by the film of agarose alone.

With regard to stage 2, i.e. the growth of liposomes promoted by forces normal to the film of lipids,[3, 42] it is important to consider the hybrid nature of the films of partially dried agarose and lipids (Figure 2.2 and Figure 2.4). We hypothesize that, as soon as water enters this hybrid film, agarose molecules within the hybrid film of agarose and lipids dissolve and hence generate hyperosmotic conditions during the initial stages of liposome formation when only small amounts of water are present between the lipid lamellae. If this hypothesis is correct, then the resulting hyperosmotic conditions would lead to an influx of water[11, 64] and thus generate forces normal to the lipid lamellae in the hybrid film, and a film of a cross-linked hydrogel would provide a reduced benefit compared to a hydrogel that can dissolve into many individual molecules. We found that a chemically cross-linked polyacrylamide gel facilitated the formation of giant liposomes in solutions of physiologic ionic strength, but typically to a smaller extent than formation from ultra-low melting temperature agarose (see Appendix A, Figure A.6). In addition, the formation of giant liposomes worked best when the agarose films were formed with a type of agarose that dissolved in water and, hence, increased the number of agarose molecules in solution; this increased number of molecules affects colligative properties, such as osmotic pressure. For instance, agarose with ultra-low and, to a smaller extent, with low melting temperature generated the highest yield of giant liposomes in solutions of physiologic ionic strength, whereas dried films of standard or high melting temperature agarose did not provide a substantial benefit compared to formation from films of lipids supported on bare glass or ITO (see Appendix A, Figure A.6). We observed that ultra-low and low melting agarose dissolved partially during one hour of liposome formation, while films from standard and high melting temperature

agarose did not dissolve noticeably. Moreover, swelling of films from standard and high melting temperature agarose proceeded more evenly and slowly (over the course of 1 h) than swelling of films of ultra-low and low melting agarose types, which occurred within the first seconds of formation.

One additional effect that could promote stage 2 of liposome formation is that the presence of partially hydrophilic agarose molecules in this heterogeneous film of agarose and lipids might promote the influx of water into the lipid film.[11, 64] Such facilitated hydration may further promote the separation of lipid bilayers in the nascent liposomes and generate forces normal to the lipid bilayers. To test this hypothesis, we immersed glass slides containing a film of agarose in PBS for 30 s. Films of ultra-low melting and of low melting agarose appeared to hydrate completely during this short immersion in PBS; these hydrated, swollen, and partially dissolved films could be displaced from the surface of the glass by a stream of pressurized air. In contrast, films of standard and high melting temperature agarose did not swell noticeably during the 30 s immersion in PBS (or even after 2 min of hydration) and remained as thin films that adhered firmly to the surface of the glass. These films did not dissolve noticeably, but did swell into a firm gel, within 1 h.

Phase contrast microscopy observations during the early stages of liposome formation provided additional evidence for swelling of films of agarose after immersing the slides in aqueous solution. Specifically, this swelling increased the thickness of the film and hence moved the nascent layer of liposomes out of the focal plane of the microscope away from the surface of the glass. We followed the swelling by adjusting the focal plane of the microscope as the hybrid film of agarose and lipids moved away

from the surface of the glass slide. Given that the entire film swelled observably, agarose molecules must have undergone translational motion at a microscopic level. This conclusion agrees with findings by Fialkowski *et al.*, who related the influx of water to increased elastic energy in hydrogels.[64] Since the films were composed of both agarose and lipids, it follows that forces acting on the agarose film also acted directly or indirectly on lipids and on lipid lamellae in the film. In this sense, the swelling hydrogel film may provide benefits similar to the forces provided by alternating electric fields in electroformation.[42]

In order to investigate if applying alternating electric fields would provide an additional benefit, we formed giant liposomes in deionized water from hybrid films of agarose and lipids with and without an applied AC electric field as well as from ITO plates without agarose in the presence (electroformation) and absence (gentle hydration) of an electric field. We found that, in deionized water, the yield of giant liposomes from hybrid films of agarose and lipids was not affected by the presence of an applied AC electric field; it was similar to the yield from standard electroformation. In contrast, the yield of giant liposomes by gentle hydration from bare glass surfaces without electric fields was significantly lower (see Appendix A, Figure A.7) compared to formation from hybrid films of agarose and lipids. Importantly, standard electroformation did not generate giant liposomes in PBS whereas giant liposomes formed readily in PBS from hybrid films of agarose and lipids, and they did so with or without an electric field.

With regard to stage 3, the fusion of adjacent liposomes, time-lapse series of phase contrast micrographs revealed numerous fusion events of giant liposomes in

PBS solutions, in particular during the first minutes of formation (Figure 2.6). We did not detect such fusion events in control experiments with lipid films on bare glass, presumably due to the low density of liposomes that formed on bare glass in PBS. Films of agarose hence strongly promoted fusion of liposomes probably due to crowding and the associated mechanical stresses[46] of the large number of liposomes that grew outward from the porous agarose film into the solution above the hybrid films and possibly due to mechanical stresses generated by the swelling hydrogel film.[41] One may ask if liposomes grown from hybrid films of agarose and lipid formulations that contained negatively charged lipids or PEGylated lipids (Figure 2.3C,E,G,M,O,Q,S) also fused during the formation process. In this context, it is instructive that in other methods of formation, such as electroformation or freeze-and-thaw, fusion of adjacent liposome membranes is also a key characteristic in formation of giant liposomes,[3, 12, 13] and these methods also yield giant liposomes from lipid compositions that include PEGylated lipids[65] or anionic lipids.[66] Therefore, the repulsive forces generated by these specialized lipid formulations, which are often used to promote initial bilayer orientation and separation, can be overcome by appropriate mechanical stresses,[67, 68] such as those generated by an electric field, osmotic pressure during freeze-and-thaw cycles, or as proposed here, by a swelling hydrogel film. Figure 2.6 also illustrates that films of agarose promoted rapid formation of giant liposomes in PBS: typically, giant liposomes formed within 5 min upon addition of aqueous solutions to hybrid films of agarose and lipids.

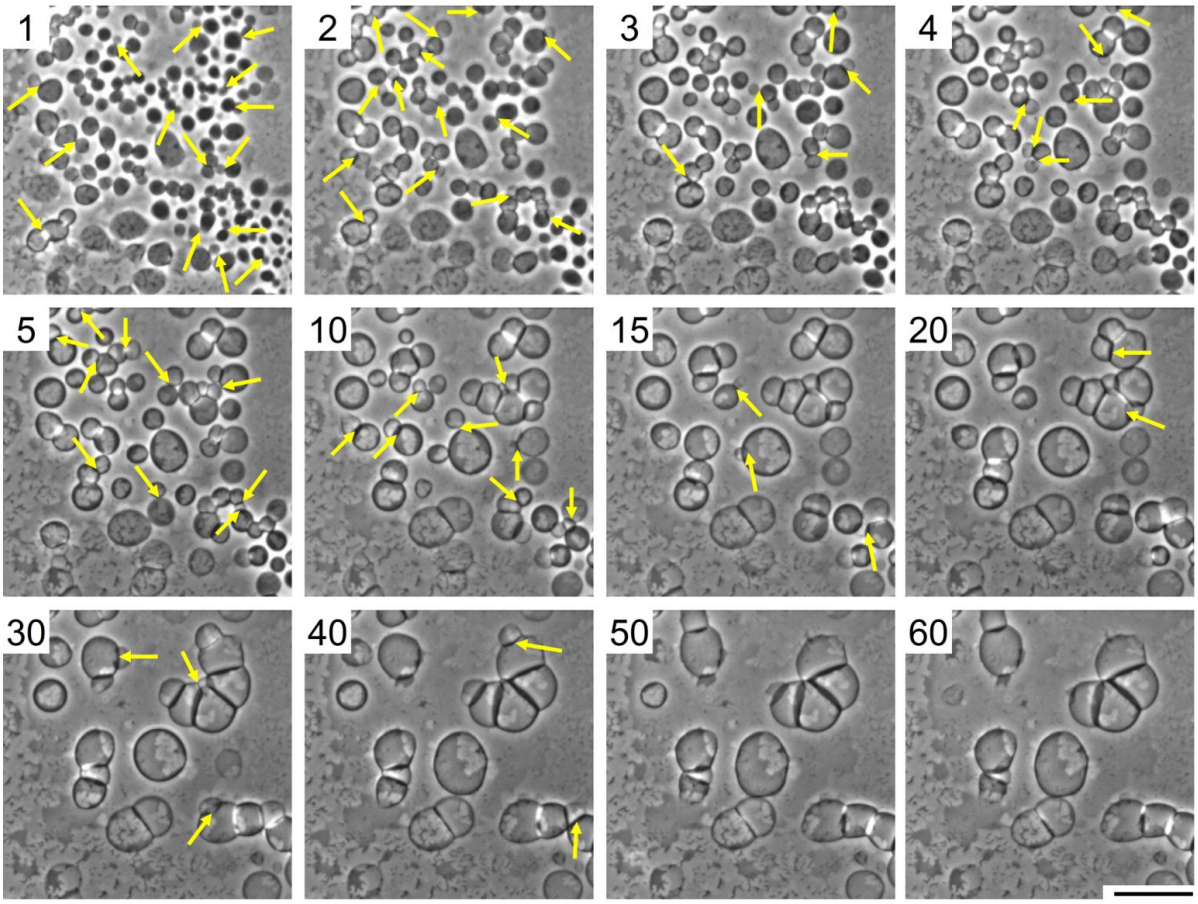

Figure 2.6. Time-lapse series of phase contrast micrographs during the formation of giant liposomes in PBS from a hybrid film of ultra-low melting temperature agarose (Type IX-A) and pure POPC lipids. Image capture began within seconds after adding PBS to the formation chamber and the micrographs depict the same location on the glass slide throughout the entire time series. Yellow arrows indicate fusion events that occurred before the next time point of image capture. Numbers in the upper left corner of each frame indicate elapsed time in minutes from the start of the time series. Scale bar = 100 µm.

2.2.4 Lamellarity of giant liposomes formed from films of agarose and lipids

One important aspect of the method presented here is the lamellarity of the resulting giant liposomes in solutions of physiologic ionic strength.[(69),(70),(71)] In order to address this question, we analyzed the fluorescence intensity of the membranes using a confocal microscope.[(8, 10)] We formed liposomes composed of POPC doped with 1%

1,2-dipalmitoyl-*sn*-glycero-3-phosphoethanolamine-N-(lissamine rhodamine B sulfonyl) (ammonium salt) (referred to as DPPE-rhodamine) and liposomes composed of POPC with 5% PEG-PE and 1% DPPE-rhodamine in PBS from films of ultra-low melting temperature agarose. We measured the fluorescence intensity at multiple locations on the membranes of free-floating giant liposomes procured from these preparations and determined the size and average intensity of each liposome (Figure 2.7).

Akashi *et al.* showed previously that the fluorescence intensity of unilamellar liposomes varied with the size of the liposomes. In order to account for this effect, we constructed histograms of fluorescence intensity and carried out a best curve fit with a lognormal function. We conducted this analysis first on liposomes that contained 5% PEGylated lipids. Liposomes with such a high content in PEGylated lipids have been reported to be predominantly unilamellar, even in the presence of ionic solutions.[(10, 44)]

Figure 2.7 shows that almost all giant liposomes with 5% PEGylated lipids had fluorescence intensities between 300 and 750 arbitrary units and that a lognormal curve with a single maximum at ~577 arbitrary units fit the data very well. Figure 2.7 also shows that the same analysis on POPC liposomes (without PEGylated lipids) that were formed from agarose films in PBS solution also yielded a peak with a maximum intensity at ~577 arbitrary units. This result suggests that a significant fraction of free-floating giant liposomes was unilamellar when these liposomes were formed from agarose in PBS, even in the absence of PEGylated lipids. Figure 2.7 also shows, however, two additional small peaks of fluorescence intensity that appeared in the histograms of POPC liposomes at ~1,000 arbitrary units and at ~1,500 arbitrary units (dashed red line). These intensities suggest the presence of two and three bilayers in the

liposomes, respectively. Moreover, this preparation also contained liposomes with fluorescence intensities that indicate a larger number of bilayers than three. Formation of giant liposomes from hybrid films of agarose and lipids hence appeared to generate both unilamellar and multilamellar liposomes in PBS solutions.

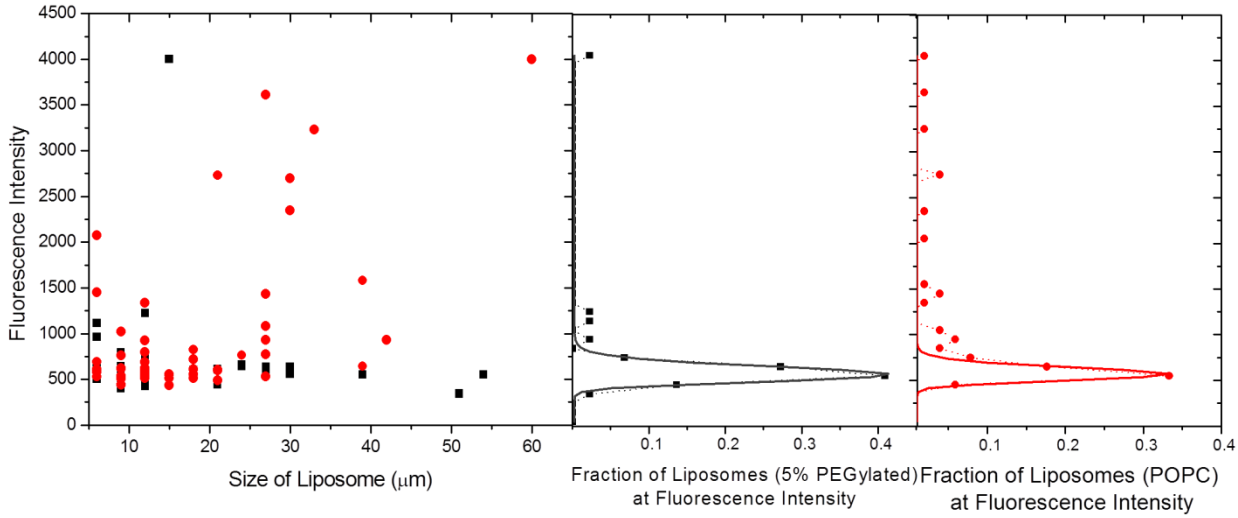

Figure 2.7. Average fluorescence intensity of giant liposomes as a function of liposome diameter and corresponding Gaussian fits to the distribution in fluorescence intensity. The panel on the left displays the average fluorescence intensities of free-floating liposomes formed for three hours in PBS from hybrid films of ultra-low melting temperature agarose and lipids. Black squares represent giant liposomes composed of POPC with 5 mol% PEGylated lipids and 1% DPPE-rhodamine; red circles represent giant liposomes composed of POPC with 1% DPPE-rhodamine. Each symbol in the left panel corresponds to one liposome (total count = 95; 51 were composed of POPC and 44 contained PEGylated lipids). The center panel shows the distribution of the average fluorescence intensities of giant liposomes composed of POPC with 5 mol% PEGylated lipids and 1% DPPE-rhodamine (indicated by the black squares connected with a dashed black line) and the fit of a lognormal function to the main peak of intensities (solid gray line). The panel on the right shows the distribution of the average fluorescence intensities of giant liposomes composed of POPC with 1% DPPE-rhodamine (indicated by the red circles connected with a dashed red line) and the fit of a lognormal function to the main peak of intensities (solid red line). Note, the camera saturated at fluorescence intensities above 4,000.

2.2.5 Encapsulation of water-soluble macromolecules into giant liposomes

One possible application of giant liposomes in physiologic buffer is to carry out reactions inside these liposomes. To this end, it would be useful to encapsulate molecules inside the liposomes. We tested this possibility by forming giant liposomes from hybrid films of agarose and lipids in a flow chamber[22] in a solution that contained 0.1 mM Tris (pH 7.4) with 0.5 μM dextran (MW 70,000) labeled covalently with fluorescein isothiocyanate (FITC). After 3 h of formation, we replaced the fluid in the chamber with a 0.1 mM Tris solution (pH 7.4) that did not contain FITC-conjugated dextran. We found that giant liposomes, when formed from hybrid films of agarose and lipids, did encapsulate FITC-conjugated dextran but at a lower concentration inside the liposomes than was present in the surrounding solution (see Appendix A, Figure A.8). In addition, a fraction of the encapsulated dextran remained in giant liposomes after the solution was exchanged. These results demonstrated that this method of forming giant liposomes from films of agarose may be useful for encapsulating large water-soluble molecules within giant liposomes, thus opening up the possibility to use them as microreactors.

2.3 Conclusion

Gentle hydration of hybrid films of partially dried agarose and lipids provides a straight-forward, rapid, and reproducible procedure to generate giant liposomes in high yield in solutions of physiologic ionic strength. This method does not require any specialized equipment and makes it possible to generate giant liposomes in PBS from a variety of lipids, including lipid compositions that typically pose problems for formation of

giant liposomes, such as pure phosphatidylserine, pure phosphatidylglycerol, or asolectin. During the formation process, agarose molecules associate with the lipid membranes of the resulting liposomes while the lipids in the liposomes maintain fluidity. This interaction of macromolecular carbohydrate molecules with liposome membranes may have a similar beneficial effect as PEGylated lipids for the formation of giant liposomes in solutions with physiologic ionic strength. Analysis of free-floating giant liposomes prepared from hybrid films of partially dried agarose and lipids revealed that this method appeared to generate both unilamellar and multilamellar giant liposomes in PBS, even in the absence of PEGylated or charged lipids. The short time of formation, reliability, and high yield of the simple method presented here is appealing for generating giant liposomes in physiologic solutions and provides the opportunity to extend studies with giant liposomes to physiologically relevant conditions. Moreover, the remarkably strong benefit of hybrid films of agarose and lipids with regard to the yield of giant liposomes in ionic solutions supports several proposed mechanisms of formation of these important models of cell membranes[1, 3, 10, 41, 42] and may thus contribute to the understanding of the formation of giant liposomes.

2.4 Experimental Section

2.4.1 Formation of a film of agarose on glass slides by dip-coating

We investigated the formation of giant liposomes on the following four types of agarose (all from Sigma-Aldrich, St. Louis, MO): Type IX-A ultra-low melting agarose (gel point, $T_g \leq 17^{\circ}C$; melting point, $T_m \leq 60^{\circ}C$; electroendosmosis, EEO ≤ 0.11), Type VII-A low melting agarose (T_g ~$26^{\circ}C$; $T_m \leq 65.5^{\circ}C$; EEO ≤ 0.12), Type II-A medium EEO

agarose (T_g ~36°C; T_m ~ 87°C; EEO = 0.16-0.19), and Type VI-A high melting agarose (T_g ~41°C; T_m ~95°C; EEO ≤ 0.14). For each type of agarose, we prepared a 1% (w/w) solution in deionized water. We boiled the suspension of agarose in water in a microwave oven, mixed the resulting solution, returned it to a boil, and mixed again to promote complete solubilization of the agarose powder. We poured the warm agarose solution into a Petri dish and allowed it to cool either at room temperature (22°C overnight) or in a refrigerator (4°C for 1-2 h) to form a gel. Immediately before dip-coating the glass slides, we heated the agarose gel in the Petri dish for 10-30 s in the microwave oven, just long enough to re-melt the gel into liquid form, and mixed the solution gently. We found that dip-coating slides after this re-melting procedure facilitated homogeneous surface coverage of the slides with the agarose solution.

To dip-coat the glass slides, we contacted only one side of each glass slide (75 x 50 x 1 mm, Corning Glass Works, Corning, NY) with the surface of the melted agarose solution. We held the coated slides vertically for a few seconds to remove excess solution and placed the slides with the agarose-coated side facing up on a temperature-controlled hotplate (Barnstead Intl, Dubuque, IA) at a temperature of 40°C. Sometimes the solution of agarose did not wet the glass surface evenly; in this case, we placed the slide onto the hotplate and used a micropipette to deposit ~300 µL of agarose solution onto the surface of the slide. Using the long edge of the pipette tip, we spread the solution of agarose over the surface of the slide by sweeping back and forth slowly until the solution of agarose remained spread over the surface. We left the agarose-coated slides on the hotplate until the water evaporated such that a clear, seemingly dry film of agarose formed. This process of drying occurred typically within 1-3 h. In the case of

agarose with ultra-low and low melting temperatures, the solution did not form a gel state before drying into a film, whereas standard and high melting temperature agarose types gelled before drying into a thin film. The resulting films of agarose adhered firmly to the surface of the slides. These agarose films had a thickness of ~2 μm, as measured by scanning electron microscopy (SEM) of the cross-sections of these films.

2.4.2 Formation of a film of polyacrylamide on glass slides

For comparison with agarose films, we formed films of polyacrylamide gel by mixing 10 mL of a 10% (w/v) solution of 37.5:1 acrylamide:N,N'-methylene-bis-acrylamide (Bio-Rad Laboratories, Inc., Hercules, CA) with 10 μL of ammonium persulfate (APS) (Bio-Rad Laboratories, Inc.) and 1 μL of tetramethylethylene-diamine (TEMED) (Bio-Rad Laboratories, Inc). Immediately after depositing the solution onto a glass slide, we placed a second slide on top of the solution and allowed the solution to gel for ~20 min. We removed one of the glass slides and placed the gel (supported on the other glass slide) in deionized water while stirring for ~4 h to remove non-polymerized acrylamide monomers. (Note, acrylamide monomers are toxic). After this rinsing process, we placed the glass-supported gel on a hot plate at 40°C for 1-3 h to dry the surface of the gel. Note, we dried the polyacrylamide gel only partially in order to prevent the film from detaching from the surface of the glass.

2.4.3 Formation of films of lipids on films of agarose or on polyacrylamide

To generate a film of lipids on and inside the films of agarose or polyacrylamide, we spread solutions with a concentration of 3.75 mg mL^{-1} lipids (all lipids were purchased from Avanti Polar Lipids, Inc., Alabaster, AL; except soybean asolectin, which we obtained from Sigma-Aldrich, St. Louis, MO) dissolved in either pure chloroform ($CHCl_3$)

(EMD Chemicals, Inc., Gibbstown, NJ) or in 90% $CHCl_3$ and 10% (v/v) methanol (MeOH) (EMD Chemicals, Inc.). Figure 2.8 illustrates the procedure. (Note, chloroform vapors are toxic; this step must be performed in a chemical flow hood). We used the following ten lipid compositions to form lipid films (all in mol%): 1) pure 1-palmitoyl-2-oleoyl-sn-glycero-3-phosphatidylcholine (POPC); 2) pure 1,2-dioleoyl-sn-glycero-3-[phospho-L-serine](sodium salt) (DOPS); 3) pure 1-palmitoyl-2oleoyl-sn-glycero-3-[phosphor-rac-(1-glycerol)] (POPG); 4) asolectin from soybean; 5) 90% POPC with 10% cholesterol; 6) 80% POPC with 20% cholesterol; 7) 90% POPC with 10% POPG; 8) 50% POPC with 50% POPG; 9) 90% POPC with 10% DOPS; and 10) 95% POPC with 5% 1,2-dipalmitoyl-sn-glycero-3-phosphatidylethanolamine-N-[methoxy (polyethylene glycol)-2000] (PEG-PE, also referred to as PEGylated lipids). For viewing liposomes or lipid films in epifluorescence mode, we doped the lipid solution with 0.5 mol% or 1 mol% 1,2-dipalmitoyl-sn-glycero-3-phosphoethanolamine-N-(lissamine rhodamine B sulfonyl) (ammonium salt) (DPPE-rhodamine). For fluorescence recovery after photobleaching experiments, we used 97% POPC with 3% 1,2-dimyristoyl-*sn*-glycero-3-phosphoethanolamine-N-(7-nitro-2-1,3-benzoxadiazol-4-yl)(ammonium salt) (DMPE-NBD).

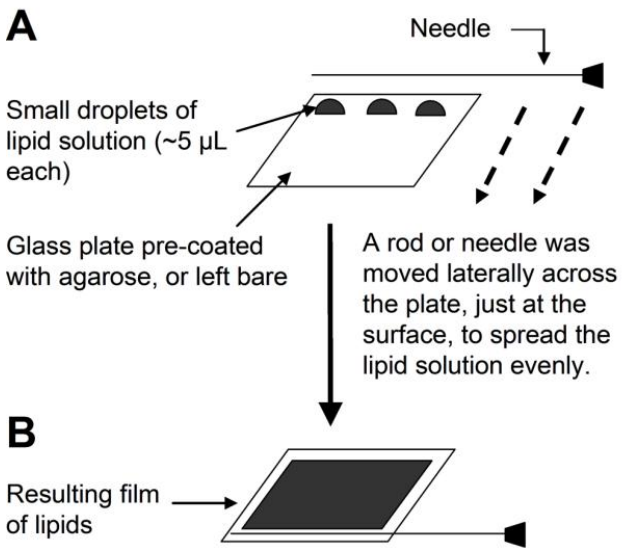

Figure 2.8. Formation of a film of lipids on glass slides that were pre-coated with a film of agarose (or on bare glass without a film of agarose for control experiments). A) Two to three droplets of lipid solution (~5 µL each) were deposited close to one edge of the slide. B) Lateral movement of a rod or needle across the slide, just at the surface, was used to spread the lipid solution into an even film. Steps A and B were repeated to deposit a total volume of 30 µL of lipid solution.

We deposited a total of 30 µL of lipid solution onto each glass slide using the two steps illustrated in Figure 2.8. We placed the lipid-coated plates under vacuum (approx. -730 mmHg) for at least 20 min to remove residual $CHCl_3$ and MeOH. Although the lipid solution was coated over the film of agarose, lipids penetrated through the agarose film and resulted in a hybrid film of lipids and agarose (see Figure 2.4).

2.4.4 Formation of a thick film of agarose

To prepare a glass slide with a particularly thick (~16 µm) film of agarose, we repeated the dip-coating procedure described in Figure 2.2A ten times. We then deposited a single lipid film of POPC lipids doped with 0.5 mol% DPPE-rhodamine using the procedure described in Figure A.9 of Appendix A.

2.4.5 Formation of giant liposomes on glass slides

After removing the solvent from the lipid solution under vacuum, we initiated the formation of giant liposomes by placing the agarose- and lipid-coated slides in a clean Petri dish (140 x 20 mm Nunc Petri dish, Fisher Scientific, Rochester, NY) with the coated side facing upward. We slowly added aqueous solution to the dish until the solution covered the slide completely. We pre-warmed the aqueous solution either to room temperature or to 37°C in a water bath prior to adding it to the dish. The dish remained undisturbed on a leveled surface at room temperature for a period of one to three hours to form giant liposomes at the surface of the agarose. We formed giant liposomes in the following three aqueous solutions: deionized water, 150 mM potassium chloride (KCl) (EMD Chemicals, Inc., Gibbstown, NJ), and Dulbecco's phosphate buffered saline (PBS) without Ca^{2+} or Mg^{2+} (JRH Biosciences, Inc., Lenexa, KS).

2.4.6 Observation of liposomes

We observed liposomes using an inverted microscope (Nikon Eclipse TE2000-U) in phase-contrast mode with a 10× objective (Nikon, NA=0.25). We captured images of liposomes using a charge-coupled device (CCD) camera (Photometrics CoolSnap HQ camera, Roper Scientific, Trenton, NJ) and used calibrated imaging analysis software (Metamorph 7.0, Universal Imaging Corporation, Downington, PA) to determine their diameters. To observe the growth and fusion of giant liposomes on films of agarose, we recorded time-lapse series of images during the formation of giant liposomes composed of pure POPC on films of ultra-low melting agarose in PBS for one hour. We began capturing images within seconds after adding PBS to the formation chamber and recorded images from the same spot for the entire hour. Due to the swelling of the film

of agarose, we adjusted the focal plane during the time-series to keep the top surface of the swelling agarose film in focus in order to observe the formation of liposomes.

For confocal imaging, we used a 20× objective (Nikon, NA = 0.75) on an inverted microscope (Nikon Eclipse TE2000-U) equipped with an argon laser (Spectra-physics, wavelength = 488 nm), a helium-neon laser (Melles-Griot, wavelength = 543 nm), and appropriate filter settings for fluorescein, rhodamine, or NBD. We used EZ-C1 software (Nikon, version 3.5) to capture images and analyze data.

2.4.7 Characterization of films of agarose by scanning electron microscopy

In order to carry out imaging with a high resolution scanning electron microscope (HRSEM) (NOVA 200 Nanolab, FEI Company, Hillsboro, OR), we used glass plates coated with a thin film of indium tin oxide[72] (ITO) (Delta Technologies, Stillwater, MN) and agarose-coated ITO plates and coated them with a sputter coater (Hummer VI, Anatech, Hayward, CA) in gold-palladium (Au:Pd ratio of 60:40, thickness ~6 nm). To measure the thickness of the ultra-low melting agarose films, we peeled agarose films that were not coated with gold-palladium from the surface of the glass and examined the cross-sections of the films by HRSEM.

2.4.8 Characterization of films of agarose by atomic force microscopy

We scanned a randomly selected region (10 μm x 10 μm) of a film from each of the four types of agarose with a NanoScope IIa atomic force microscope (AFM) (Digital Instruments, Woodbury, NY) using a soft tip (UltraSharp Non-Contact Cantilever, MikroMasch, Madrid, Spain) with a resonance frequency of 371.014 kHz in tapping mode. We used image analysis software to flatten the topographic images to produce representations of contours of films of agarose.

2.4.9 Chemical modification of agarose to produce fluorescently-labeled agarose

In order to generate fluorescently-labeled agarose, we stirred 10 mL of a 2% solution of ultra-low melting temperature agarose at ~50°C and gradually added 200 µL of a fresh solution of fluorescein isothiocyanate (FITC) (Fisher Scientific, Rochester, NY) dissolved in anhydrous dimethylsulfoxide (DMSO) (99.9% pure, Alfa Aesar, Ward Hill, MA) with a concentration of 100 mg mL^{-1}. After mixing the FITC and agarose for 3 h, we dialyzed the solution in deionized water using a Slide-A-Lyzer 10K dialysis cassette (10,000 molecular weight cut off, Pierce, Rockford, IL) for 3 days while changing the water twice daily. We dip-coated glass slides with films of agarose from a solution that contained 0.9% (w/w) ultra-low melting temperature agarose and 0.1% FITC-labeled ultra-low melting temperature agarose.

2.5 Acknowledgements

This material is based upon work supported by the National Science Foundation (MM, CAREER award, grant No. 0449088), the National Institute of Health, NIH, (MM, Grant No. 1RO1GM081705), a Rackham Engineering Award fellowship (KSH), and a Microfluidics in Biomedical Sciences Training Program (KSH, Grant No. T32EB005582 from the National Institute of Biomedical Imaging and Bioengineering at NIH). We thank Sheereen Majd and Ming Yong for valuable discussion and advice, Dr. Jeffrey Uram for assistance with SEM, Ashish Agarwal for assistance with AFM, Chloe Funkhouser for assistance with confocal imaging, and Dr. Douglas Weibel for the protocol to label agarose with FITC.

References

1. Angelova, M. I., and Dimitrov, D. S. (1986) Liposome Electroformation, *Faraday Discussions 81*, 303-311.

2. Kuribayashi, K., Tresset, G., Coquet, P., Fujita, H., and Takeuchi, S. (2006) Electroformation of giant liposomes in microfluidic channels, *Meas. Sci. Technol. 17*, 3121-3126.

3. Menger, F. M., and Angelova, M. I. (1998) Giant vesicles: Imitating the cytological processes of cell membranes, *Accounts of Chemical Research 31*, 789-797.

4. Seredyuk, V. A., and Menger, F. M. (2004) Membrane-Bound Protein in Giant Vesicles: Induced Contraction and Growth, *Journal of the American Chemical Society 126*, 12256-12257.

5. Dimova, R., Aranda, S., Bezlyepkina, N., Nikolov, V., Riske, K. A., and Lipowsky, R. (2006) A practical guide to giant vesicles. Probing the membrane nanoregime via optical microscopy, *Journal of Physics: Condensed Matter 18*, S1151-S1176.

6. Luisi, P. L., and Walde, P., (Eds.) (2000) *Perspectives in Supramolecular Chemisty: Giant Vesicles*, Vol. 6, John Wiley & Sons, New York.

7. Hotani, H., Nomura, F., and Suzuki, Y. (1999) Giant liposomes: from membrane dynamics to cell morphogenesis, *Current Opinion in Colloid & Interface Science 4*, 358-368.

8. Akashi, K., Miyata, H., Itoh, H., and Kinosita, K. (1996) Preparation of giant liposomes in physiological conditions and their characterization under an optical microscope, *Biophysical Journal 71*, 3242-3250.

9. D'Onofrio, T. G., Hatzor, A., Counterman, A. E., Heetderks, J. J., Sandel, M. J., and Weiss, P. S. (2003) Controlling and measuring the interdependence of local properties in biomembranes, *Langmuir 19*, 1618-1623.

10. Yamashita, Y., Oka, M., Tanaka, T., and Yamazaki, M. (2002) A new method for the preparation of giant liposomes in high salt concentrations and growth of protein microcrystals in them, *Biochimica Et Biophysica Acta-Biomembranes 1561*, 129-134.

11. Reeves, J. P., and Dowben, R. M. (1969) Formation and Properties of Thin-Walled Phospholipid Vesicles, *Journal of Cellular Physiology 73*, 49-60.

12. Castile, J. D., and Taylor, K. M. G. (1999) Factors affecting the size distribution of liposomes produced by freeze-thaw extrusion, *International Journal of Pharmaceutics 188*, 87-95.

13. Oku, N., and Macdonald, R. C. (1983) Differential-Effects of Alkali-Metal Chlorides on Formation of Giant Liposomes by Freezing and Thawing and Dialysis, *Biochemistry 22*, 855-863.

14. Menger, F. M., and Gabrielson, K. D. (1995) Cytomimetic Organic-Chemistry - Early Developments, *Angewandte Chemie-International Edition in English 34*, 2091-2106.

15. Kim, S., and Martin, G. M. (1981) Preparation of Cell-Size Unilamellar Liposomes with High Captured Volume and Defined Size Distribution, *Biochimica Et Biophysica Acta 646*, 1-9.

16. Moscho, A., Orwar, O., Chiu, D. T., Modi, B. P., and Zare, R. N. (1996) Rapid preparation of giant unilamellar vesicles, *Proceedings of the National Academy of Sciences of the United States of America 93*, 11443-11447.

17. Pautot, S., Frisken, B. J., and Weitz, D. A. (2003) Production of unilamellar vesicles using an inverted emulsion, *Langmuir 19*, 2870-2879.

18. Peterlin, P., and Arrigler, V. (2008) Electroformation in a flow chamber with solution exchange as a means of preparation of flaccid giant vesicles, *Colloids and Surfaces B-Biointerfaces 64*, 77-87.

19. Estes, D. J., and Mayer, M. (2005) Electroformation of giant liposomes from spin-coated films of lipids, *Colloids and Surfaces B-Biointerfaces 42*, 115-123.

20. Menger, F. M., and Seredyuk, V. A. (2003) Internally Catalyzed Separation of Adhered Lipid Membranes, *Journal of the American Chemical Society 125*, 11800-11801.

21. Menger, F. M., Seredyuk, V. A., Kitaeva, M. V., Yaroslavov, A. A., and Melik-Nubarov, N. S. (2003) Migration of Poly-L-lysine through a Lipid Bilayer, *Journal of the American Chemical Society 125*, 2846-2847.

22. Estes, D. J., and Mayer, M. (2005) Giant liposomes in physiological buffer using electroformation in a flow chamber, *Biochimica Et Biophysica Acta-Biomembranes 1712*, 152-160.

23. Montes, L. R., Alonso, A., Goni, F. M., and Bagatolli, L. A. (2007) Giant Unilamellar Vesicles Electroformed from Native Membranes and Organic Lipid Mixtures under Physiological Conditions, *Biophys. J. 93*, 3548-3554.

24. Majd, S., Estes, D. J., and Mayer, M. (2006) Assays for Studying Annexin Binding to Artificial Bilayers, *Calcium Binding Proteins 1*, 26-29.

25. Poolman, B., Spitzer, J. J., and Wood, J. A. (2004) Bacterial osmosensing: roles of membrane structure and electrostatics in lipid-protein and protein-protein interactions, *Biochimica Et Biophysica Acta-Biomembranes 1666*, 88-104.

26. Ling, T., Majd, S., Mayer, M., and Guo, L. J. (2008) Detection and qunatification of lipid membrane binding on silica micro-tube resonator sensor, *Proceedings of SPIE - Single Molecule Spectroscopy and Imaging 6862*, 68620B68621-68620B68628.

27. Akashi, K., Miyata, H., Itoh, H., and Kinosita, K. (1998) Formation of giant liposomes promoted by divalent cations: Critical role of electrostatic repulsion, *Biophysical Journal 74*, 2973-2982.

28. Israelachvili, J. N., and McGuiggan, P. M. (1988) Forces between Surfaces in Liquids, *Science 241*, 795-800.

29. Majd, S., and Mayer, M. (2005) Hydrogel stamping of arrays of supported lipid bilayers with various lipid compositions for the screening of drug-membrane and protein-membrane interactions, *Angewandte Chemie-International Edition 44*, 6697-6700.

30. Longo, M. L., Waring, A. J., and Hammer, D. A. (1997) Interaction of the influenza hemagglutinin fusion peptide with lipid bilayers: Area expansion and permeation, *Biophys. J. 73*, 1430-1439.

31. Tresset, G., and Takeuchi, S. (2005) Utilization of cell-sized lipid containers for nanostructure and macromolecule handling in microfabricated devices, *Analytical Chemistry 77*, 2795-2801.

32. Sabin, J., Prieto, G., Ruso, J. M., Hidalgo-Alvarez, R., and Sarmiento, F. (2006) Size and stability of liposomes: A possible role of hydration and osmotic forces, *European Physical Journal E 20*, 401-408.

33. Mathivet, L., Cribier, S., and Devaux, P. F. (1996) Shape change and physical properties of giant phospholipid vesicles prepared in the presence of an AC electric field, *Biophysical Journal 70*, 1112-1121.

34. Winterhalter, M., and Helfrich, W. (1992) Bending Elasticity of Electrically Charged Bilayers - Coupled Monolayers, Neutral Surfaces, and Balancing Stresses, *Journal of Physical Chemistry 96*, 327-330.

35. Riquelme, G., Lopez, E., Garciasegura, L. M., Ferragut, J. A., and Gonzalezros, J. M. (1990) Giant Liposomes - a Model System in Which to Obtain Patch-Clamp Recordings of Ionic Channels, *Biochemistry 29*, 11215-11222.

36. Keller, B. U., Hedrich, R., Vaz, W. L., and Criado, M. (1988) Single channel recordings of reconstituted ion channel proteins: an improved technique, *Pflugers Arch 411*, 94-100.

37. Schmidt, C., Mayer, M., and Vogel, H. (2000) A chip-based biosensor for the functional analysis of single ion channels, *Angewandte Chemie International Edition 39*, 3137-3140.

38. Constantin, D., Ollinger, C., Vogel, M., and Salditt, T. (2005) Electric field unbinding of solid-supported lipid multilayers, *European Physical Journal E 18*, 273-278.

39. Fialkowski, M., Bishop, K. J. M., Klajn, R., Smoukov, S. K., Campbell, C. J., and Grzybowski, B. A. (2006) Principles and implementations of dissipative (dynamic) self-assembly, *Journal of Physical Chemistry B 110*, 2482-2496.

40. Leng, J., Egelhaaf, S. U., and Cates, M. E. (2002) Kinetic pathway of spontaneous vesicle formation, *Europhysics Letters 59*, 311-317.

41. Angelova, M., Soleau, S., Meleard, P., Faucon, J. F., and Bothorel, P. (1992) Preparation of giant vesicles by external a.c. electric fields. Kinetics and applications, *Progress in Colloid & Polymer Science 89*, 127-131.

42. Dimitrov, D. S., and Angelova, M. I. (1988) Lipid Swelling and Liposome Formation Mediated by Electric-Fields, *Bioelectrochemistry and Bioenergetics 19*, 323-336.

43. Lasic, D. D., and Needham, D. (1995) The "Stealth" liposome: A prototypical biomaterial, *Chem. Rev. 95*, 2601-2628.

44. Needham, D., McIntosh, T. J., and Lasic, D. D. (1992) Repulsive Interactions and Mechanical Stability of Polymer-Grafted Lipid-Membranes, *Biochim. Biophys. Acta 1108*, 40-48.

45. Estes, D. J., Lopez, S. R., Fuller, A. O., and Mayer, M. (2006) Triggering and visualizing the aggregation and fusion of lipid membranes in microfluidic chambers, *Biophys J 91*, 233-243.

46. Taylor, P., Xu, C., Fletcher, P. D. I., and Paunov, V. N. (2003) A novel technique for preparation of monodisperse giant liposomes, *Chem. Commun.*, 1732-1733.

47. This trial was prepared on ITO plates instead of glass slides.

48. Carrion, F. J., Delamaza, A., and Parra, J. L. (1994) The Influence of Ionic-Strength and Lipid Bilayer Charge on the Stability of Liposomes, *Journal of Colloid and Interface Science 164*, 78-87.

49. This low yield may be due, in part, because we formed these liposomes without a pre-hydration step.

50. To eliminate signal from the autofluorescence of agarose, we first viewed a film of agarose without lipids and adjusted the camera settings until we could no longer observe fluorescence from the agarose film. These settings were then used to view the agarose film with fluorescently-labeled lipids; its fluorescence was significantly stronger and easily detectable.

51. Arnott, S., Fulmer, A., Scott, W. E., Dea, I. C. M., Moorhouse, R., and Rees, D. A. (1974) Agarose Double Helix and Its Function in Agarose-Gel Structure, *Journal of Molecular Biology 90*, 269-272.

52. Foord, S. A., and Atkins, E. D. T. (1989) New X-Ray-Diffraction Results from Agarose - Extended Single Helix Structures and Implications for Gelation Mechanism, *Biopolymers 28*, 1345-1365.

53. Normand, V., Lootens, D. L., Amici, E., Plucknett, K. P., and Aymard, P. (2000) New insight into agarose gel mechanical properties, *Biomacromolecules 1*, 730-738.

54. Arndt, E. R., and Stevens, E. S. (1994) A Conformational Study of Agarose by Vacuum Uv Cd, *Biopolymers 34*, 1527-1534.

55. Fatin-Rouge, N., Wilkinson, K. J., and Buffle, J. (2006) Combining small angle neutron scattering (SANS) and fluorescence correlation spectroscopy (FCS) measurements to relate diffusion in agarose gels to structure, *Journal of Physical Chemistry B 110*, 20133-20142.

56. Schafer, S. E., and Stevens, E. S. (1995) A Reexamination of the Double-Helix Model for Agarose Gels Using Optical-Rotation, *Biopolymers 36*, 103-108.

57. Ratajska-Gadomska, B., and Gadomski, W. (2000) Critical exponents in a percolation picture of the fluorescence quenching during the sol-gel transition, *European Physical Journal B 17*, 281-288.

58. Colombo, V. E., and Spath, P. J. (1981) Structures of Various Types of Gels as Revealed by Scanning Electron-Microscopy (Sem), *Scanning Electron Microscopy*, 515-522.

59. Nipper, M. E., Majd, S., Mayer, M., Lee, J. C. M., Theodorakis, E. A., and Haidekker, M. A. (2008) Characterization of changes in the viscosity of lipid membranes with the molecular rotor FCVJ, *Biochim Biophys Acta 1778*, 1148-1153.

60. LeBerre, M., Yamada, A., Reck, L., Chen, Y., and Baigl, D. (2008) Electroformation of Giant Phospholipid Vesicles on a Silicon Substrate: Advantages of Controllable Surface Properties, *Langmuir 24*, 2643-2649.

61. Itagaki, H., Fukiishi, H., Imai, T., and Watase, M. (2005) Molecular structure of agarose chains in thermoreversible hydrogels revealed by means of a fluorescent probe technique, *Journal of Polymer Science, Part B: Polymer Physics 43*, 680-688.

62. Itagaki et al. provide additional evidence of water molecules co-crystallizing with agarose by use of a fluorescent probe (see Itagaki, H.; Fukiishi, H.; Imai, T.; Watase, M., J. Polym. Sci., Part B: Polym. Phys. 2005, 43, 680-688).

63. Arndt and Stevens discuss the presence of tightly bound water molecules within dried agarose gels as determined by vacuum UV CD (see Arndt, E.R.; Stevens, E.S., Biopolymers 1994, 34, 1527-1534).

64. Fialkowski, M., Campbell, C. J., Bensemann, I. T., and Grzybowski, B. A. (2004) Absorption of water by thin, ionic films of gelatin, *Langmuir 20*, 3513-3516.

65. Constantinescu, I., Levin, E., and Gyongyossy-Issa, M. (2003) Liposomes and blood cells: a flow cytometric study, *Artificial cells, blood substitutes, and immobilization biotechnology 31*, 395-424.

66. Claessens, M., Leermakers, F. A. M., Hoekstra, F. A., and Stuart, M. A. C. (2007) Opposing effects of cation binding and hydration on the bending rigidity of anionic lipid bilayers, *Journal of Physical Chemistry B 111*, 7127-7132.

67. Angelova, M. I., and Dimitrov, D. S. (1988) A mechanism of liposome formation, *Progress in Colloid and Polymer Science 76*, 59-67.

68. Cevc, G., and Richardsen, H. (1999) Lipid vesicles and membrane fusion, *Advanced Drug Delivery Reviews 38*, 207-232.

69. A definite analysis of lamellarity is typically obtained by micropipette aspiration to measure the bending modulus. See Akashi, K.; Miyata, H.; Itoh, H.; Kinosita, K. Biophys. J. 1996, 71, 3242-3250; Yamashita, Y.; Oka, M.; Tanaka, T.; Yamazaki, M. Biochim. Biophys. Acta 2002, 1561, 129-134; Angelova, M.; Soleau, S.; Meleard, P.; Faucon, J.F.; Bothorel, P. Prog. Colloid Polym. Sci. 1992, 89, 127-131; Needham, D.; McIntosh, T.J.; Lasic, D.D. Biochim.

Biophys. Acta 1992, 1108, 40-48; Bermudez, H.; Hammer, D.A.; Discher, D.E. Langmuir 2004, 20, 540-543.

70. Measuring the bending modulus by micropipet aspiration is difficult to perform and requires specialized equipment and expertise. See Hotani, H.; Nomura, F.; Suzuki, Y. Curr. Opin. Colloid Interface Sci. 1999, 4, 358-368; Akashi, K.; Miyata, H.; Itoh, H.; Kinosita, K. Biophys. J. 1996, 71, 3242-3250; Yamashita, Y.; Oka, M.; Tanaka, T.; Yamazaki, M. Biochim. Biophys. Acta 2002, 1561, 129-134; Bermudez, H.; Hammer, D.A.; Discher, D.E. Langmuir 2004, 20, 540-543; Farge, E.; Deveaux, P.F. Biophys. J. 1992, 61, 347-57.

71. The bending modulus can be affected by ions in the solution (see Dimova, R.; Aranda, S.; Bezlyepkina, N.; Nikolov, V.; Riske, K.A.; Lipowsky, R., J. Phys.: Condens. Matter 2006, 18, S1151-S1176) and by macromolecules associated with the membrane, such as PEG (see Yamashita, Y.; Oka, M.; Tanaka, T.; Yamazaki, M Biochim. Biophys. Acta 2002, 1561, 129-134; Bermudez, H.; Hammer, D.A.; Discher, D.E. Langmuir 2004, 20, 540-543) or possibly by agarose.

72. We conducted early experiments using a standard protocol of electroformation from agarose-coated ITO plates, but found later that the electric AC field added little or no benefit over simple hydration of the hybrid films of agarose and lipids (see Figure A.7 in Appendix A).

CHAPTER III

Functional Reconstitution of Human P-glycoprotein (ABCB1) in Giant Liposomes

Abstract

Giant proteoliposomes containing P-glycopotein (P-gp) were generated from a solution of small proteoliposomes by utilizing a film of agarose to facilitate formation. The inside-out orientation of reconstituted P-gp was confirmed with stimulation of ATP hydrolysis by the substrate, verapamil. To measure active transport of the fluorescent substrate rhodamine 123 by reconstituted P-gp, the fluorescence intensity inside giant proteoliposomes was analyzed. These experiments revealed the apparent membrane permeability (P_s) and a rate constant of active transport (k_T) for this substrate. The apparent P_s value of rhodamine 123 was larger in membranes containing P-gp under any condition than membranes that lacked P-gp and indicates that the presence of P-gp in the membrane increases its leakiness. The rate of active transport was significantly higher in the presence of ATP than without ATP or in the presence of the competitive inhibitor verapamil and verifies that P-gp was functionally active after reconstitution in

giant proteoliposomes. Lastly, patch clamp experiments on giant proteoliposomes showed detectable ion channel activity that was consistent with a co-purified chloride ion channel protein. Together, these results confirm that this reconstitution technique enables functional assays with transmembrane proteins, such as P-gp or ion channel proteins, and demonstrate the advantage of using giant proteoliposomes for characterization of transporter properties.

3.1 Introduction

Giant liposomes are useful models to study diffusion or transport of solutes across biological membranes because their interiors are isolated from the surrounding fluid by a self-enclosing membrane and can be observed individually by optical microscopy.[1-3] To study protein-mediated transport, functional transmembrane proteins must be incorporated into the membrane of giant liposomes that consist of a single lipid bilayer (giant unilamellar vesicle, GUV). Few methods exist for the production of such giant proteoliposomes with active ion channels or transporter proteins due to the sensitive and fragile nature of many transmembrane proteins and GUVs.[4, 5]

Many of the current methods of forming giant proteoliposomes are variations of the classic protocols of gentle hydration or electroformation, but with a carefully executed, gentle dehydration step to prevent denaturation of the proteins.[5-14] To this end, most methods involve reconstituting transmembrane proteins into small unilamellar vesicles (SUVs), and then partially drying the SUVs into a film under controlled conditions before finally rehydrating the film in an aqueous solution.[10-13] For example, during partial dehydration, the surfaces coated with proteoliposome solution can be

dried under a flow of inert gas or placed in a desiccator with low humidity (e.g., by the presence of a saturated salt solution or anhydrous calcium chloride crystals in a dessicator).[10-12] Carbohydrates or other hydrophilic molecules, such as ethylene glycol, may also be added to the solution of proteoliposomes before dehydration to protect the protein from denaturing.[11-14]

Other methods of forming giant proteoliposomes have been reported, but have limitations with regard to their final composition. For example, Yanagisawa *et al*. reported a water-in-oil droplet transfer technique of incorporating transmembrane proteins into giant proteoliposomes.[15] Many integral membrane proteins require undisrupted contact with lipids or detergent, however, so this method may not be suitable for all proteins.[4] Another method of forming giant proteoliposomes is based on fusion of small proteoliposomes with pre-formed GUVs[16] and was recently refined by pre-concentrating GUVs to increase the efficiency of proteoliposome-GUV fusion.[17] Fusing small proteoliposomes to GUVs often results in low protein-lipid ratio and frequently requires specific lipid compositions, fusion peptides, or other physical or chemical inducers to promote membrane fusion.[4, 5, 18]

Here, we present a novel approach for forming giant proteoliposomes and use it to incorporate the human multidrug resistance-linked ATP-binding cassette (ABC) transporter, ABCB1, commonly known as P-glycoprotein (P-gp). Previously, we described the use of a hybrid film of dried agarose and lipids to promote formation of GUVs in solutions of physiologic ionic strength.[19] We had demonstrated that the dried film of agarose retained a water content of ~15 wt% after drying on a hot plate at 40°C for >4 h. Therefore, we hypothesized that a dried film of agarose might be useful also

for reconstituting proteins into giant proteoliposomes because the inherent water retention may protect the proteins from denaturing during the dehydration step. To demonstrate the usefulness of this approach, we reconstituted purified P-gp and then assessed their orientation and functionality by measuring the rate of ATP hydrolysis, determining the transport rate by a fluorescence flux assay, and performing patch clamp experiments of a putative chloride channel that appeared to co-purify with P-gp.[20]

The ability to assay P-gp for drug screening and development is of interest due to the role of P-gp in the blood-brain barrier and in cancer cells.[21-24] P-gp is a transporter protein belonging to the ATP binding cassette (ABC) family of proteins with two ATP binding domains and 12 transmembrane α-helices.[21-25] P-gp uses ATP hydrolysis to mediate active efflux of a broad range of hydrophobic molecules, and thus its (over)expression plays a significant role in multi-drug resistance (MDR) by cancer cells.[21-25] Attempts to study P-gp thus far have been restricted primarily to cell-based assays, and so measured transport rates, with or without potential modulators, can be complicated by the presence of other transporter proteins and cellular constituents.[22, 24, 26] Liposome-based studies using purified P-gp have been conducted using primarily small proteoliposomes due, in part, to the difficulty of incorporating P-gp into giant proteoliposomes.[4, 27-29] Sasaki *et al*. recently described a transport assay using commercially available giant proteoliposomes containing reconstituted P-gp.[30] These proteoliposomes had diameters less than 3 μm and were immobilized in microfluidic channels for observation. The fluorescent substrate was restricted to sub-μM concentrations because the signal inside the liposomes would otherwise be affected by accumulation of fluorescent substrate on or in the membrane. The use of larger giant

proteoliposomes (>10 μm), as demonstrated here, could be useful because, in these large GUVs, the internal fluorescence measured near the center of the liposomes is located at a sufficient distance from the liposome membrane, thereby minimizing background signal from membrane-partitioned fluorescent substrate molecules.[2] Giant proteoliposomes with diameters >10 μm are also easy to distinguish individually to provide liposome-specific transport data.[2] Another advantage of giant proteoliposomes with large diameters is that they are well suited for patch clamp experiments. We explored this benefit by performing inside-out current recordings on the same preparation of giant liposomes with reconstituted P-gp as used for the transport assays with fluorescent substrates. To our surprise, we detected single ion channel activity that was consistent with a chloride channel with regard to the effect of specific chloride channel blockers and the single channel conductance. Previous reports have indicated an association between P-gp and a chloride channel protein.[26, 27, 31-34] Based on these results, we propose that reconstitution of purified P-gp into giant proteoliposomes that are greater than 10 μm in diameter provides a useful model system for studying the direct effects of potential inhibitors on the rate of transport by P-gp and potentially other transport or ion channel proteins. We expect these systems to aid in drug development and in studying potential interactions of transport proteins with ion channel proteins.

3.2 Results and Discussion

3.2.1 Formation of giant proteoliposomes from small proteoliposomes

We formed giant proteoliposomes that contained P-glycoprotein (P-gp) in the phospholipid membrane by first forming small proteoliposomes with P-gp, dehydrating the small proteoliposomes onto a dried film of ultra-low melting agarose, and then

rehydrating the film. Giant liposomes formed readily from small proteoliposomes that contained P-gp (Figure 3.1C) and also from small liposomes that did not contain proteins (Figure 3.1A) that were used for control experiments. Since the procedure of forming small proteoliposomes was previously demonstrated to reconstitute P-gp in the inside-out orientation,[27, 35] we hypothesized that at least a portion of the proteins would reconstitute into giant proteoliposomes in the same inside-out orientation such that the ATP-binding domain would remain accessible on the exterior of the liposome. Since ATP hydrolysis enables active transport by P-gp, the inside-out orientation results in transport into the liposome instead of efflux (as naturally occurs in cells).

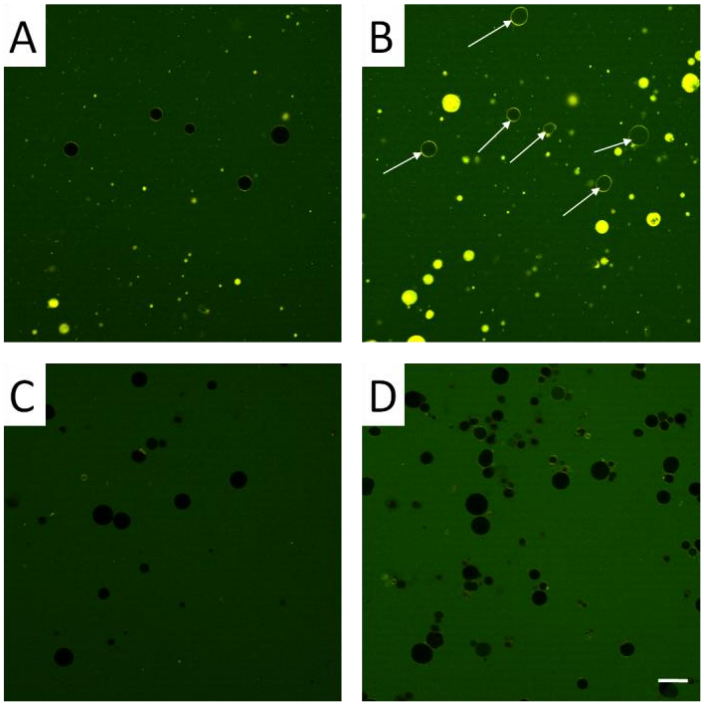

Figure 3.1. Confocal images of giant liposomes with or without reconstituted P-glycoprotein (P-gp) in a solution containing 1 μM of the fluorescent substrate rhodamine 123 (Rho123). A) Giant proteoliposomes formed with P-gp, 2 min after immersion in Rho123 solution. B) Giant proteoliposomes formed with P-gp, 30 min after immersion in Rho123 solution. White arrows indicate proteoliposomes with interiors that exhibited a change in fluorescence intensity over time and were included in the data analysis to obtain apparent permeabilities and transport rates. C) Control experiment with giant

liposomes that did not contain P- gp, 2 min after immersion in Rho123 solution. D) Giant liposomes that did not contain P-gp, 30 min after immersion in Rho123 solution. Scale bar = 50 μm.

Giant liposomes that formed from hybrid films of ultra-low melting agarose and small liposomes with P-gp showed elevated levels of ATPase activity following stimulation with the well-known P-gp substrate verapamil (see Appendix B, Table B.1) compared to levels of ATPase activity before adding verapamil. This substrate-induced ATP hydrolysis suggested that a fraction of P-gp was measurably active with the ATP-binding domain accessible to the external solution after the process of reconstitution via dried films of ultra-low melting agarose.[23, 35, 36]

We observed a notable change in fluorescence intensity inside giant proteoliposomes that were formed with P-gp 30 min after their immersion in a solution containing a fluorescent substrate of P-gp, rhodamine 123 (Rho123),[22, 23, 30, 37, 38] but did not observe a similar change after immersion in Rho123 solution for GUVs that lacked P-gp. This difference indicated that P-gp was indeed present at or in the membranes of giant liposomes following the reconstitution process and thus affected the flux of Rho123 across the membrane of liposomes.

To test for active transport of a P-gp substrate into giant proteoliposomes, we collected time-lapse series of images following immersion of giant proteoliposomes in a solution containing Rho123. We noted a frequent occurrence of brightly fluorescent rings in confocal images of the membranes of giant liposomes containing P-gp (as compared to the background or to the fluorescence of the liposome interior). In contrast, giant liposomes that were generated without P-gp rarely showed these bright fluorescent membranes (see Figure 3.1). This difference indicated that Rho123

associated preferentially with P-gp, while interacting to a smaller extent with the phospholipid membrane itself. We observed this interaction of Rho123 with P-gp-containing membranes in both the presence and absence of ATP or verapamil (see Appendix B, Figure B.1). These results indicate that ATP was not required for Rho123 to associate with P-gp and that the presence of verapamil, a known competitive inhibitor of P-gp-mediated transport of Rho123,[22, 23, 35, 39] was not able to out-compete this association completely. This incomplete inhibition could be due possibly to a lower concentration of verapamil in the membranes of giant proteoliposomes along with increased lipid membrane area compared to the membranes of small proteoliposomes.

To quantify transport, we monitored the fluorescence intensity inside and outside the giant liposomes over time. The fluorescence intensity started low and increased significantly in some of the giant proteoliposomes that were formed with P-gp (Figure 3.1B), whereas the fluorescence intensity remained low in nearly all GUVs that lacked P-gp (Figure 3.1D). When the fluorescence intensity of the interior started low, we surmised the giant liposome was filled initially with the fluid used to reconstitute the liposome and, therefore, any measurable change in fluorescence intensity would be due to active transport and/or passive diffusion of Rho123 from the external solution, across the membrane, and into the internal solution. In images of giant proteoliposomes that were formed with reconstituted P-gp, we also observed the occurrence of liposomes that were filled with bright fluorescence shortly after immersion in Rho123 solution and did not change in fluorescence intensity over time (see Figure 3.1 and Appendix B, Figure B.2). These liposomes were present in images of giant proteoliposomes when active transport was enabled (e.g., with ATP) as well as impeded (e.g., without ATP or

in the presence of an inhibitor). These brightly fluorescent liposomes even occurred occasionally in giant liposomes that did not contain reconstituted P-gp (see Appendix B, Figure B.2A). We attributed these bright spots to giant liposomes that were filled with smaller liposomes. In fact, most of these liposomes showed inhomogeneous low fluorescence indicating the presence of other liposomes inside of them (e.g., Figure 3.1B). We surmised that the change in fluorescence intensity inside these giant liposomes was caused by the close proximity of adjacent membranes, leading to possible membrane-to-membrane transfer of Rho123 and subsequent additive increase of the fluorescence intensity inside these giant liposomes.[30] These brightly fluorescent liposomes were excluded from the data analysis.

3.2.2 Assessment of protein function using a transport assay

To determine if the reconstituted P-gp proteins were functional, we analyzed the rate of change in fluorescence intensity inside the liposomes with respect to the background fluorescence in each image and compared the rate of change under four different assay conditions: 1) with P-gp and 1 mM ATP, 2) with P-gp but without ATP, 3) with P-gp and 1 mM ATP and 30 μM verapamil to inhibit the transport of Rho123 by P-gp, and 4) without P-gp.

The change in the concentration of Rho123 inside a liposome is due to the molecules of Rho123 crossing the membrane of the liposome. Molecules can cross a membrane via passive diffusion from the solution of high concentration to the solution of low concentration in a manner dependent on the area of membrane and a rate constant of diffusion, P_s. Alternatively, molecules can cross the membrane via active transport in the presence of active transporter proteins that depends on the number of P-gp (given by the surface density of P-p times the area of membrane), the concentration of ATP

and a rate constant of transport. In our analysis, we combined the concentration of ATP and the rate constant of transport into one variable, k_T. Figure 3.2 depicts schematically the role of passive diffusion and active transport on the change in the concentration of Rho123 inside a liposome.

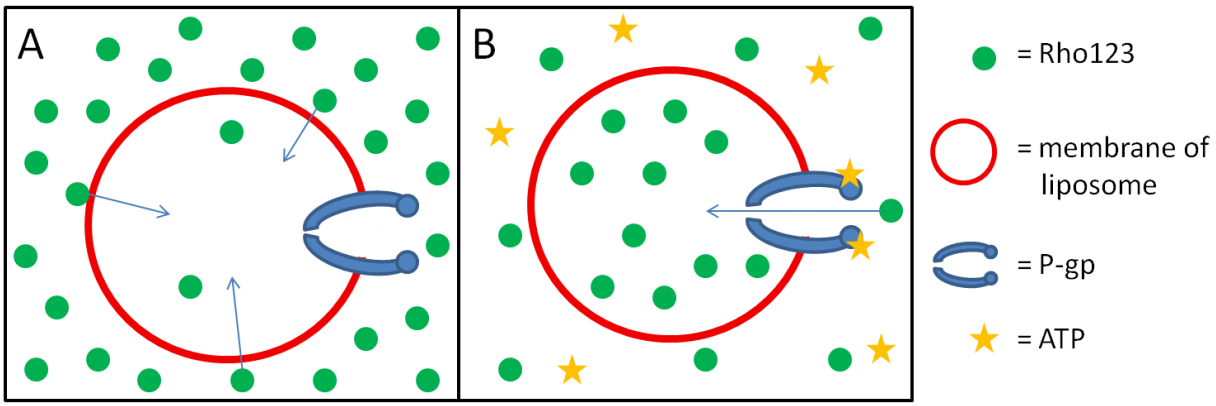

Figure 3.2. Schematic depiction of passive diffusion and active transport of rhodamine 123 (Rho123) across the membrane of a liposome. A) Passive diffusion is the net movement of molecules from high concentration to lower concentration. Accumulation inside a spherical liposome depends on the concentration difference across the membrane, the area of membrane that separates the two solutions, and a permeability rate constant. B) Active transport of Rho123 requires the presence of functional transporter protein and ATP. Since ATP was only added to the external solution, active transport yielded a net flux from outside to inside the liposome, independent of the concentration inside the liposome. Therefore, the rate of active transport depends on the number of transporter proteins, the concentration of ATP, and a rate constant of transport.

The change in the concentration of Rho123 in giant liposomes, as demonstrated in this work, is given by Equation 3.1,[2, 40, 41] where V is the volume $[m^3]$, C is the concentration [µM], P_s is the apparent membrane permeability $\left[\frac{m}{s}\right]$; A is the surface area $[m^2]$; $(C_{out} - C_{in})$ is the difference in concentration of solute across the membrane (from

external solution to the interior); and Γ_{Pgp} is the surface density of P-gp in the membrane $\left[\frac{mol}{m^2}\right]$.

$$V\frac{dC}{dt} = \mathrm{P_s\,A}(C_{out} - C_{in}) + \mathrm{k_T\,\Gamma_{Pgp}\,A\,C_{out}} \quad (3.1)$$

By assuming a relatively constant external concentration of Rho123 surrounding the liposome, and with liposomes being spherical and of constant volume, integrating Equation 3.1 from 0 μM (C_{in} at t_0) to C_{in} and t_0 to t yields Equation 3.2, where t is the time $[s]$; C_{out} is the concentration of solute in the external solution; C_{in} is the concentration of solute inside the liposome at time t; and $\frac{3}{r}$ is the surface area of a sphere divided by its volume, where r is the radius $[m]$. We calculated the surface density of P-gp in the membranes of liposomes to be $7.6\times10^{-11}\ \frac{mol}{m^2}$, based on the ratio of starting materials (see Appendix B, Section B.3).

$$\frac{C_{in}}{C_{out}} = \left(1 + \frac{\mathrm{k_T\,\Gamma_{Pgp}}}{\mathrm{P_s}}\right)\left(1 - \mathrm{e}^{-\frac{3\,\mathrm{P_s}}{\mathrm{r}}(t-t_0)}\right) \quad (3.2)$$

The fluorescence intensity inside giant liposomes formed with P-gp increased rapidly in the first 10-15 min after immersion in 1 μM Rho123 assay solution (see Appendix B, Figure B.3). We determined the time-dependent concentration of Rho123 from calibration of the fluorescence intensity. We then accounted for the slight change in concentration outside the liposome by evaluating the ratio in concentration between internal and external solution $\left(\frac{C_{in}}{C_{out}}\right)$ at each time point. We fitted this ratio to Equation 3.2 using Origin 8.0 to determine $\mathrm{k_T}$, $\mathrm{P_s}$, and t_0 for each liposome that contained P-gp. Liposomes that lacked P-gp, however, did not include the active transport term, $\mathrm{k_T}$, because the surface density of P-gp in this case was zero. Figure 3.3 shows box plots of the apparent $\mathrm{P_s}$ and $\mathrm{k_T}$ values determined from these fits.

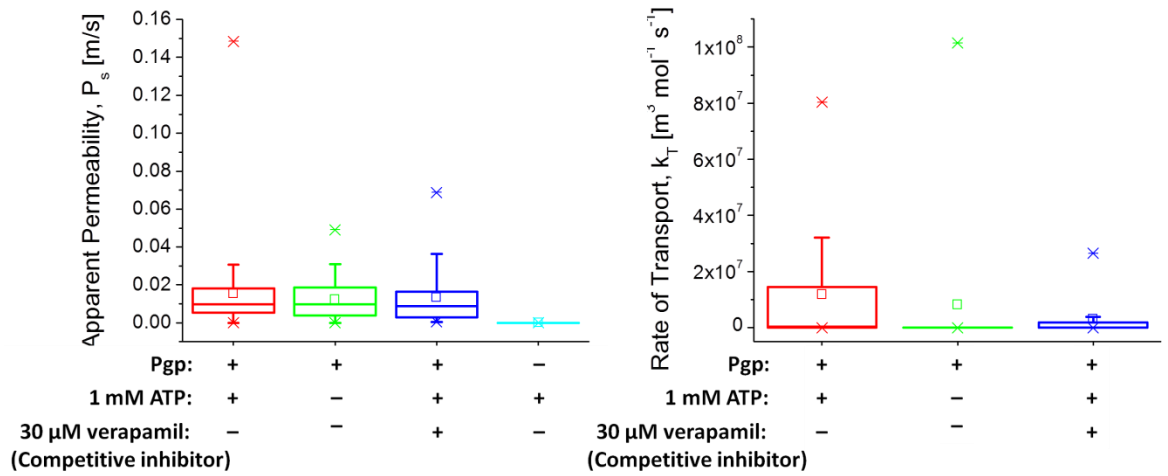

Figure 3.3. Box plots of apparent membrane permeability (P_s) and rate constant of transport (k_T) of rhodamine 123 into giant liposomes under different test conditions. The median apparent P_s values for each condition (from left to right, all in m/s) were: 0.0098, 0.0096, 0.0088, and 1.1×10^{-7}. Kruskal-Wallis ANOVA revealed that the left three conditions have a similar apparent P_s value, whereas liposomes without P-gp had an apparent P_s value that was significantly lower than the liposomes that contained P-gp ($p \ll 0.001$). The median k_T values for each condition (from left to right, all in m^3 mol^{-1} s^{-1}) were: 3.7×10^5, 0, and 0. The k_T value for liposomes without P-gp was not evaluated because the surface density of P-gp in these membranes was zero. Kruskal-Wallis ANOVA revealed that the k_T value for liposomes with active transport (i.e., containing P-gp and assayed with ATP and without verapamil) was significantly higher than the k_T value for liposomes assayed without ATP ($p = 0.027$) or in the presence of verapamil ($p = 0.033$).

We found that when P-gp was reconstituted into giant liposomes under any assay condition, the apparent P_s was significantly higher than the apparent P_s for liposomes that lacked P-gp. Moreover, the apparent P_s was similar under all assay conditions for liposomes that contained P-gp. The membrane permeability is used typically to characterize passive diffusion across membranes, such as into liposomes. When comparing the P_s values under different conditions, a higher P_s value corresponds

to a faster rate of diffusion. As the diffusion rate of a solute across a membrane increases, the rate of accumulation of the solute inside the liposome also increases in a manner that is dependent on the size of the liposome. Therefore, these results indicate that the presence of P-gp in the membrane increased the membrane permeability to Rho123, even when active transport was not enabled. We could not differentiate, however, whether the increased permeability was due to leakiness of the membrane itself (for example, due to packing defects in the membrane induced by the nearby presence of P-gp) or due to passage along the surface of P-gp (for example, via passive transport caused by random changes of conformation from inward-facing to outward-facing and vice versa).

The k_T values for liposomes containing P-gp in the presence of an inhibitor or without ATP were significantly lower than the k_T value for liposomes containing P-gp in the presence of ATP without an inhibitor. Similar to the membrane permeability coefficient, the rate of accumulation of solute inside the liposome due to active transport is also dependent on the size of the liposome and increases with increasing values of k_T. In our analysis, the k_T value also accounts for the concentration of ATP (1 mM for all assay conditions that included ATP). Since active transport of Rho123 across the lipid membrane by functional P-gp in the inside-out orientation contributes to an increased rate of accumulation of fluorescent molecules inside giant liposomes, we attributed the observed increased k_T values under the appropriate conditions to be due to active transport by functional P-gp. Additional evidence for active transport stems from the observation that the fluorescence intensity inside the liposomes exceeded the intensity outside the liposomes for several liposomes if the assay was carried out for at

least 20 min and seemed to be following an upward trend, whereas the fluorescence intensity inside liposomes without ATP or with inhibitor seemed to plateau (see Appendix B, Figure B.3). These results indicate that functionally active P-gp proteins were reconstituted from small proteoliposomes into giant proteoliposomes via a dried film of ultra-low melting agarose. Furthermore, ATP-mediated transport of Rho123 into giant proteoliposomes supports the hypothesis that at least a portion of the active P-gp retained their inside-out orientation.

Next, we evaluated the rate of change in fluorescence intensity to determine the rate of active transport (see Appendix B, Section B.3 for detailed calculations). We assumed that proteins and lipids reconstituted into giant proteoliposomes in the same ratio as in the small proteoliposomes prior to coating on a dried agarose film. Based on this ratio and the average surface area of lipids and of P-gp, we determined the theoretical number of P-gp to be ~59,000 for a giant proteoliposome with a diameter of 20 μm. At a transport rate of ~1 molecule per second per protein,[(42)] the theoretical transport rate is $4.5 \times 10^{13} \frac{molecules}{m^2 s}$. We then calculated the active transport-related flux as the number of molecules per elapsed time from the portion of Equation 3.2 related to active transport (i.e., without the portion of Equation 3.2 related to passive diffusion). Using the median k_T value determined from the fits to Equation 3.2, under the conditions of active transport (assayed with ATP without inhibitor), we determined the transport flux per area to be $1.7 \times 10^{16} \frac{molecules}{m^2 s}$.

A number of factors may contribute to the three orders of magnitude discrepancy between the experimentally determined transport rate and the theoretical transport rate: the transport rate of Rho123 by individual P-gp proteins may be faster than 1 molecule

per second under the experimental conditions of our work, and the concentration of Rho123 in the membrane where transport occurs was likely higher than 1 μM (e.g., we had noted brighter membrane fluorescence, see Figure 3.1 and Appendix B, Figure B.1). Another possibility is that some lipid or P-gp molecules may have interacted with the agarose film preferentially and not been reconstituted into giant liposomes in the same ratio as was present in small proteoliposomes. One other explanation is that, given the range of values determined from the fits of Equation 3.2, the true k_T value may differ from the median value.

A significant benefit of using giant proteoliposomes for transport analyses is the ability to discern and evaluate vesicles individually. The concentration (or number) of molecules transported into the liposome is dependent on the surface area of the vesicle. Methods of generating giant proteoliposomes, however, yield a heterogeneous population with a broad range of sizes. Here we report a liposome-based transport assay that is simple to construct and perform, yields concentration data of fluorescent substrates with respect to vesicle size, and provides the ability to visually assess individual liposomes for irregularities and artifacts that could affect the influx of substrates. For example, as discussed previously, bright spots inside liposomes corresponded to multilamellar liposomes or to giant liposomes filled with small vesicles. The presence of such liposomes is not unusual for methods of generating giant liposomes with embedded membrane proteins based on variations of the gentle hydration method,[43] but could skew the results when liposomes are too small to discern individually due to the brightness of the membrane fluorescence. The giant

proteoliposomes prepared with the method presented here make it possible to exclude some of these artifacts from the analysis.

3.2.3 Evaluation of ion channel activity of chloride channels co-purified with P-gp

Previous reports have associated P-gp with chloride channel activity,[26, 27, 31-34] presumably by co-purification of these channels with P-gp. Therefore, as an additional means of testing the functionality of proteins reconstituted in giant proteoliposomes via the method introduced here, we performed patch clamp experiments employing the inside-out mode from giant proteoliposomes and compared the current recordings of membranes containing P-gp with the current recordings of membranes without P-gp (Figure 3.4).

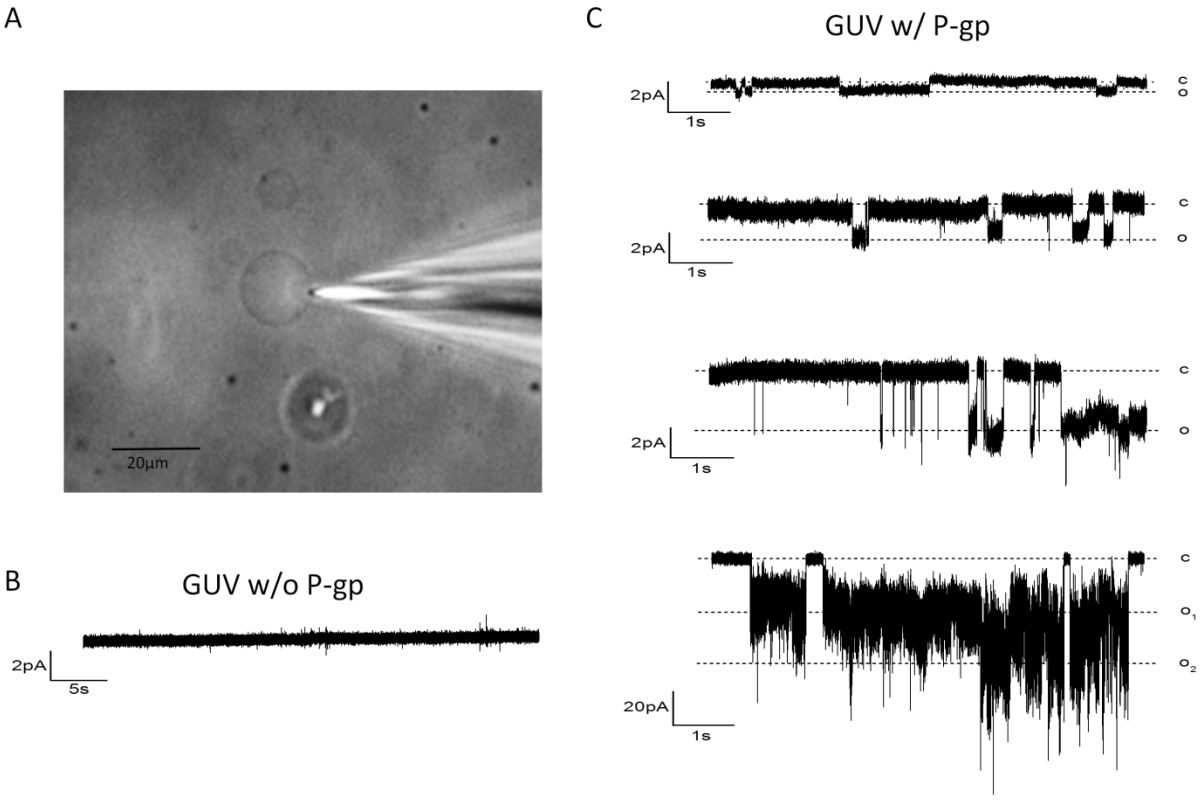

Figure 3.4. Patch clamp recordings from giant liposomes formed on an agarose film from small liposomes that contained or did not contain purified P-glycoprotein (P-gp). Single channel currents were recorded after excising a membrane patch from the

proteoliposomes in the inside-out configuration at a holding potential of -100 mV. The cut-off filter frequency was 5 kHz and the sampling rate was 25 kHz. (A) Phase contrast image of a patch pipette sealed to a giant proteoliposome suspended in bath solution. (B) Current trace of single channel recordings from a GUV without P-gp. (C) Current traces of single channel recordings from giant proteoliposomes reconstituted with purified P-gp. Traces (from top to bottom panel) were filtered at 1 kHz, 2 kHz, 2 kHz and 5 kHz, respectively. The mean single channel conductance values of open states (from top to bottom panel) were: 6, 19, 37, and 238 pS, respectively.

We observed transient, and distinct, open and closed states in the patch clamp recordings of membrane patches from giant proteoliposomes that contained P-gp (Figure 3.4C). In comparison, patch clamp recordings of membrane patches from GUVs that lacked P-gp did not show current fluctuations beyond baseline noise (Figure 3.4B). These results indicate that functional ion channel proteins were reconstituted in giant proteoliposomes when reconstituting the purified P-gp preparation by the method reported here.

To investigate if these ion channel events originated from chloride ion channel proteins that co-purified with P-gp from the host insect cells, we applied potent chloride channel inhibitors (Figure 3.5). Channel activity was blocked in the presence of 100 µM of the potent chloride channel inhibitor, 5-Nitro-2-(3-phenylpropylamino)benzoic acid (NPPB), but was restored after washing out the inhibitor.[44, 45] Channel activity was irreversibly blocked after application of 50 µM Gd^{3+}, as expected for chloride channels.[44, 46] The responses observed with these chloride channel inhibitors indicate the presence of chloride channel proteins in giant proteoliposomes containing purified P-gp and agree with previous studies.[45, 47, 48] For instance, Ehring *et al*. reported single channel conductance values of 6.1 pS and 25.2 pS from multi-drug resistance cell lines[45] while Duan *et al*. reported a single channel conductance value of 40 pS.[48] In

addition, Schwiebert *et al*. observed a large conductance Cl^- channel with a single channel conductance value of 305 pS.[47] The initial currents at a holding potential of 100 mV revealed two open states at 4.1 and 15.2 pS.

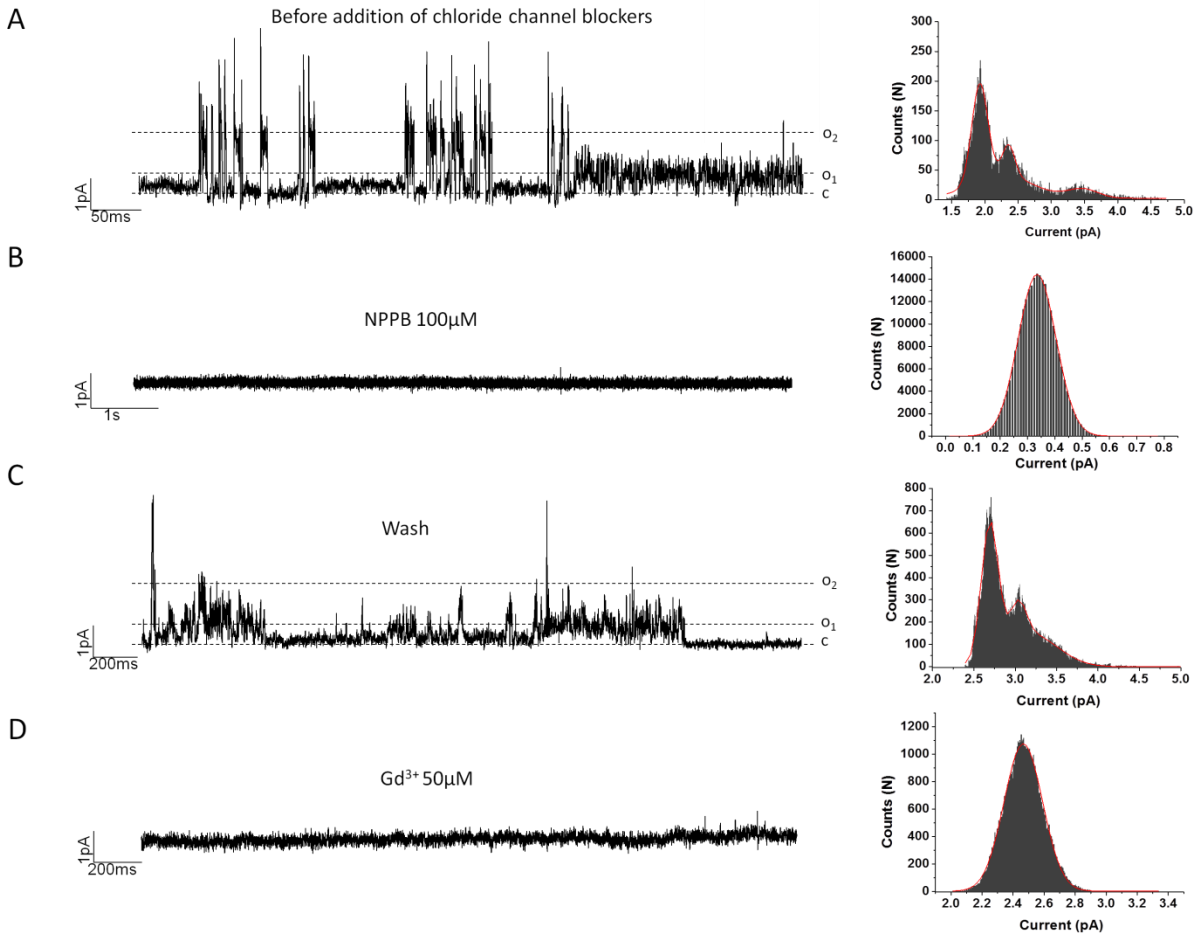

Figure 3.5. Single channel recordings of Cl^- currents in giant proteoliposomes that contained purified P-glycoprotein (P-gp) and their corresponding histograms. Recordings were performed in the inside-out configuration at a holding potential of 100 mV. The recording cut-off filter frequency was 5 kHz and the sampling rate was 25 kHz. Traces were filtered at 1 kHz. (A) Original single channel Cl^- currents. The single channel conductance values of two open states were 4.1 and 15.2 pS, respectively. (B) Current trace in the presence of 5-Nitro-2-(3-phenylpropylamino)benzoic acid (NPPB), a potent Cl^- channel inhibitor, at a concentration of 100 µM, and (C) after washing out NPPB with standard bath solution. The conductance values of two open states are 3.8 and 14.4 pS, respectively. (D) Current trace in the presence of 50 µM Gd^{3+}, another chloride channel inhibitor. The dashed lines indicate the closed state (c) and two open states (o_1 and o_2). Peaks in the histogram reveal the open state current amplitudes.

3.2.4 Comparison with a previously described method

When choosing a method for reconstituting proteins into giant proteoliposomes, the properties of the resulting liposomes must be considered. For example, to study ion channels using the traditional, pipette-based patch clamp technique, only a few giant proteoliposomes need to be present because the experimentalist can select a proteoliposome of choice from a heterogeneous population. For semi-automated, suction-based planar patch clamp assays,[49-51] however, a high concentration of unilamellar proteoliposomes with large diameters is desirable to ensure acceptable success rates of bilayer formation over micro- or nano-pores.[4] Similarly, for transport assays as described in the work presented here, the ideal case would be an abundance of unilamellar proteoliposomes with diameters larger than 10 µm so that influx of solutes into liposomes can be readily monitored and analyzed using time series of images. To compare the agarose-based method presented here with an existing method for producing giant proteoliposomes, we formed giant liposomes containing P-gp using the gentle hydration method presented by Riquelme *et al*.[52] Both methods produced a similar yield of giant liposomes after collecting free-floating liposomes using a pipette (see Appendix B, Figure B.4). Formation of giant proteoliposomes using the previously described method of gentle hydration was, however, less reliable (some trials yielded very few free-floating giant proteoliposomes) than formation from a film of ultra-low melting agarose (every trial produced a good yield of giant proteoliposomes). We also found that the previously described method[52] typically produced liposomes that were more often packed with small liposomes compared to the method presented here (see Appendix B, Figure B.4). While these internal liposomes did not interfere with the patch

clamp studies performed by Riquelme *et al*.,[52] these types of liposomes were not suitable for transport assays that measure the fluorescence intensity inside liposomes as described here. Therefore, the fractional yield of suitable proteoliposomes for fluorescent flux assays was higher when formation was facilitated by a film of ultra-low melting agarose in comparison to the previously established protocol.

3.3 Conclusion

Dried films of ultra-low melting agarose facilitated the formation of giant proteoliposomes from small proteoliposomes. The resulting giant proteoliposomes contained purified P-gp transporters and exhibited (i) increased ATPase activity following stimulation with a known transport substrate compared to pre-stimulation activity, (ii) elevated apparent membrane permeabilities to Rho123 in liposomes containing P-gp compared to liposomes lacking P-gp, (iii) elevated rates of transport under conditions conducive to active transport by P-gp compared to conditions lacking ATP or with an inhibitor, and (iv) patch clamp recordings that are consistent with co-purified chloride channel proteins. Together, these results demonstrate that this technique yielded functional reconstitution of purified transmembrane proteins, such as P-gp and co-purified chloride ion channels, into giant proteoliposomes. At least a portion of the P-gp proteins remained in the inside-out configuration, wherein the ATP-binding and substrate-binding domains were exposed to the external solution. Unlike cellular assays, this configuration allows straightforward and rapid alteration of the environment surrounding these domains and provides a means of studying direct effects of potential inhibitors and ATP concentration on the rate of transport. Agarose-

mediated reconstitution of transmembrane proteins into giant liposomes resulted in a high yield of giant proteoliposomes that were suitable for transport studies and may enable experiments with semi-automated planar patch clamp experiments on reconstituted and purified proteins.

3.4 Experimental Section

Chemicals were purchased from Sigma-Aldrich (St. Louis, MO), except when noted otherwise.

3.4.1 Isolation of crude membranes from P-gp-expressing High Five insect cells

We prepared crude membranes from High Five insect cells infected with recombinant baculovirus carrying the 6×His-tagged human MDR1 cDNA (kindly provided by S.V. Ambudkar, Laboratory of Cell Biology, Center for Cancer Research, National Cancer Institute, NIH, Bethesda, MD) as described previously.[(53)] We incubated cells on ice for 45 min in a lysis buffer containing 50 mM trizma hydrochloride (Tris-HCl), pH 7.5, 50 mM mannitol, 2 mM ethylene glycol tetraacetic acid (EGTA), 2 mM dithiothreitol (DTT), 1 mM 4-(2-aminoethyl)benzenesulfonyl fluoride (AEBSF), and 1% (w/v) aprotinin (Roche Diagnostics, Indianapolis, IN) and subsequently disrupted the cells using a Dounce homogenizer (30 strokes with pestle A). We removed undisrupted cells and nuclear debris by centrifugation at 500×*g* for 10 min. We diluted the supernatant 2-fold in resuspension buffer containing 50 mM Tris-HCl (pH 7.5), 300 mM mannitol, 1 mM EGTA, 1 mM DTT, 1 mM AEBSF, and 1% (w/v) aprotinin. We collected the membranes by centrifugation for 60 min at 100,000×*g* and resuspended the pellet in resuspension buffer containing 10% (v/v) glycerol. We stored the membranes in small

aliquots at -70°C. We revealed the protein content of each preparation using the Amido Black protein method described by Schaffner and Weissmann[36] with bovine serum albumin (BSA) as a standard.

3.4.2 Solubilization of P-gp

We solubilized membranes prepared from insect cells using octyl *β*-D-glucopyranoside as described[35] with modifications. We resuspended crude membranes at a concentration of 2.0 mg/mL in a buffer containing: 20 mM Tris-HCl (pH 8.0), 20% (v/v) glycerol,150 mM NaCl, 2 mM *β*-mercaptoethanol, 2.0% (w/v) octyl glucoside, 1.5 mM $MgCl_2$, 1 mM AEBSF, 2 *μ*g/mL pepstatin, 2 *μ*g/mL leupeptin, 1% (w/v) aprotinin and a 0.4% (w/v) lipid mixture consisting of *Escherichia coli* bulk phospholipid, phosphatidylcholine, phosphatidylserine, and cholesterol (all from Avanti Polar Lipids, Alabaster, AL) at 60:17.5:10:12.5 (w/w), respectively. After 20 min of incubation on ice, we removed insoluble material by centrifugation at 100,000×*g* for 1 h. The supernatant, which we call detergent extract, contained the solubilized P-gp.

3.4.3 Purification of P-gp by metal affinity chromatography

We incubated the detergent extract (10 mg of protein) in the presence of 2 mM imidazole (final concentration) for 30 min at 4°C on a rotary shaker with 0.5 mL of 50% (w/v) Talon metal affinity resin in non-buffered 20% ethanol (Clontech, Mountain View, CA). The resin was prewashed once with buffer A composed of 20 mM Tris-HCl (pH 8.0), 100 mM NaCl, 20% (v/v) glycerol, 2.5 mM *β*-mercaptoethanol, 1.25% (w/v) octyl glucoside, 1 mM $MgCl_2$, 1 mM AEBSF, 2 *μ*g/mL pepstatin, 2 *μ*g/mL leupeptin, 1% (w/v) aprotinin and a 0.1% (w/v) lipid mixture (same composition as the solubilization reaction). We pelleted the metal affinity beads by centrifugation for 5 min at 500×*g* and

washed twice by resuspending and incubating in 10 mL of buffer A at 4°C for 10 min on a rotary shaker. We resuspended the beads in 1 mL of buffer A and transferred them to a 4 mL disposable column (Bio-Rad, Hercules, CA). After being washed twice in 5 mL of buffer A containing 500 mM KCl, we eluted the proteins stepwise in 2 mL each of buffer B (same as buffer A except with 20 mM Tris-HCl at pH 6.8 instead of at pH 8.0) containing 10, 100, and 200 mM imidazole. We concentrated the fractions eluted from the column using Centriprep-50 concentrators (Amicon, Beverly, MA) and stored in aliquots at -70°C. We analyzed the protein content of the purified sample by the Amido Black protein method and performed sodium dodecyl sulfate polyacrylamide gel electrophoresis (SDS-PAGE) and immunoblot analysis as previously described.[35, 36] We estimate the purity of this P-gp preparation to be 70 to 80%.

3.4.4 Reconstitution of P-gp into small proteoliposomes

For reconstitution, we used 160-250 µg of purified and concentrated P-gp. We mixed the protein sample with 4-5 mg of tip sonicated phospholipid mixture (same composition as the solubilization reaction at 50 mg/mL in 50 mM Tris-HCl, pH 7.4), 1.25% octylglucoside, and 50 mM Tris-HCl, pH 7.4, in a final volume of 1 ml. We incubated the mixture for 20 min on ice and formed proteoliposomes or liposomes (prepared without protein) at 23-25°C by a 1:25 dilution into buffer C composed of 50 mM Tris-HCl, pH 7.4, 1 mM DTT, and 1× protease inhibitor cocktail (Roche Diagnostics, Indianapolis, IN). We concentrated the proteoliposomes or liposomes by centrifugation at 100,000×g, washed once, and resuspended in 150 µL of buffer C containing protease inhibitors and 2.5 mM $MgCl_2$.

3.4.5 Formation of giant proteoliposomes

To form giant proteoliposomes from small proteoliposomes, we extended a technique that we described previously for the formation of liposomes without reconstituted proteins.[19] We prepared ~10 mL of a solution of 1% (w/w) ultra-low melting agarose (Type IX-A from Sigma-Aldrich, St. Louis, MO) in deionized water by boiling the suspension of agarose powder and water twice in a microwave with gentle agitation between heating. After the solution cooled to room temperature, we reheated it for 10 s in a microwave and immediately dip-coated one side of a cover glass (24 × 50 × 0.15 mm, from Fisher Scientific, Rochester, NY) in the agarose solution. We placed the cover glass with the agarose-coated side facing upward on a temperature-controlled hot plate (Barnstead Intl, Dubuque, IA) and covered the glass with the lid from a Petri dish set at an angle to allow water vapor to escape while also preventing dust from settling onto the agarose film. The cover glass remained on the hot plate with the temperature set to 40°C until the solution appeared dry (typically ~20 min).

After the agarose solution dried into a clear film, we hand-cut a rectangular frame of poly-dimethylsiloxane (PDMS) (Sylgard 184 Silicone, Dow Corning Corporation, Midland, MI) to the size of the cover glass and placed the PDMS frame onto the agarose-coated side of the cover glass. Using a pipette, we dispersed 150 µL of the solution containing small proteoliposomes in small droplets (~10 µL each) onto the dried film of agarose while trying to cover the entire surface enclosed within the PDMS frame. We dragged the pipette tip over the tops of the droplets until they coalesced into a single film of solution while taking care not to disturb the underlying agarose film. We placed the lid from a Petri dish set at an angle over the cover glass and kept the cover

glass undisturbed overnight at room temperature, or until the solution appeared dry. In the last few trials, we applied a vacuum (~500 mmHg) to shorten the drying time to less than 2 h.

When the solution of small liposomes appeared dry, we added 1 mL of 190 mM sucrose, 1 mM DTT, and 1× protease inhibitor cocktail in 50 mM Tris-HCl, pH 7.0, placed the lid of a Petri dish over the cover glass, and left it undisturbed for 3 h to allow formation of giant proteoliposomes. After formation, we transferred the giant proteoliposomes to a microcentrifuge tube (1.5 mL volume, Eppendorf, Westbury, NY) while taking care not to transfer visible pieces of the agarose film.

3.4.6 Assessment of protein activity after reconstitution into giant liposomes

In order to determine the rate of ATP hydrolysis of reconstituted liposomes, we incubated them with 30 µM verapamil (a substrate of P-gp) in the presence and absence of 300 µM vanadate in ATPase assay buffer for 10 min at 37ºC. This ATPase assay buffer contained 50 µM KCl, 5 mM NaN_3, 2 mM EGTA, 10 mM $MgCl_2$, 1 mM DTT, 2 mM ouabain, and 50 mM Tris-HCl, pH 7.5. We used vanadate to inhibit the ATPase activity of P-gp. We started the reaction by adding 5 mM ATP and incubated for 20 min at 37ºC. We terminated the reaction with the addition of SDS solution (0.1 mL of 5% w/v SDS) and quantified the amount of inorganic phosphate released by a sensitive colorimetric reaction as described previously.[25] We recorded the specific activity of the transporter as vanadate-sensitive ATPase activity.[25]

3.4.7 Measurement of P-gp transport rate

We prepared assay solutions at 2× the desired final concentration of magnesium ions, rhodamine 123 (Rho123), and adenosine triphosphate (ATP) to account for

dilution of these molecules when mixed with an equal volume of solution containing giant liposomes. We used a concentration of sorbitol that was isoosmolar to the sucrose solution used to form giant proteoliposomes such that the giant proteoliposomes would settle quickly due to the density gradient (see Appendix B, Figure B.5) with minimal or no swelling or shrinking from water flux across the membrane. Assay solution without ATP consisted of 207 mM sorbitol, 50 mM Tris, pH 7.0, 8 mM $MgCl_2$, and 2 µM Rho123. Assay solution with ATP was the same but contained also 2 mM ATP. To inhibit the P-gp-mediated transport of Rho123 competitively, we transferred a portion of the solution containing giant proteoliposomes to a separate microcentrifuge tube, added verapamil to a final concentration of 30 µM, and incubated them at room temperature for >15 min before use. Assay solution with inhibitor was the same as assay solution with ATP but contained also 30 µM verapamil.

For microscopic observation of transport, we punched 5 mm diameter holes in a slab of PDMS (approximately 2 mm thick) and adhered the pre-punched PDMS to a cover glass to form wells for viewing giant liposomes. We incubated these wells with 5% milk (w/v nonfat dry milk powder in phosphate buffered saline) to prevent non-specific adsorption that may lead to rupture of giant liposomes on the surface of the glass. We then placed 30 µL of assay solution into an observation well, added 30 µL of solution containing giant liposomes, and mixed the contents of the well gently using the pipette. After waiting ~1 min to allow the giant liposomes to settle to the bottom of the well, we focused on a region that contained multiple liposomes and used a confocal microscope (Nikon EZ-C1 software, version 3.20) to capture confocal images at 1 min intervals for 30–60 min using an inverted microscope (Nikon Eclipse TE2000-U) with a

20× objective (Nikon, NA=0.75) and equipped with an argon laser (Spectra-physics, wavelength = 488 nm), a helium-neon laser (Melles-Griot, wavelength = 543 nm), appropriate filter settings for Rho123, and a pinhole diameter of 33.3 μm.

3.4.8 Data analysis

We used EZ-C1 Freeviewer (Nikon, version 3.50) to measure the diameter of liposomes and the fluorescence intensity of their interiors and of the surrounding solution as a function of time. Some liposomes were filled with smaller vesicles and appeared as bright spots in confocal images. These filled liposomes were not analyzed because the fluorescence intensity appears to be due to membrane-associated Rho123 instead of Rho123 transported from the external to the internal solution.

We determined that the fluorescence intensity was linearly related to the concentration of Rho123 (see Appendix B, Fig. B.2). The detection sensitivity of the confocal imaging software, however, was different between days and even each time the program was opened. Therefore, for each date we performed the assay, we used a two point calibration to determine the Rho123 concentration from fluorescence intensity values using the average intensity inside GUVs without P-gp at the starting time (concentration of Rho123 ~0 μM) and the average intensity of the solution outside of GUVs at the starting time (concentration of Rho123 ~1 μM).

The change in the concentration of Rho123 inside a liposome is due to the molecules of Rho123 crossing the membrane of the liposome. Molecules can cross a membrane via passive diffusion in a manner that depends on the difference in concentration on each side of the membrane and a rate constant of diffusion, P_s, or via active transport in the presence of active transporter proteins that depends on the

concentration of ATP and a rate of transport. In our analysis, we combined the concentration of ATP and the rate of transport into one variable, k_T. The change in the concentration of Rho123 in giant liposomes, as demonstrated in this work, is given by Equation 3.1,[2, 40, 41] where V is the volume $[m^3]$, C is the concentration [μM], P_s is the apparent membrane permeability $\left[\frac{m}{s}\right]$; A is the surface area $[m^2]$; $(C_{out} - C_{in})$ is the difference in concentration of solute across the membrane (from external solution to the interior); and Γ_{Pgp} is the surface density of P-gp in the membrane $\left[\frac{mol}{m^2}\right]$.

$$V\frac{dC}{dt} = P_s\, A(C_{out} - C_{in}) + k_T\, \Gamma_{Pgp}\, A\, C_{out} \qquad (3.1)$$

By assuming a relatively constant external concentration of Rho123 surrounding the liposome, and with liposomes being spherical and of constant volume, integrating Equation 3.1 from 0 μM (C_{in} at t_0) to $C_{in,t}$ and t_0 to t yields Equation 3.2, where t is the time $[s]$; C_{out} is the concentration of solute in the external solution; C_{in} is the concentration of solute inside the liposome at time t; and $\frac{3}{r}$ is the surface area of a sphere divided by its volume, where r is the radius $[m]$.

$$\frac{C_{in}}{C_{out}} = \left(1 + \frac{k_T\, \Gamma_{Pgp}}{P_s}\right)\left(1 - e^{-\frac{3\,P_s}{r}(t - t_0)}\right) \qquad (3.2)$$

We calculated the surface density of P-gp in the membranes of liposomes to be $7.6\times10^{-11}\ \frac{mol}{m^2}$, based on the ratio of starting materials (see Supporting Information). We then accounted for the slight change in concentration outside the liposome by evaluating the ratio in concentration between external and internal solution $\left(\frac{C_{in}}{C_{out}}\right)$ at each time point. We fitted this ratio to Equation 3.2 using Origin 8.0 to determine k_T, P_s, and t_0 for each liposome that contained P-gp. Liposomes that lacked P-gp, however,

did not include the active transport term, k_T, because the surface density of P-gp in this case was zero.

For this analysis, we did not evaluate the fluorescence intensity of liposomes that were clearly not unilamellar or that visibly contained small vesicles inside because these results would not be due solely to active transport by P-gp. Of the liposomes analyzed per Equation 3.2, most fit well to the expected trend with an adjusted R^2 >0.98. Data from some liposomes did not follow the expected trend and may have been due to multilamellar liposomes or to liposomes with defects. Therefore, we did not include data from liposomes with a poor fit to the expected trend (adjusted R^2 <0.90) in the test for statistical significance. We used Kruskal-Wallis ANOVA in Origin 8.0 to assess statistical significance of the data for each experimental condition.

3.4.9 Patch clamp experiments with proteoliposomes

We placed a 20 µL drop of proteoliposome suspension in the center of a 35 mm glass bottom Petri dish (MatTek, Ashland, MA) that we had pretreated with 5% milk (w/v dry nonfat milk powder in phosphate buffered saline) for 30 min. Then we covered the dish with 2 mL of bath solution while taking care to keep the giant proteoliposomes near the center of the dish. Most of the giant proteoliposomes settled to the bottom of the dish within a few minutes. The bath solution consisted of 130 mM KCl, 1 mM $MgCl_2$, and 10 mM HEPES with a pH titrated to 7.2 using KOH. The pipette solution was identical to the bath solution supplemented with 5 mM ATP. We fabricated the patch electrodes with resistances of 5.0–10.0 MΩ from borosilicate glass (Sutter Instruments, Novato, CA) using a P-87 puller (Sutter Instruments, Novato, CA). After formation of a Giga seal, we pulled the patch electrode away from the giant proteoliposome and quickly went

through the water-air interface in order to ensure the inside out configuration. We recorded the single channel current at room temperature using an Axopatch 200B amplifier (Molecular Devices, Sunnyvale, CA) and digitized the recordings using a Digidata 1322A (Molecular Devices, Sunnyvale, CA). Data acquisition was done using pClamp9 software (Molecular Devices, Sunnyvale, CA).

3.5 Acknowledgements

This work was supported by a National Science Foundation Career Award (M.M., grant no. 0449088) and the National Institutes of Health (M.M., grant no. 1R01GM081705). Drs. S. Shukla and S.V. Ambudkar were supported by the Intramural Research Program of the NIH, National Cancer Institute, Center for Cancer Research. K.S.H. acknowledges a Microfluidics in Biomedical Sciences Training Program fellowship from NIH (Grant No. T32EB005582 from the National Institute of Biomedical Imaging and Bioengineering at NIH) and a Rackham Engineering Award Fellowship.

References

1. Luisi, P. L., and Walde, P., (Eds.) (2000) *Perspectives in Supramolecular Chemisty: Giant Vesicles*, Vol. 6, John Wiley & Sons, New York.

2. Li, S., Hu, P. C., and Malmstadt, N. (2010) Confocal Imaging to Quantify Passive Transport across Biomimetic Lipid Membranes, *Analytical Chemistry 82*, 7766-7771.

3. Maherani, B., Arab-Tehrany, E., Mozafari, M. R., Gaiani, C., and Linder, M. (2011) Liposomes: A Review of Manufacturing Techniques and Targeting Strategies, *Curr. Nanosci. 7*, 436-452.

4. Tiefenauer, L., and Demarche, S. (2012) Challenges in the Development of Functional Assays of Membrane Proteins, *Materials 5*, 2205-2242.

5. Walde, P., Cosentino, K., Engel, H., and Stano, P. (2010) Giant Vesicles: Preparations and Applications, *Chembiochem 11*, 848-865.

6. Reeves, J. P., and Dowben, R. M. (1969) Formation and Properties of Thin-Walled Phospholipid Vesicles, *Journal of Cellular Physiology 73*, 49-60.

7. Angelova, M. I., and Dimitrov, D. S. (1986) Liposome Electroformation, *Faraday Discussions 81*, 303-311.

8. Morales-Penningston, N. F., Wu, J., Farkas, E. R., Goh, S. L., Konyakhina, T. M., Zheng, J. Y., Webb, W. W., and Feigenson, G. W. (2010) GUV preparation and imaging: Minimizing artifacts, *Biochimica Et Biophysica Acta-Biomembranes 1798*, 1324-1332.

9. Shaklee, P. M., Semrau, S., Malkus, M., Kubick, S., Dogterom, M., and Schmidt, T. (2010) Protein Incorporation in Giant Lipid Vesicles under Physiological Conditions, *Chembiochem 11*, 175-179.

10. Girard, P., Pecreaux, J., Lenoir, G., Falson, P., Rigaud, J. L., and Bassereau, P. (2004) A new method for the reconstitution of membrane proteins into giant unilamellar vesicles, *Biophysical Journal 87*, 419-429.

11. Keller, B. U., Hedrich, R., Vaz, W. L., and Criado, M. (1988) Single channel recordings of reconstituted ion channel proteins: an improved technique, *Pflugers Arch 411*, 94-100.

12. Riquelme, G., Lopez, E., Garcia-Segura, L. M., Ferragut, J. A., and Gonzalez-Ros, J. M. (1990) Giant liposomes: a model system in which to obtain patch-clamp recordings of ionic channels, *Biochemistry 29*, 11215-11222.

13. Doeven, M. K., Folgering, J. H. A., Krasnikov, V., Geertsma, E. R., van den Bogaart, G., and Poolman, B. (2005) Distribution, lateral mobility and function of membrane proteins incorporated into giant unilamellar vesicles, *Biophysical Journal 88*, 1134-1142.

14. Battle, A. R., Petrov, E., Pal, P., and Martinac, B. (2009) Rapid and improved reconstitution of bacterial mechanosensitive ion channel proteins MscS and MscL into liposomes using a modified sucrose method, *Febs Letters 583*, 407-412.

15. Yanagisawa, M., Iwamoto, M., Kato, A., Yoshikawa, K., and Oiki, S. (2011) Oriented Reconstitution of a Membrane Protein in a Giant Unilamellar Vesicle: Experimental Verification with the Potassium Channel KcsA, *Journal of the American Chemical Society 133*, 11774-11779.

16. Kahya, N., Pecheur, E. I., de Boeij, W. P., Wiersma, D. A., and Hoekstra, D. (2001) Reconstitution of membrane proteins into giant unilamellar vesicles via peptide-induced fusion, *Biophysical Journal 81*, 1464-1474.

17. Varnier, A., Kermarrec, F., Blesneac, I., Moreau, C., Liguori, L., Lenormand, J. L., and Picollet-D'hahan, N. (2010) A Simple Method for the Reconstitution of Membrane Proteins into Giant Unilamellar Vesicles, *Journal of Membrane Biology 233*, 85-92.

18. Estes, D. J., Lopez, S. R., Fuller, A. O., and Mayer, M. (2006) Triggering and visualizing the aggregation and fusion of lipid membranes in microfluidic chambers, *Biophys J 91*, 233-243.

19. Horger, K. S., Estes, D. J., Capone, R., and Mayer, M. (2009) Films of Agarose Enable Rapid Formation of Giant Liposomes in Solutions of Physiologic Ionic Strength, *Journal of the American Chemical Society 131*, 1810-1819.

20. Hardy, S. P., Goodfellow, H. R., Valverde, M. A., Gill, D. R., Sepulveda, F. V., and Higgins, C. F. (1995) PROTEIN-KINASE C-MEDIATED PHOSPHORYLATION OF THE HUMAN MULTIDRUG-RESISTANCE P-GLYCOPROTEIN REGULATES CELL VOLUME-ACTIVATED CHLORIDE CHANNELS, *Embo J. 14*, 68-75.

21. Ambudkar, S. V., Kimchi-Sarfaty, C., Sauna, Z. E., and Gottesman, M. M. (2003) P-glycoprotein: from genomics to mechanism, *Oncogene 22*, 7468-7485.

22. Ramachandran, C., and Melnick, S. J. (1999) Multidrug resistance review in human tumors - Molecular diagnosis and clinical significance, *Molecular Diagnosis 4*, 81-94.

23. Sharom, F. J. (2011) The P-glycoprotein multidrug transporter, In *Essays in Biochemistry: Abc Transporters* (Sharom, F. J., Ed.), pp 161-178, Portland Press Ltd, London.

24. Palmeira, A., Sousa, E., Vasconcelos, M. H., and Pinto, M. M. (2012) Three Decades of P-gp Inhibitors: Skimming Through Several Generations and Scaffolds, *Curr. Med. Chem. 19*, 1946-2025.

25. Ambudkar, S. V. (1998) Drug-stimulatable ATPase activity in crude membranes of human MDR1-transfected mammalian cells, *Methods Enzymol. 292*, 504-514.

26. Wielinga, P. R., Heijn, N., Westerhoff, H. V., and Lankelma, J. (1998) A method for studying plasma membrane transport with intact cells using computerized fluorometry, *Analytical Biochemistry 263*, 221-231.

27. Howard, E. M., and Roepe, P. D. (2003) Purified human MDR 1 modulates membrane potential in reconstituted proteoliposomes, *Biochemistry 42*, 3544-3555.

28. Al-Shawi, M. K., and Omote, H. (2005) The remarkable transport mechanism of P-glycoprotein: A multidrug transporter, *Journal of Bioenergetics and Biomembranes 37*, 489-496.

29. Bucher, K., Belli, S., Wunderli-Allenspach, H., and Kramer, S. D. (2007) P-glycoprotein in proteoliposomes with low residual detergent: The effects of cholesterol, *Pharmaceutical Research 24*, 1993-2004.

30. Sasaki, H., Kawano, R., Osaki, T., Kamiya, K., and Takeuchi, S. (2012) Single-vesicle estimation of ATP-binding cassette transporters in microfluidic channels, *Lab on a Chip 12*, 702-704.

31. Higgins, C. F. (1995) P-glycoprotein and cell volume-activated chloride channels, *Journal of Bioenergetics and Biomembranes 27*, 63-70.

32. Valverde, M. A., Diaz, M., Sepulveda, F. V., Gill, D. R., Hyde, S. C., and Higgins, C. F. (1992) Volume-regulated chloride channels associated with the human multidrug-resistance P-glycoprotein, *Nature 355*, 830-833.

33. Johnstone, R. W., Ruefli, A. A., and Smyth, M. J. (2000) Multiple physiological functions for multidrug transporter P-glycoprotein?, *Trends Biochem.Sci. 25*, 1-6.

34. Mizutani, T., Masuda, M., Nakai, E., Furumiya, K., Togawa, H., Nakamura, Y., Kawai, Y., Nakahira, K., Shinkai, S., and Takahashi, K. (2008) Genuine functions of P-glycoprotein (ABCB1), *Curr. Drug Metab. 9*, 167-174.

35. Ambudkar, S. V., Lelong, I. H., Zhang, J. P., Cardarelli, C. O., Gottesman, M. M., and Pastan, I. (1992) Partial-purification and reconstitution of the human multidrug-resistance pump - characterization of the drug-stimulatable ATP hydrolysis, *Proceedings of the National Academy of Sciences of the United States of America 89*, 8472-8476.

36. Schaffner, W., and Weissman, C. (1973) Rapid, sensitive, and specific method for determination of protein in dilute-solution, *Analytical Biochemistry 56*, 502-514.

37. Shapiro, A. B., and Ling, V. (1998) Stoichiometry of coupling of rhodamine 123 transport to ATP hydrolysis by P-glycoprotein, *Eur. J. Biochem. 254*, 189-193.

38. Chearwae, W., Anuchapreeda, S., Nandigama, K., Ambudkar, S. V., and Limtrakul, P. (2004) Biochemical mechanism of modulation of human P-glycoprotein (ABCB1) by curcumin I, II, and III purified from Turmeric powder, *Biochem. Pharmacol. 68*, 2043-2052.

39. Shukla, S., Wu, C. P., and Ambudkar, S. V. (2008) Development of inhibitors of ATP-binding cassette drug transporters - present status and challenges, *Expert Opin. Drug Metab. Toxicol. 4*, 205-223.

40. Chakrabarti, A. C., and Deamer, D. W. (1992) Permeability of lipid bilayers to amino-acids and phosphate, *Biochimica Et Biophysica Acta 1111*, 171-177.

41. Michelson, S., and Slate, D. (1992) A MATHEMATICAL-MODEL OF THE P-GLYCOPROTEIN PUMP AS A MEDIATOR OF MULTIDRUG RESISTANCE, *Bull. Math. Biol. 54*, 1023-1038.

42. Ambudkar, S. V., Cardarelli, C. O., Pashinsky, I., and Stein, W. D. (1997) Relation between the turnover number for vinblastine transport and for vinblastine-stimulated ATP hydrolysis by human P-glycoprotein, *Journal of Biological Chemistry 272*, 21160-21166.

43. Rodriguez, N., Pincet, F., and Cribier, S. (2005) Giant vesicles formed by gentle hydration and electroformation: A comparison by fluorescence microscopy, *Colloids and Surfaces B-Biointerfaces 42*, 125-130.

44. de Tassigny, A. D., Souktani, R., Ghaleh, B., Henry, P., and Berdeaux, A. (2003) Structure and pharmacology of swelling-sensitive chloride channels, I-Cl,I-swell, *Fundam. Clin. Pharmacol. 17*, 539-553.

45. Ehring, G. R., Osipchuk, Y. V., and Cahalan, M. D. (1994) Swelling-activated chloride channels in multidrug-sensitive and multidrug-resistant cells, *Journal of General Physiology 104*, 1129-1161.

46. Suzuki, M., Morita, T., and Iwamoto, T. (2006) Diversity of Cl- channels, *Cell. Mol. Life Sci. 63*, 12-24.

47. Schwiebert, E. M., Mills, J. W., and Stanton, B. A. (1994) Actin-based cytoskeleton regulates a chloride channel and cell-volume in a renal cortical collecting duct cell-line, *Journal of Biological Chemistry 269*, 7081-7089.

48. Duan, D., Winter, C., Cowley, S., Hume, J. R., and Horowitz, B. (1997) Molecular identification of a volume-regulated chloride channel, *Nature 390*, 417-421.

49. Demarche, S., Sugihara, K., Zambelli, T., Tiefenauer, L., and Voros, J. (2011) Techniques for recording reconstituted ion channels, *Analyst 136*, 1077-1089.

50. Bruggemann, A., Stoelzle, S., George, M., Behrends, J. C., and Fertig, N. (2006) Microchip technology for automated and parallel patch-clamp recording, *Small 2*, 840-846.

51. Schmidt, C., Mayer, M., and Vogel, H. (2000) A chip-based biosensor for the functional analysis of single ion channels, *Angewandte Chemie International Edition 39*, 3137-3140.

52. Riquelme, G., Lopez, E., Garciasegura, L. M., Ferragut, J. A., and Gonzalezros, J. M. (1990) Giant Liposomes - a Model System in Which to Obtain Patch-Clamp Recordings of Ionic Channels, *Biochemistry 29*, 11215-11222.

53. Ramachandra, M., Ambudkar, S. V., Chen, D., Hrycyna, C. A., Dey, S., Gottesman, M. M., and Pastan, I. (1998) Human P-glycoprotein exhibits reduced affinity for substrates during a catalytic transition state, *Biochemistry 37*, 5010-5019.

CHAPTER IV

Conclusions and Future Directions

4.1 Improvements in the Field

This work describes a novel method of generating giant liposomes, both with and without integral proteins. The method is simple and easy to perform and uses low cost materials that are available commonly in most laboratories. Unlike previously described methods of generating giant liposomes or proteoliposomes, we formed giant liposomes and proteoliposomes effectively, reliably, and without the typical sensitivity to lipid type or ionic strength.

4.2 Future Work Based on Chapter II

Chapter II described experiments that delve into how an agarose film facilitates formation of giant liposomes, but other work can be performed to explore the limitations of the technique. For example, the method is useful for formation of giant unilamellar vesicles (GUVs) in physiologically relevant solutions, but higher salt concentration may be desired if the giant liposomes will be used as microreactors.[(1)] I did test a few different pHs (pH 5 and 9) with success, but the ionic concentration of these pHs did not

exceed the salt concentration of the solutions we had used previously. Additionally, divalent cations have been problematic historically to the formation of giant liposomes.[2, 3] Therefore, we avoided solutions containing Mg^{2+} and Ca^{2+} during the formation of giant liposomes. These ions purportedly form an ionic bridge between lamellae so that the lipid sheets do not separate readily[3]. The swiftness and ease of the formation of GUVs from an agarose film, however, may help overcome the disadvantage these divalent cations cause with separating lamellae, but we have not yet tested this possibility.

In Chapter II, we demonstrated the benefit of an agarose film to be limited to ultra-low melting agarose because the agarose film, as it dried, remained in a conformation that could later easily dissolve, swelled during formation before it dissolved partially from the film, and associated with the membranes of liposomes. A similar benefit may be obtained from other types of agarose (i.e., with a higher melting point than the ultra-low melting agarose) by maintaining a temperature above the gel temperature of the agarose while it is drying into a film, but we did not yet examine this possibility. We did, however, investigate the benefit of a gelatin film on formation of giant liposomes (unpublished results) with successful formation of GUVs. Frequently, large pieces of the gelatin film disrupted from the surface during formation or while collecting free-floating liposomes, and so we considered the use of a gelatin film as less beneficial than an agarose film.

Other investigations into the method of forming giant liposomes from an agarose film can focus on optimizing the procedure to enhance specific qualities of the liposomes. For example, we initially used a larger amount of lipids coated onto the

agarose film, but obtained formation of a multitude of liposomes that included a wide variety of sizes along with giant liposomes filled with smaller liposomes. The frequency of forming these filled liposomes seemed to decrease when we decreased the amount of lipids per area (based on personal observations, unpublished data). Additionally, my early attempts at forming GUVs from small unilamellar liposomes (SUV) formed very few giant liposomes. We obtained formation of giant liposomes in greater yield after calculating the amount of SUV suspension to coat on the agarose film based on the amount of lipids in chloroform that were previously successful in forming GUVs. We did not conduct further exploration of the optimal concentration of lipids to coat either as SUV suspension or dissolved in chloroform for successful formation of primarily unilamellar liposomes.

4.3 Future Work Based on Chapter III

Chapter III described a method for reconstitution of P-glycoprotein (P-gp) and an associated chloride ion channel protein by coating a solution of SUVs on an agarose film, and this method may be applicable to other proteins. I tested the method for reconstitution of acetylcholine receptor from crude membrane. I was unsuccessful in reconstituting the protein in giant proteoliposomes by coating a film of agarose with crude membrane, but we did not try solubilized protein or acetylcholine receptor in small proteoliposomes. We also attempted, unsuccessfully, to reconstitute giant proteoliposomes by applying solubilized P-gp proteins and small liposomes to an agarose film and diluting out the detergent (unpublished data). We formed giant liposomes as indicated by phase contrast and fluorescence microscopy, but an ATPase

assay revealed that the proteins were not functional. I concluded from these experiments that P-gp proteins do not reconstitute functionally by a detergent dilution method even when facilitated by an agarose film. An agarose film may, however, be suitable for reconstitution of other proteins that can be incorporated into SUVs using the method described in Chapter III considering that P-gp is a large, complex protein with multiple transmembrane domains.

In Chapter III, we determined that a portion of the P-gp proteins reconstituted in an inside-out orientation. One extension of the transport assay we used is to determine an estimate of the fraction of proteins reconstituted in this orientation. To do so, we would need to combine confocal microscopy with a micropipette similar to those used for patch clamp experiments. After collecting a time lapse series of images to determine the rate of transport of rhodamine 123 into a giant proteoliposome, we would replace the external solution with a solution that does not contain ATP and rhodamine 123, attach a micropipette filled with a solution containing ATP to one of the giant proteoliposomes in the field of view, and rupture the small patch of membrane within the micropipette. ATP would diffuse from the micropipette into the giant proteoliposome and enable active transport by the P-gp proteins in an outward facing orientation. We would collect a time lapse series of images to determine the rate of transport out of the giant proteoliposome. We should be able to estimate the fraction of outward facing P-gp proteins by comparing the rates of transport in and out of giant proteoliposomes.

One important benefit of generating giant liposomes, with or without proteins, is to use them for the formation of a planar membrane. To this end, formation of unilamellar giant liposomes in high yield increases the likelihood of forming a planar

membrane that completely covers a micro- or nanopore. The membrane-covered pore would ideally separate two chambers with a small volume so that passive diffusion, active transport, or ion channel activity can be measured and studied.

4.4 Applications in Industry

To be useful, scientific work should either reveal new fundamental insight or have the capacity to be extended beyond the research laboratory. The results from this work are likely to be most useful for research applications, such as: 1) using the transport assay to screen for potential therapeutics that will affect P-gp function, or 2) using giant proteoliposomes with ion channel proteins for planar patch clamp assays. The potential exists, however, for commercialization. For example, microscope slides, petri dishes, or flat-bottom glass wells can be pre-coated with agarose and lipids or proteoliposomes and then frozen to preserve their integrity for shipment. The end user would simply add rehydration solution of choice and wait 2–3 hours for giant liposomes or proteoliposomes to form and be ready for use. Such a system may need some investigation to determine optimal amounts, establish a working protocol, and be patented before it would be ready to be marketed.

The coating process might be facilitated by combining the techniques described in this work with hydrogel stamping as described by Majd, *et al.*[4, 5] Briefly, a suspension of small proteoliposomes would be applied to the surface of a hydrogel stamp and then pressed onto a dried agarose film. One benefit of using such a technique is that the hydrogel would absorb most of the solution from the suspension of proteoliposomes and thereby shorten the dehydration time. Shortening the preparation

time would provide a longer period of time to perform assays before the proteins naturally degrade and become non-functional. Another significant benefit is the ability to then automate the process of pre-coating a high density of proteoliposomes onto a surface before freezing it for later use. If the surface to be coated consists of multiple wells, different proteins or lipids can be applied to each well so that GUVs or giant proteoliposomes of different compositions can be reconstituted simultaneously.

References

1. Yamashita, Y., Oka, M., Tanaka, T., and Yamazaki, M. (2002) A new method for the preparation of giant liposomes in high salt concentrations and growth of protein microcrystals in them, *Biochimica Et Biophysica Acta-Biomembranes 1561*, 129-134.

2. Cevc, G., and Richardsen, H. (1999) Lipid vesicles and membrane fusion, *Advanced Drug Delivery Reviews 38*, 207-232.

3. Estes, D. J., Lopez, S. R., Fuller, A. O., and Mayer, M. (2006) Triggering and visualizing the aggregation and fusion of lipid membranes in microfluidic chambers, *Biophys J 91*, 233-243.

4. Majd, S., and Mayer, M. (2005) Hydrogel stamping of arrays of supported lipid bilayers with various lipid compositions for the screening of drug-membrane and protein-membrane interactions, *Angewandte Chemie-International Edition 44*, 6697-6700.

5. Majd, S., and Mayer, M. (2008) Generating Arrays with High Content and Minimal Consumption of Functional Membrane Proteins, *Journal of the American Chemical Society 130*, 16060-16064.

APPENDICES

APPENDIX A

Supporting Information

Films of Agarose Enable Rapid Formation of Giant Liposomes in Solutions of Physiologic Ionic Strength

A.1 Yield of Free-floating Giant Liposomes That Were Formed from Films of Agarose

Since many experiments involving giant liposomes require the use of free-floating liposomes (i.e. liposomes that are not attached to the surface of formation or to each other), we compared the yield of free-floating giant liposomes obtained by hydration (without an electric field) of hybrid films of agarose and lipids in PBS and in deionized water with the yield of free-floating giant liposomes formed by standard electroformation. We procured free-floating liposomes by prying apart the formation chamber and allowing the contents to drip into a collection vessel or by applying gentle aspiration through a pipette or needle and syringe to remove the solution from the chamber. Figure A.1A shows free-floating giant liposomes in deionized water that we obtained in this manner after generation by electroformation on bare ITO plates. Figure A.1B,C depicts free-floating giant liposomes that we collected using the same technique

after formation from hybrid films of agarose and lipids. The yield of free-floating giant liposomes was higher in deionized water than in PBS, which is not surprising since the yield of giant liposomes that formed on the surface of the films was also higher in deionized water than PBS. The yield of free-floating giant liposomes in deionized water was similar when formed from hybrid films of agarose and lipids compared to standard electroformation, and suggests that either of these techniques can be used to obtain a good yield of free-floating giant liposomes in deionized water. Formation from hybrid films of agarose and lipids, however, has the important benefit of being capable of producing free-floating giant liposomes in solutions of physiologic ionic strength, such as PBS, whereas electroformation did not generate giant liposomes in PBS.

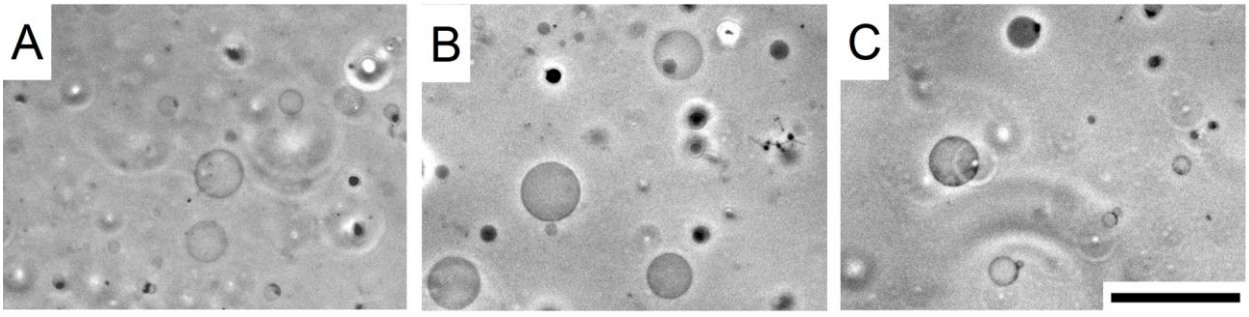

Figure A.1. Free-floating giant liposomes. Liposomes composed of POPC were formed for one hour (A) by electroformation (1.5 V peak-to-peak, 4 Hz) on bare ITO plates in deionized water, (B) by hydration of a hybrid film of ultralow melting temperature agarose and lipids in deionized water without an electric field, and (C) by hydration of a hybrid film of ultralow melting temperature agarose and lipids in PBS without an electric field. Scale bar = 100 μm.

A.2 Formation of Giant Liposomes in Three Types of Aqueous Solutions

To explore the effect of ions present in solution on the formation of giant liposomes, we formed giant liposomes from hybrid films of ultralow melting temperature

agarose and lipids in three aqueous solutions: deionized water, 150 mM KCl, and PBS. These and all other experiments did not employ AC electric fields unless specifically mentioned. Figure A.2 shows giant liposomes composed of POPC in each of the three aqueous solutions. Formation in deionized water yielded giant liposomes with large diameters (>>10 μm) over most of the surface. In contrast to formation in deionized water, the formation of giant liposomes from films of agarose in ionic solutions was not uniform over the entire surface. Figure A.2 depicts regions of formation with a good yield of liposomes. Other regions contained fewer or smaller liposomes than these selected regions. Formation of giant liposomes was typically better (in terms of number and size of liposomes) in 150 mM KCl than in PBS. Nonetheless, ~30–80% of the total surface area of the liposome formation chamber (100% ≈ 896 mm^2) contained liposomes comparable to those depicted in Figure A.2B,C.

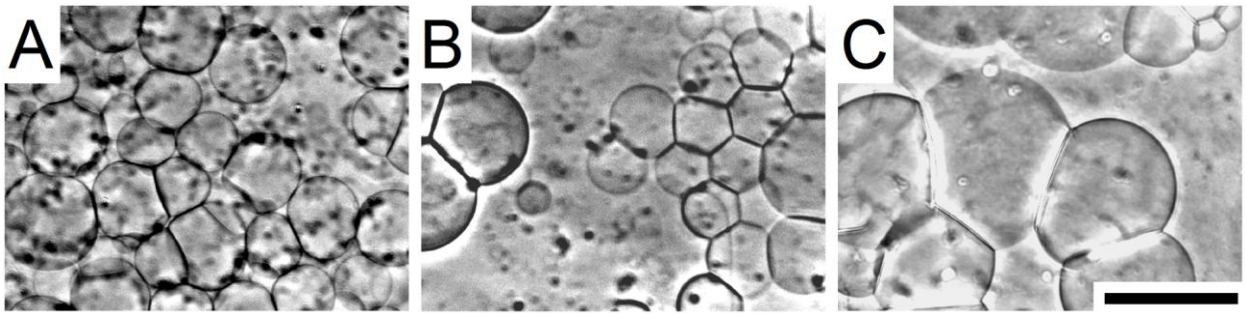

Figure A.2. Giant liposomes composed of 100% POPC formed from films of ultralow melting temperature agarose for 1 h in three types of aqueous solutions: (A) deionized water, (B) 150 mM KCl, and (C) PBS without Ca^{2+} and Mg^{2+}. Scale bar = 100 μm.

A.3 Surface Topography of Films of Different Types of Agarose as Determined by SEM and AFM

The different types of agarose used in this work were distinguished by their melting temperature. Factors that affect the melting temperature of agarose gels

include the average molecular weight (MW) of the molecules and the extent of cross-linking between molecules.[1, 2] Generally, a reduced MW and a reduced number of cross-links results in a lower melting temperature of the gels.[2] To provide additional characterization of films formed from each of these types of agarose, we assessed the surface topography by SEM (Figure A.3, row A) and AFM (Figure A.3, row B). The seemingly porous character of the films in these images, together with the observation that lipids penetrate the agarose films and thus form a hybrid film of agarose and lipids (see Chapter II, Figure 2.4), suggests that these hybrid films of lipids and porous agarose provide a large interface between agarose molecules and lipid molecules.

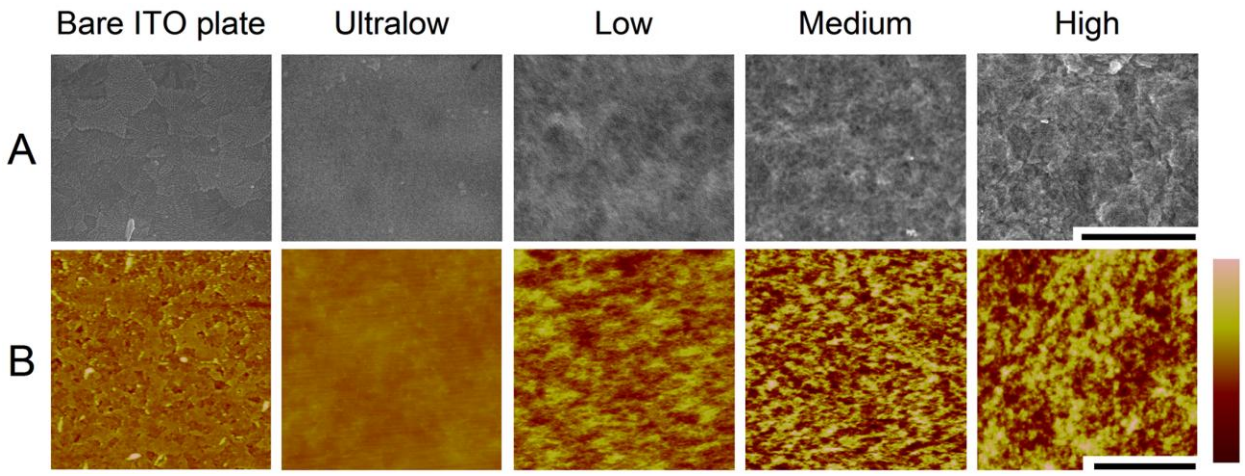

Figure A.3. Comparison of the surface topography of bare ITO plates with films of agarose from four different types of agarose. (Row A) SEM images of a bare ITO plate and of films of agarose with different melting temperatures as specified in the column headings. Scale bar = 1 μm. (Row B) AFM images of a bare ITO plate and different films of agarose as specified in the column headings. The color bar represents a range in the z-direction (height) of 0 to 40 nm. Scale bar = 2 μm.

A.4 Fluorescence Intensities of Giant Liposomes Formed from a Hybrid Film of Fluorescently Labeled Agarose and Lipids and from a Hybrid Film of Nonlabeled Agarose and Lipids

To determine if agarose molecules associated with giant liposomes when formed from hybrid films of agarose and lipids, we formed giant liposomes from films of fluorescently labeled, ultralow melting temperature agarose. If agarose associated with the membranes of giant liposomes, we expected the fluorescence intensities of liposomes formed from films of fluorescently labeled agarose to be higher than the intensities of liposomes formed from nonlabeled agarose. The fluorescence intensities shown in Figure A.4 confirmed this hypothesis, suggesting that agarose indeed associated with the membranes of liposomes. Agarose molecules, which are macromolecular carbohydrates, may hence provide a similar benefit to the formation of giant liposomes as PEGylated lipids.[3, 4]

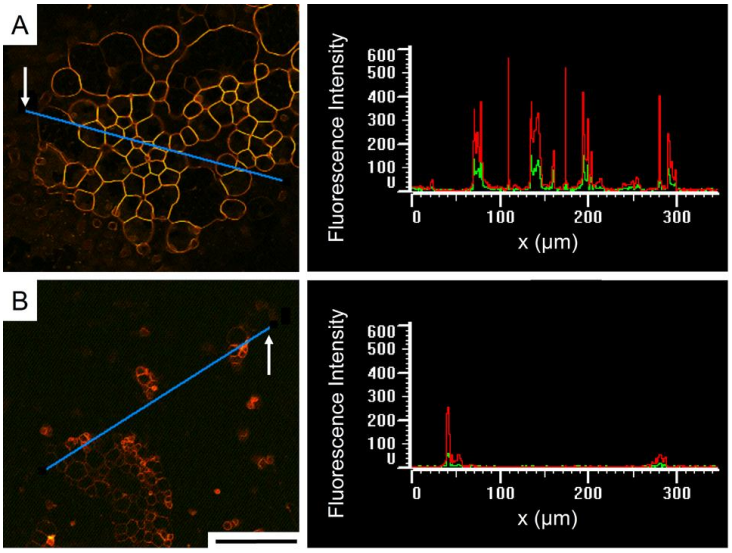

Figure A.4. Fluorescence intensities of giant liposomes formed from films of fluorescently labeled agarose and from nonlabeled agarose. Confocal microscopy images in the column on the left contain blue lines representing the position of line

scans whose corresponding fluorescence intensities are shown in the column on the right. The arrow in the micrograph denotes the starting location of the line scan. Giant liposomes composed of POPC were formed for one hour in PBS. (A) Giant liposomes formed from films of fluorescently labeled agarose. (B) Giant liposomes formed from films of nonlabeled agarose. Note, the low levels of fluorescence from nonlabeled, ultralow melting temperature agarose originated from weak autofluorescence of the agarose.[5] The images in A and B were taken at the same microscopy settings (laser intensity, sensitivity of the camera, etc.), and thus the fluorescence intensity values in the graphs in the column on the right are quantitatively comparable to each other; however, the images in the column on the left were contrast enhanced for clarity. Scale bar = 100 μm.

A.5 Determination of Membrane Fluidity by Fluorescence Recovery After Photobleaching (FRAP)

Since agarose molecules associated with the membranes of giant liposomes that were formed from hybrid films of agarose and lipids, we determined if this association impeded diffusion of lipids within these membranes. To assess the fluidity of the membranes, we used the technique of fluorescence recovery after photobleaching (FRAP) and compared the recovery curve of giant liposomes formed from hybrid films of agarose and lipids to the recovery curve of giant liposomes formed by electroformation. Using a confocal microscope, we scanned the laser beam to bleach only a portion of the membranes of giant liposomes for 30 s. During the 10 min recovery period, we scanned a bigger field of view every 10 s. For each image, we determined the peak fluorescence intensity of four locations on the bleached portion of the membrane and calculated the average of these fluorescence intensities. Recovery curves were generated by plotting the average fluorescence intensity of the bleached area versus the elapsed time of recovery. To fit the data, we determined the best curve fit of the data to Equation A.1.[6] In order to carry out the best curve fit, we set the

parameter F_o to zero, which assumes that the lipids in the exposed portion of membrane were completely photobleached,[6] set the parameter a to one, which assumes unperturbed Brownian motion of lipids,[6] and ran 100 iterations with an initial guess of F_i = 30 and $t_{1/2}$ = 30. Figure A.5 and the fitting parameters listed in the figure caption show that the recovery curves of giant liposomes formed in deionized water were similar for liposomes formed from hybrid films of agarose and lipids compared to liposomes formed from bare ITO (i.e. without the presence of agarose) by electroformation. The fluorescence intensities of giant liposomes formed in PBS from hybrid films of agarose and lipids were higher, but the recovery curve shows a similar trend and value for $t_{1/2}$ (half-time for recovery). Therefore, we conclude that the association of agarose molecules with the giant liposomes formed from hybrid films of agarose and lipids did not significantly alter the diffusion constant of lipids within the membrane.

$$y = \frac{F_0 + F_i * \left(\frac{x}{t_{1/2}} \right)^a}{1 + \left(\frac{x}{t_{1/2}} \right)^a} \qquad \text{(A.1)}$$

where: F_0 = fluorescence intensity immediately after photobleaching ($t = 0$)
F_i = fluorescence intensity as $t \to \infty$
x = x-coordinate of the plot; here x corresponds to time, t
$t_{1/2}$ = half time for recovery
a = time exponent; diffusion is Brownian if a = 1, or anomalous if a < 1
y = y-coordinate of the plot; here y corresponds to fluorescence intensity

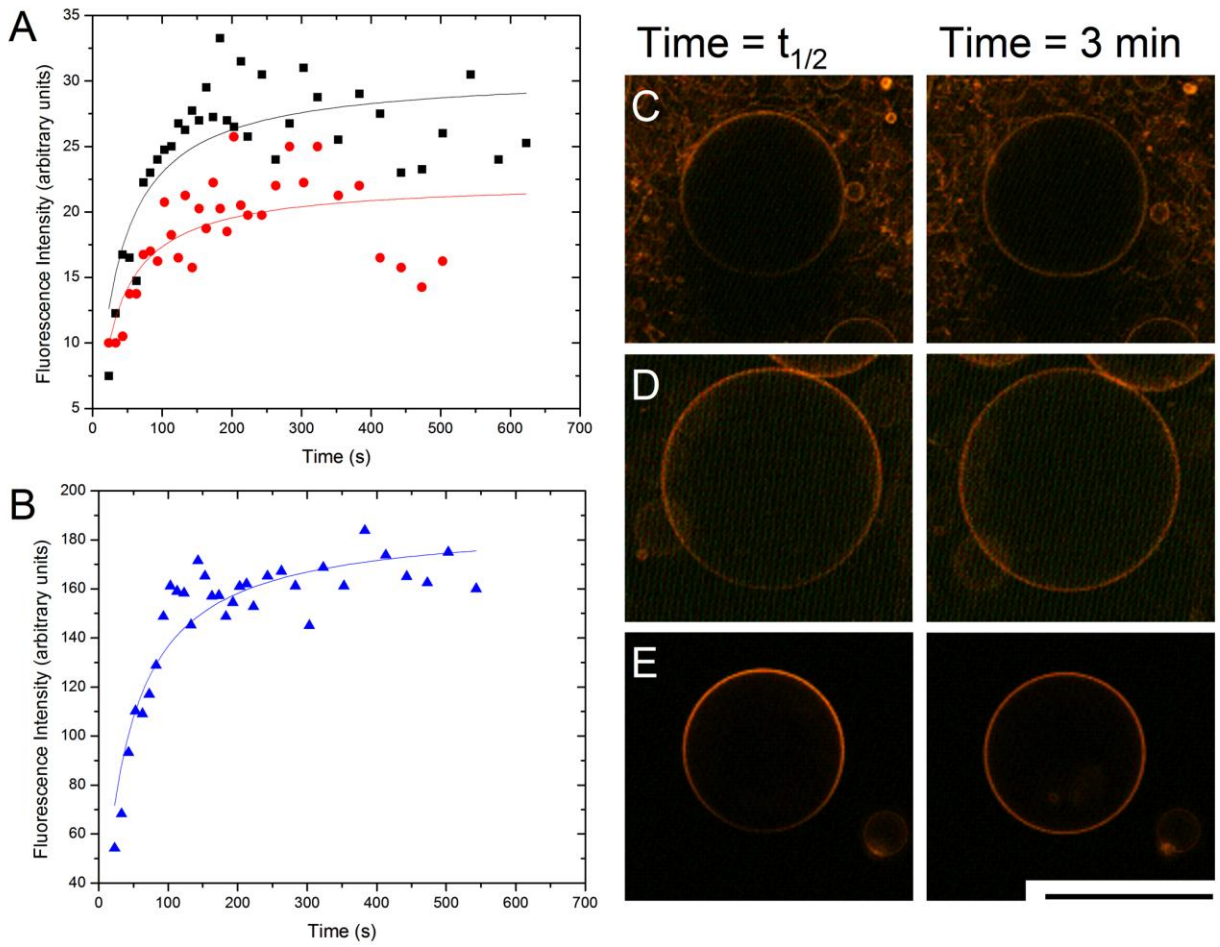

Figure A.5. Fluorescence recovery curves and micrographs obtained from FRAP experiments using confocal microscopy on giant liposomes containing 97% POPC with 3% DMPE-NBD. Liposomes were formed for 2 h, photobleached for 30 s, and scanned during recovery every 10 s for 10 min. The fluorescence intensity of the bleached area of the membrane was plotted versus time to generate each recovery curve. (A) Fluorescence recovery curves of giant liposomes formed in deionized water. Red circles represent the fluorescence intensity of a giant liposome formed from a hybrid film of agarose and lipids. The solid red line represents a fit to the red circles (F_i = 22.4, $t_{1/2}$ = 28.7 ± 8.7). Black squares represent the fluorescence intensity of a giant liposome formed by electroformation from a bare ITO surface (without agarose). The solid black line represents a fit to the black squares (F_i = 30.6, $t_{1/2}$ = 32.8 ± 7.2). (B) Fluorescence recovery curve of giant liposomes formed in PBS from a hybrid film of agarose and lipids (blue triangles). The solid blue line represents a fit to the blue triangles (F_i = 187.5, $t_{1/2}$ = 37.1 ± 4.9). (C) Confocal microscopy image of a giant liposome that was laser-bleached after being formed in deionized water by electroformation at the time points during recovery indicated in the column headings. (D) Confocal microscopy image of a giant liposome that was laser-bleached after being formed in deionized water from a hybrid film of agarose and lipids at the time points

during recovery indicated in the column headings. (E) Confocal microscopy image of a giant liposome that was laser-bleached after being formed in PBS from a hybrid film of agarose and lipids at the time points during recovery indicated in the column headings. Fluorescence intensities used to generate recovery curves were obtained using the same microscopy settings (laser intensity, sensitivity of the camera, etc.). The images for C,D,E were contrast enhanced for clarity, but were enhanced to the same extent for both time points in each given condition of formation. Scale bar = 50 μm.

A.6 Residual Water Content of Partially Dried Agarose Films

To quantify the amount of residual water in partially dried films of agarose (1–3 h at 40 ^{o}C), we weighed 10 cover glass slides (24 x 50 mm) before and after coating with agarose solution, after partially drying the agarose solution on a hotplate at 40 ^{o}C, after drying the agarose film in an oven at a temperature above 100 ^{o}C, and after exposing the oven-dried agarose film to water-saturated nitrogen for 20 min (prehydration). The mass of agarose solution deposited onto the 10 slides was 0.7280 g (72.8 mg per slide), after subtracting the mass of the slides themselves. Based on a 1% (w/w) solution, the theoretical mass of agarose deposited onto each slide was 0.73 mg. The mass of the films of agarose on 10 slides after all films no longer appeared wet was 0.0088 g (0.88 mg per slide). These measurements indicate that the films of agarose consisted of ~15% water (0.15 mg per slide) and 85% agarose after drying on a hotplate at 40 ^{o}C. Drying these films at 40 ^{o}C for an additional 3 h did not measurably change the mass. In contrast, after drying the films of agarose on the slides overnight at a temperature >100 ^{o}C resulted in agarose films with a total mass of 0.0073 g (0.73 mg per slide). This result suggest that all (or nearly all) of the residual water in the agarose films evaporated in the oven, and the resulting film contained <1% water and >99% agarose. Prehydration of agarose films resulted in an increase in their mass by ≤5%. These results indicate that traditional prehydration of oven-dried films of agarose

results in lower water content in the films than the residual water content of partially dried films of agarose.

A.7 Formation of Giant Liposomes from a Hybrid Film of Cross-linked Hydrogel and Lipids as well as from Hybrid Films of Other Types of Agarose and Lipids

To determine if giant liposomes could be formed from films of lipids that were coated over four different types of agarose (identified by melting temperature) or over a chemically cross-linked hydrogel (polyacrylamide), we carried out the experiments shown in Figure A.6 by hydrating hybrid films of lipids and each type of hydrogel for 1 h in deionized water and in solutions of PBS. Hybrid films of lipids and agarose with ultralow and low melting temperature generated the highest yield of giant liposomes in all aqueous solutions. In deionized water, all types of agarose produced a good yield of giant liposomes. In PBS, on the other hand, giant liposomes formed consistently only from hybrid films of lipids and ultralow melting or low melting types of agarose. The yield of giant liposomes from hybrid films of lipids and low melting temperature agarose was lower in PBS in terms of numbers of giant liposomes and surface coverage compared to the yield from hybrid films of lipids and ultralow melting temperature agarose in PBS. The yield of giant liposomes from low melting temperature agarose was higher, however, than formation on bare ITO plates or from types of agarose with higher melting temperatures. We found that films of polyacrylamide and lipids also facilitated the formation of giant liposomes in solutions of physiologic ionic strength compared to formation from bare glass (or bare ITO), but to a lesser extent than from

ultralow melting temperature agarose. Interestingly, polyacrylamide appeared to *hinder* the formation of giant liposomes in deionized water.

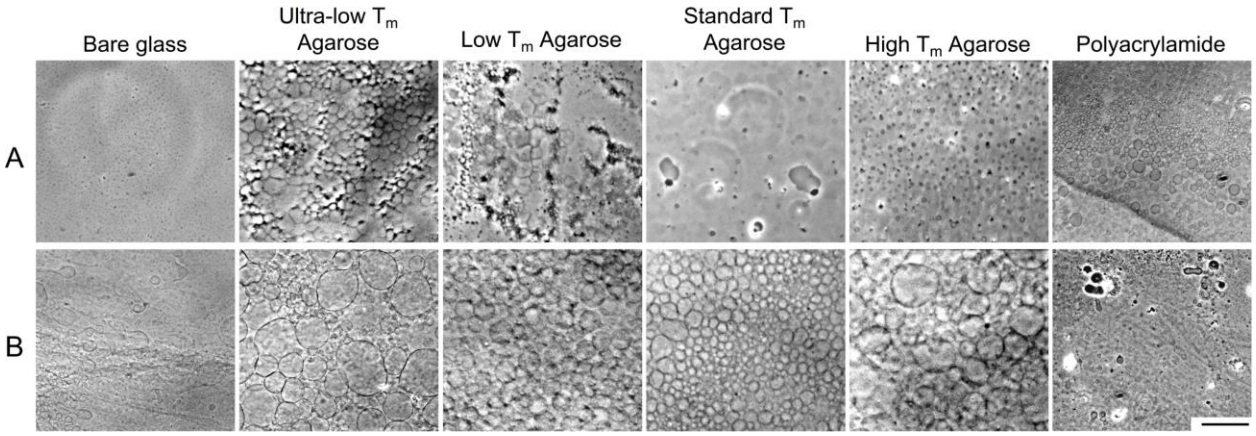

Figure A.6. Giant liposomes consisting of 100% POPC formed for 1 h from different hydrogels in PBS (row A) and in deionized water (row B). Note that although the selected image of liposomes formed from polyacrylamide in PBS shows a large number of giant liposomes and hence demonstrates that formation of giant liposomes from polyacrylamide films can proceed in solutions of physiologic ionic strength, we found that most of the area (~90%) of the polyacrylamide film did not yield giant liposomes. Scale bar = 100 μm.

A.8 Effect of an Electric AC Field on the Formation of Giant Liposomes from Hybrid Films of Agarose and Lipids

To determine if the generation of giant liposomes from hybrid films of agarose and lipids is comparable to established protocols, we compared the yield of giant liposomes formed from hybrid films of ultralow melting agarose and lipids with the yield of giant liposomes formed by electroformation (without agarose). The method of electroformation uses an electric field of alternating current (AC) to stimulate the swelling of giant liposomes from the electrodes, such as glass plates coated with a thin film of indium tin oxide (ITO).[7-10] Production of giant liposomes by electroformation is typically limited to solutions with low ionic strength (<50 mM), and the best yield is

obtained using deionized water.[9] When we carried out formation from hybrid films of agarose and lipids, we also obtained the best yield of giant liposomes using deionized water, as shown in Figure A.2. To compare the yield of giant liposomes from hybrid films of agarose and lipids with the yield obtained by electroformation, we performed both techniques in deionized water. Additionally, we determined if an electric field would provide an additional benefit on the formation of giant liposomes from hybrid films of agarose and lipids by applying an AC electric field of 1.5 V peak-to-peak at 4 Hz for 1 h to ITO plates that were coated with agarose and lipids. Figure A.7 shows that, when forming giant liposomes from hybrid films of agarose and lipids, an AC electric field did not provide a significant benefit, and the area covered by giant liposomes was similar to the results of electroformation. In contrast, the AC electric field was essential for the formation of giant liposomes on bare ITO plates (i.e. without agarose) in deionized water within 1 h.

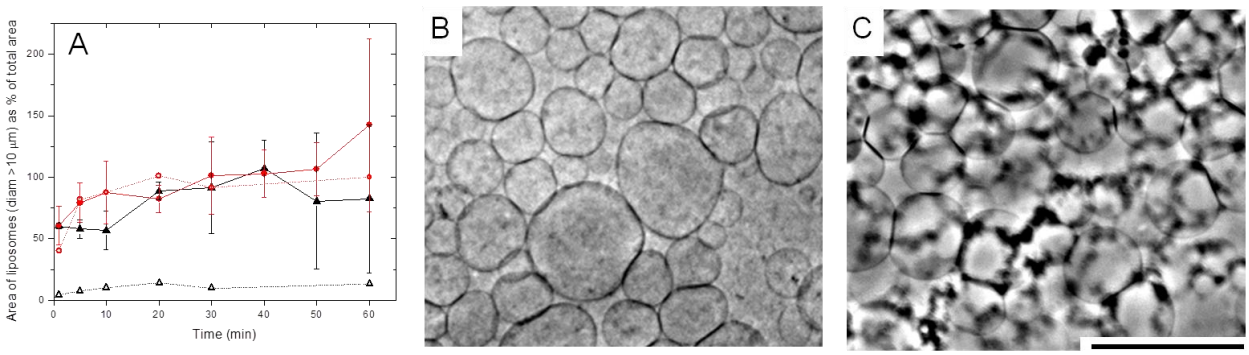

Figure A.7. Time course of formation of giant liposomes from hybrid films of ultralow melting agarose and lipids or from lipid films on bare ITO plates in the presence and absence of an AC electric field and phase contrast micrographs of giant liposomes formed from hybrid films of agarose and lipids in the presence of an AC electric field after one hour of formation. (A) Time course of formation. Liposomes were composed of 95% POPC and 5% PEG-PE and were formed in deionized water. The field of view (~0.6 mm^2) had been selected randomly *before* initiating formation. The following conditions of formation were used: (●) from hybrid films of agarose and lipids with an AC electric field (1.5 V, 4 Hz); (○) from hybrid films of agarose and lipids without

an AC field; (▲) from films of lipids on bare ITO plates with an AC field (1.5 V, 4 Hz); and (△) from films of lipids on bare ITO plates without an AC field. The fraction of the field of view occupied by giant liposomes was quantified by calculating the total area covered with giant liposomes with diameter >10 μm (normalized by the area of the field of view, 0.6 mm^2). Note, this fraction may be greater than unity because liposomes formed in more than one plane and could thus appear to overlap. Data for formation from hybrid films of agarose and lipids are averages from three independent experiments; error bars represent the standard deviation. (B) Phase contrast micrograph of giant liposomes composed of pure POPC formed for 1 h in deionized water from a hybrid film of agarose and lipids in the presence of an AC electric field (1.5 V, 4 Hz). (C) Phase contrast micrograph of giant liposomes composed of pure POPC formed for 1 h in PBS from a hybrid film of agarose and lipids in the presence of an AC electric field (1.5 V, 4 Hz). Scale bar = 100 μm.

A.9 Encapsulation of Water-soluble Macromolecules into Giant Liposomes

To determine if giant liposomes formed from films of agarose were capable of encapsulating and retaining macromolecules,[9] we formed giant liposomes consisting of POPC doped with 1% DPPE-rhodamine from hybrid films of agarose and lipids in a flow chamber that was similar to the apparatus described by Estes *et al.*[8, 9] The dimensions of the chamber used for the experiment described here was 6 cm x 0.6 cm x 0.25 cm with a total volume of 0.9 mL. We filled the chamber with a solution of 0.1 mM Tris(hydroxymethyl)aminomethane (Tris) (from Fisher Scientific, Rochester, NY), buffered to pH 7.4, containing a concentration of 0.5 μM FITC-conjugated dextran 70,000 (MW 70,000; from Sigma-Aldrich, St. Louis, MO) and allowed formation to proceed for a period of 3 h. We then exchanged the solution for 1 h with a solution of 0.1 mM Tris (pH 7.4) without dextran at a flow rate of 5 mL h^{-1}.

We found that a fraction of the giant liposomes formed in this fashion from hybrid films of agarose and lipids encapsulated FITC-conjugated dextran 70,000 during the

formation process, as indicated by the green fluorescence shown in Figure A.8A. Most of these giant liposomes, however, displayed a fluorescence intensity that was lower than the intensity of the surrounding solution. This observation indicates that the concentration of encapsulated FITC-conjugated dextran was lower in many of the giant liposomes than the concentration of the solution used to form them. In other words, the developing liposomes seemed to experience a greater influx of water molecules than macromolecules relative to the surrounding solution. This observation is not surprising since water can flux through lipid bilayers, while dextran can enter liposomes only before they form an enclosed structure. After exchanging the solution with a solution that did not contain dextran, a fraction (~10%) of the giant liposomes retained at least a portion of the encapsulated dextran, as indicated by the green fluorescence shown in Figure A.8B.

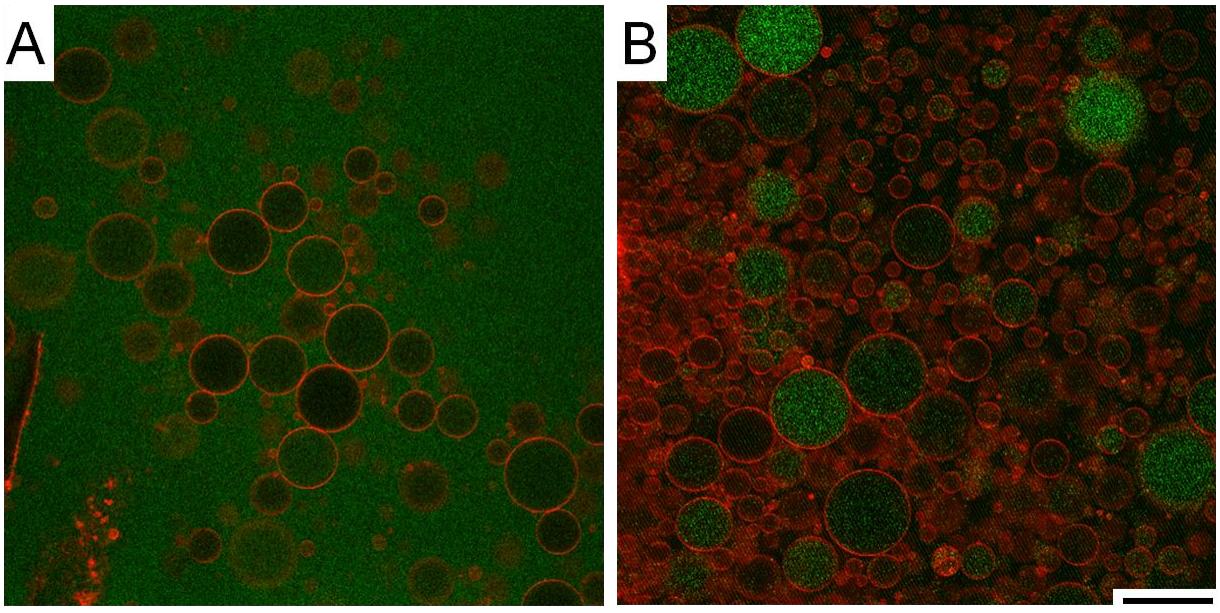

Figure A.8. Confocal micrographs of giant liposomes formed from hybrid films of agarose and lipids in the presence of fluorescently labeled, water-soluble macromolecules. Liposomes consisting of POPC doped with 1% DPPE-rhodamine were formed from hybrid films of agarose and lipids for 3 h in a flow chamber filled with an aqueous solution of 0.1 mM Tris (pH 7.4) containing a concentration of 0.5 μM FITC-

conjugated dextran 70,000 (MW 70,000). After formation, the solution was exchanged for 1 h at a flow rate of 5 mL h^{-1} with a solution of 0.1 mM Tris (pH 7.4) without dextran. (A) Giant liposomes at the end of the three hour period of formation but before exchange of solutions. (B) Giant liposomes after exchange of solutions. The images in A and B were taken at the same microscopy settings (laser intensity, sensitivity of the camera, etc.) but were contrast enhanced for clarity. Scale bars = 50 μm.

A.10 Experimental Section

A.10.1 Formation of a film of agarose on glass slides by dip-coating

We investigated the formation of giant liposomes on the following four types of agarose (all from Sigma-Aldrich, St. Louis, MO): Type IX-A ultralow melting agarose (gel point, T_g ≤17 ^oC; melting point, T_m ≤60 ^oC; electroendosmosis, EEO ≤0.11), Type VII-A low melting agarose (T_g ~26 ^oC; T_m ≤65.5 ^oC; EEO ≤0.12), Type II-A medium EEO agarose (T_g ~36 ^oC; T_m ~87 ^oC; EEO = 0.16–0.19), and Type VI-A high melting agarose (T_g ~41 ^oC; T_m ~95 ^oC; EEO ≤0.14). For each type of agarose, we prepared a 1% (w/w) solution in deionized water. We boiled the suspension of agarose in water in a microwave oven, mixed the resulting solution, returned it to a boil, and mixed again to promote complete solubilization of the agarose powder. We poured the warm agarose solution into a Petri dish and allowed it to cool either at room temperature (22 ^oC overnight) or in a refrigerator (4 ^oC for 1–2 h) to form a gel. Immediately before dip-coating the glass slides, we heated the agarose gel in the Petri dish for 10–30 s in the microwave oven, just long enough to re-melt the gel into liquid form, and mixed the solution gently. We found that dip-coating slides after this re-melting procedure facilitated homogeneous surface coverage of the slides with the agarose solution.

To dip-coat the glass slides, we contacted only one side of each glass slide (75 x 50 x 1 mm, Corning Glass Works, Corning, NY) with the surface of the melted agarose

solution. We held the coated slides vertically for a few seconds to remove excess solution and placed the slides with the agarose-coated side facing up on a temperature-controlled hotplate (Barnstead Intl, Dubuque, IA) at a temperature of 40 ^{o}C. Sometimes the solution of agarose did not wet the glass surface evenly; in this case, we placed the slide onto the hotplate and used a micropipette to deposit ~300 μL of agarose solution onto the surface of the slide. Using the long edge of the pipette tip, we spread the solution of agarose over the surface of the slide by sweeping back and forth slowly until the solution of agarose remained spread over the surface. We left the agarose-coated slides on the hotplate until the water evaporated such that a clear, seemingly dry film of agarose formed. This process of drying occurred typically within 1–3 h. In the case of agarose with ultralow and low melting temperatures, the solution did not form a gel state before drying into a film, whereas standard and high melting temperature agarose types gelled before drying into a thin film. The resulting films of agarose adhered firmly to the surface of the slides. These agarose films had a thickness of ~2 μm, as measured by scanning electron microscopy (SEM) of the cross-sections of these films.

A.10.2 Formation of a film of polyacrylamide on glass slides

For comparison with agarose films, we formed films of polyacrylamide gel by mixing 10 mL of a 10% (w/v) solution of 37.5:1 acrylamide:N,N'-methylene-bis-acrylamide (Bio-Rad Laboratories, Inc., Hercules, CA) with 10 μL of ammonium persulfate (APS) (Bio-Rad Laboratories, Inc.) and 1 μL of tetramethylethylenediamine (TEMED) (Bio-Rad Laboratories, Inc). Immediately after depositing the solution onto a glass slide, we placed a second slide on top of the solution and allowed the solution to gel for ~20 min. We removed one of the glass slides and placed the gel (supported on the other glass slide) in deionized water while stirring for ~4 h to remove non-

polymerized acrylamide monomers. (Note, acrylamide monomers are toxic). After this rinsing process, we placed the glass-supported gel on a hot plate at 40 ^{o}C for 1–3 h to dry the surface of the gel. Note, we dried the polyacrylamide gel only partially in order to prevent the film from detaching from the surface of the glass.

A.10.3 Formation of films of lipids on films of agarose or on polyacrylamide

To generate a film of lipids on and inside the films of agarose or polyacrylamide, we spread solutions with a concentration of 3.75 mg mL^{-1} lipids (all lipids were purchased from Avanti Polar Lipids, Inc., Alabaster, AL; except soybean asolectin, which we obtained from Sigma-Aldrich, St. Louis, MO) dissolved in either pure chloroform ($CHCl_3$) (EMD Chemicals, Inc., Gibbstown, NJ) or in 90% $CHCl_3$ and 10% (v/v) methanol (MeOH) (EMD Chemicals, Inc.). Figure A.9 illustrates the procedure. (Note, chloroform vapors are toxic; this step must be performed in a chemical flow hood). We used the following ten lipid compositions to form lipid films (all in mol%): (1) pure 1-palmitoyl-2-oleoyl-*sn*-glycero-3-phosphatidylcholine (POPC); (2) pure 1,2-dioleoyl-*sn*-glycero-3-[phospho-L-serine](sodium salt) (DOPS); (3) pure 1-palmitoyl-2-oleoyl-*sn*-glycero-3-[phosphor-*rac*-(1-glycerol)] (POPG); (4) asolectin from soybean; (5) 90% POPC with 10% cholesterol; (6) 80% POPC with 20% cholesterol; (7) 90% POPC with 10% POPG; (8) 50% POPC with 50% POPG; (9) 90% POPC with 10% DOPS; and (10) 95% POPC with 5% 1,2-dipalmitoyl-*sn*-glycero-3-phosphatidylethanol-amine-*N*-[methoxy (polyethylene glycol)-2000] (also referred to as PEG-PE or PEGylated lipids). For viewing liposomes or lipid films in epifluorescence mode, we doped the lipid solution with 0.5 mol% or 1 mol% 1,2-dipalmitoyl-*sn*-glycero-3-phosphoethanolamine-*N*-(lissamine rhodamine B sulfonyl) (ammonium salt) (DPPE-rhodamine). For fluorescence recovery after photobleaching experiments, we used 97% POPC with 3%

1,2-dimyristoyl-*sn*-glycero-3-phosphoethanolamine-*N*-(7-nitro-2-1,3-benzoxadiazol-4-yl) (ammonium salt) (DMPE-NBD).

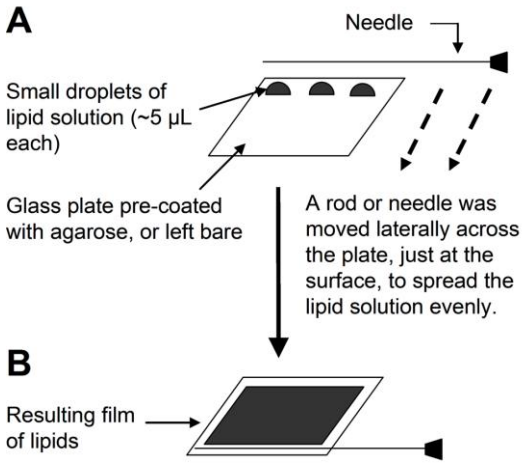

Figure A.9. Formation of a film of lipids on glass slides that were pre-coated with a film of agarose (or on bare glass without a film of agarose for control experiments). A) Two to three droplets of lipid solution (~5 μL each) were deposited close to one edge of the slide. B) Lateral movement of a rod or needle across the slide, just at the surface, was used to spread the lipid solution into an even film. Steps A and B were repeated to deposit a total volume of 30 μL of lipid solution.

We deposited a total of 30 μL of lipid solution onto each glass slide using the two steps illustrated in Figure A.9. We placed the lipid-coated plates under vacuum (approximately −730 mmHg) for at least 20 min to remove residual $CHCl_3$ and MeOH. Although the lipid solution was coated over the film of agarose, lipids penetrated through the agarose film and resulted in a hybrid film of lipids and agarose (see Chapter II, Figure 2.4).

A.10.4 Formation of a thick film of agarose

To prepare a glass slide with a particularly thick (~16 μm) film of agarose, we repeated the dip-coating procedure described in Figure 2.8A (of Chapter II) ten times. We then deposited a single lipid film of POPC lipids doped with 0.5 mol% DPPE-rhodamine using the procedure described in Figure A.9.

A.10.5 Formation of giant liposomes on glass slides

After removing the solvent from the lipid solution under vacuum, we initiated the formation of giant liposomes by placing the agarose- and lipid-coated slides in a clean dish (140 x 20 mm Nunc Petri dish, Fisher Scientific, Rochester, NY) with the coated side facing upward. We slowly added aqueous solution to the dish until the solution covered the slide completely. We pre-warmed the aqueous solution either to room temperature or to 37 ^{o}C in a water bath prior to adding it to the dish. The dish remained undisturbed on a leveled surface at room temperature for a period of 1–3 h to form giant liposomes at the surface of the agarose. We formed giant liposomes in the following three aqueous solutions: deionized water, 150 mM potassium chloride (KCl) (EMD Chemicals, Inc., Gibbstown, NJ), and Dulbecco's phosphate buffered saline (PBS) without Ca^{2+} or Mg^{2+} (JRH Biosciences, Inc., Lenexa, KS).

A.10.6 Observation of liposomes

We observed liposomes using an inverted microscope (Nikon Eclipse TE2000-U) in phase-contrast mode with a 10x objective (Nikon, NA = 0.25). We captured images of liposomes using a charge-coupled device (CCD) camera (Photometrics CoolSnap HQ camera, Roper Scientific, Trenton, NJ) and used calibrated imaging analysis software (Metamorph 7.0, Universal Imaging Corporation, Downington, PA) to determine their diameters. To observe the growth and fusion of giant liposomes on films of agarose, we recorded time-lapse series of images during the formation of giant liposomes composed of pure POPC on films of ultra-low melting agarose in PBS for one hour. We began capturing images within seconds after adding PBS to the formation chamber and recorded images from the same spot for the entire hour. Due to the swelling of the film of agarose, we adjusted the focal plane during the time-series

to keep the top surface of the swelling agarose film in focus in order to observe the formation of liposomes.

For confocal imaging, we used a 20x objective (Nikon, NA = 0.75) on an inverted microscope (Nikon Eclipse TE2000-U) equipped with an argon laser (Spectra-physics, wavelength = 488 nm), a helium-neon laser (Melles-Griot, wavelength = 543 nm), and appropriate filter settings for fluorescein, rhodamine, or NBD. We used EZ-C1 software (Nikon, version 3.5) to capture images and analyze data.

A.10.7 Characterization of films of agarose by scanning electron microscopy

In order to carry out imaging with a high resolution scanning electron microscope (HRSEM) (NOVA 200 Nanolab, FEI Company, Hillsboro, OR), we used glass plates coated with a thin film of indium tin oxide[(11)] (ITO) (Delta Technologies, Stillwater, MN) and agarose-coated ITO plates and coated them with a sputter coater (Hummer VI, Anatech, Hayward, CA) in gold-palladium (Au:Pd ratio of 60:40, thickness ~6 nm). To measure the thickness of the ultra-low melting agarose films, we peeled agarose films that were not coated with gold-palladium from the surface of the glass and examined the cross-sections of the films by HRSEM.

A.10.8 Characterization of films of agarose by atomic force microscopy

We scanned a randomly selected region (10 μm x 10 μm) of a film from each of the four types of agarose with a NanoScope IIa atomic force microscope (AFM) (Digital Instruments, Woodbury, NY) using a soft tip (UltraSharp Non-Contact Cantilever, MikroMasch, Madrid, Spain) with a resonance frequency of 371.014 kHz in tapping mode. We used image analysis software to flatten the topographic images to produce representations of contours of films of agarose.

A.10.9 Chemical modification of agarose to produce fluorescently-labeled agarose

In order to generate fluorescently labeled agarose, we stirred 10 mL of a 2% solution of ultralow melting temperature agarose at ~50 ^{o}C and gradually added 200 μL of a fresh solution of fluorescein isothiocyanate (FITC) (Fisher Scientific, Rochester, NY) dissolved in anhydrous dimethylsulfoxide (DMSO) (99.9% pure, Alfa Aesar, Ward Hill, MA) with a concentration of 100 mg mL^{-1}. After mixing the FITC and agarose for 3 h, we dialyzed the solution in deionized water using a Slide-A-Lyzer 10K dialysis cassette (10,000 molecular weight cut off, Pierce, Rockford, IL) for 3 days while changing the water twice daily. We dip-coated glass slides with films of agarose from a solution that contained 0.9% (w/w) ultralow melting temperature agarose and 0.1% FITC-labeled ultralow melting temperature agarose.

References:

1. Guiseley, K. B., Kirkpatrick, F. H., Provonchee, R. B., Dumais, M. M., and Nochumson, S. (1993) A Further Fractionation of Agarose, *Hydrobiologia 261*, 505-511.

2. Normand, V., Lootens, D. L., Amici, E., Plucknett, K. P., and Aymard, P. (2000) New insight into agarose gel mechanical properties, *Biomacromolecules 1*, 730-738.

3. Garbuzenko, O., Barenholz, Y., and Priev, A. (2005) Effect of grafted PEG on liposome size and on compressibility and packing of lipid bilayer, *Chem. Phys. Lipids 135*, 117-129.

4. Kenworthy, A. K., Hristova, K., Needham, D., and McIntosh, T. J. (1995) Range and Magnitude of the Steric Pressure between Bilayers Containing Phospholipids with Covalently Attached Poly(Ethylene Glycol), *Biophys. J. 68*, 1921-1936.

5. Ratajska-Gadomska, B., and Gadomski, W. (2000) Critical exponents in a percolation picture of the fluorescence quenching during the sol-gel transition, *European Physical Journal B 17*, 281-288.

6. Feder, T. J., BrustMascher, I., Slattery, J. P., Baird, B., and Webb, W. W. (1996) Constrained diffusion or immobile fraction on cell surfaces: A new interpretation, *Biophysical Journal 70*, 2767-2773.

7. Angelova, M., Soleau, S., Meleard, P., Faucon, J. F., and Bothorel, P. (1992) Preparation of giant vesicles by external a.c. electric fields. Kinetics and applications, *Progress in Colloid & Polymer Science 89*, 127-131.

8. Estes, D. J., Lopez, S. R., Fuller, A. O., and Mayer, M. (2006) Triggering and visualizing the aggregation and fusion of lipid membranes in microfluidic chambers, *Biophys J 91*, 233-243.

9. Estes, D. J., and Mayer, M. (2005) Giant liposomes in physiological buffer using electroformation in a flow chamber, *Biochimica Et Biophysica Acta-Biomembranes 1712*, 152-160.

10. Estes, D. J., and Mayer, M. (2005) Electroformation of giant liposomes from spin-coated films of lipids, *Colloids and Surfaces B-Biointerfaces 42*, 115-123.

11. We conducted early experiments using a standard protocol of electroformation from agarose-coated ITO plates, but found later that the electric AC field added little or no benefit over simple hydration of the hybrid films of agarose and lipids (see Figure A.7).

APPENDIX B

Supporting Information

Functional Reconstitution of P-glycoprotein in Giant Liposomes

B.1 ATPase Assay

We tested the functionality of reconstituted proteins by conducting an ATPase assay [(1)] on giant liposomes that formed from films of ultra-low melting agarose and small liposomes with human P-glycoprotein (P-gp). We prepared a solution containing small proteoliposomes, coated this solution on a dried film of ultra-low melting agarose, and rehydrated the films the following morning to form giant proteoliposomes. For the ATPase assay, we removed a 20 µL sample from the chamber in which the giant proteoliposomes were prepared in this manner and tested ATPase activity on these 20 µL in a microvial. For comparison, we also tested a 10 uL sample of small proteoliposomes on the day they were produced (that is, one day prior to testing giant proteoliposomes).

Table B.1. Basal and verapamil-stimulated ATP hydrolysis by P-gp in small and giant proteoliposomes

Sample	Basal activity (nmol Pi/mg protein/min)	Stimulated activity* (nmol Pi/mg protein/min)	Fold increase
Small proteoliposomes	42.09	166.53	4
Giant proteoliposomes	7.62	53.37	7

* Stimulated activity was determined in the presence of 30 μM verapamil

The basal levels of ATPase activity were typically lower for GUVs than SUVs because, to estimate protein concentrations within the sample after reconstitution, we assumed all of the P-gp from the small proteoliposomes reconstituted into giant proteoliposomes. This scenario is unlikely since residue was visually evident in the formation chamber following reconstitution into giant proteoliposomes, so the activity levels of small proteoliposomes cannot be compared directly to activity levels of giant proteoliposomes. Importantly, however, the 7-fold increased level of ATPase activity following stimulation of P-gp by verapamil addition indicates that active P-gp was present in membranes after formation of giant liposomes.

B.2 Rhodamine 123 Fluorescence in GUVs Containing P-gp

We noted a frequent occurrence of bright membrane fluorescence (as compared to the background) for giant liposomes containing P-gp in the presence and absence of ATP and inhibitor (see Figure B.1). These results indicate that ATP was not required for Rho123 to associate with P-gp and that the presence of verapamil, a known inhibitor of P-gp-mediated transport of Rho123 [(2-5)], was not able to out-compete this association completely.

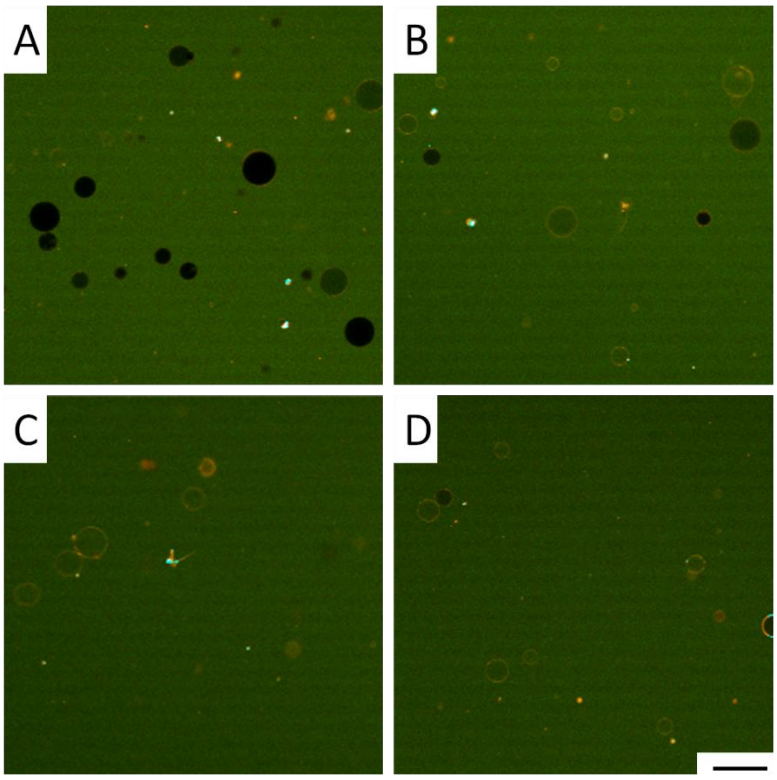

Figure B.1. Confocal images of giant liposomes in solution containing 1 µM Rhodamine 123 (Rho123). The images shown here were recorded ~20 minutes after immersion in Rho123 solution under the following conditions: A) Giant liposomes that did not contain P-glycoprotein (P-gp). B) Giant liposomes containing P-gp, without ATP or verapamil. C) Giant liposomes containing P-gp, with 1 mM ATP but without verapamil. D) Giant liposomes containing P-gp that were incubated for >15 min in 30 µM verapamil and assayed with 1 mM ATP. Scale bar = 50 µm.

We observed the occurrence of spots that were uniformly bright and did not change in fluorescence intensity. These bright spots occurred in giant proteoliposomes when active transport was impeded (e.g., without ATP or with an inhibitor) and occasionally, but less frequently, in giant liposomes that lacked reconstituted P-gp (see Figure B.2).

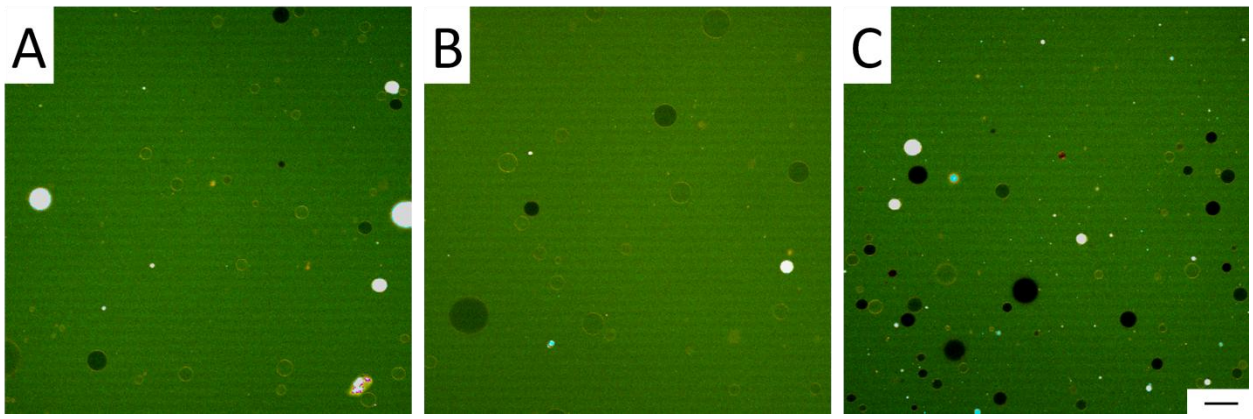

Figure B.2. Confocal images of giant liposomes in solution containing 1 µM Rhodamine 123 (Rho123). The images shown here were recorded ~13 minutes after immersion in Rho123 solution under the following conditions: A) Giant proteoliposomes containing reconstituted P-glycoprotein (P-gp) in an assay solution that did not contain ATP. B) Giant proteoliposomes containing P-gp that were incubated for >15 min in 30 µM verapamil and assayed with 1 mM ATP and 30 µM verapamil. C) Giant liposomes that did not contain P-gp. Scale bar = 50 µm.

To determine if the reconstituted P-gp proteins were functional, we analyzed the rate of change in fluorescence intensity inside the liposomes with respect to the background fluorescence. The fluorescence intensity inside giant proteoliposomes formed with P-gp increased quickly in the first 10-15 min after immersion in 1 µM Rho123 assay solution (see Figure B.3), whereas the fluorescence intensity inside giant liposomes without P-gp typically remained low. As expected for active transport of Rho123, the fluorescence intensity inside giant proteoliposomes increased above the intensity of the background fluorescence most often in the presence of 1 mM ATP (Figure B.3A). Although we observed the fluorescence intensity inside a few giant proteoliposomes to rise higher than the background fluorescence when assayed without ATP (Figure B.3B), it is important to note that these levels of intensity appeared to have

reached a plateau whereas, in the presence of ATP, the levels of intensity appeared to be continuing to rise in many of the proteoliposomes (Figure B.3A).

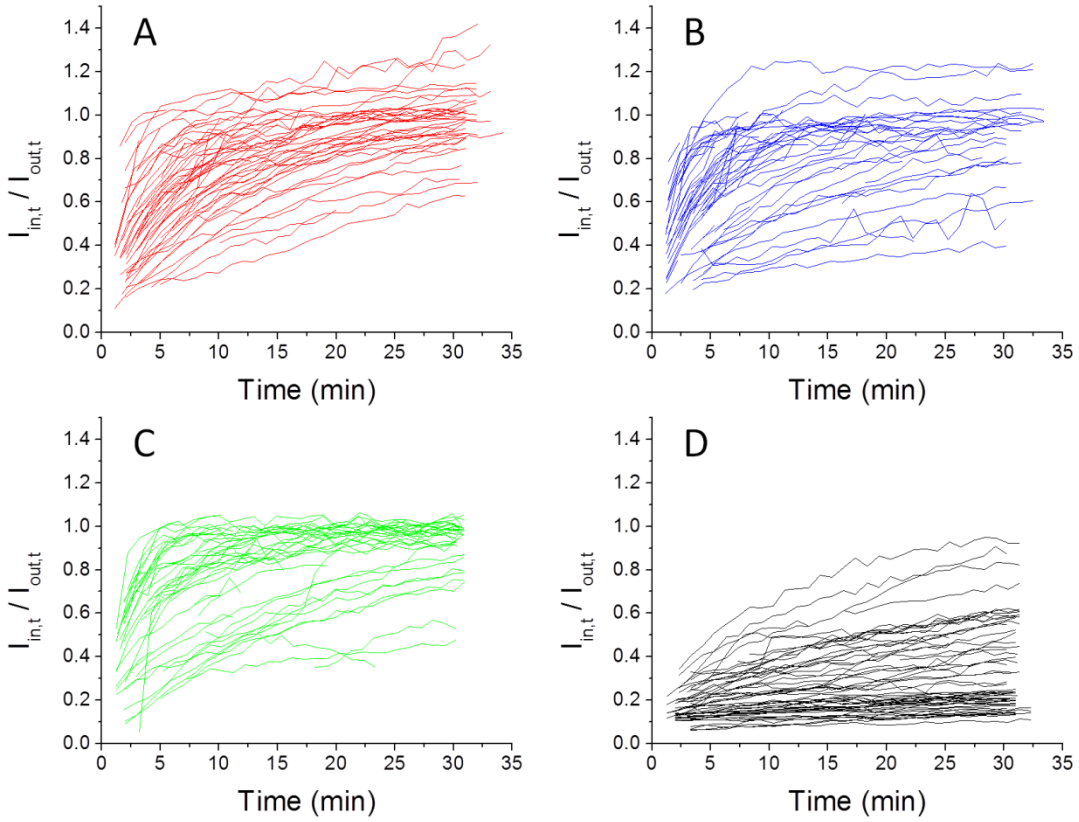

Figure B.3. Time-dependent fluorescence intensity inside giant liposomes ($I_{in,t}$) divided by the fluorescence intensity of the background ($I_{out,t}$). Giant liposomes were assayed in the presence of 1 µM of the fluorescent substrate rhodamine 123. A) Giant proteoliposomes formed with P-gp and 1 mM ATP in the assay solution. B) Giant proteoliposomes formed with P-gp and in an assay solution without ATP. C) Giant proteoliposomes formed with P-gp in an assay solution with 1 mM ATP and with 30 µM verapamil. D) Giant liposomes formed without P-gp.

B.3 Theoretical Number of Proteins and Transport Rate Per Area

B.3.1 Theoretical number of P-gp

We started with 250 µg of proteins and 25:1 lipid:protein ratio wt:wt (starting amount of lipids was 6,250 µg). We expected only 10% recovery of active proteins [4, 6]

at a purity of about 70-80%, so we expect about 0.70 × 0.10 × 250 µg = 17.5 µg of active P-gp with 6,250 µg lipids in the small proteoliposomes.

The total area of lipids or active proteins is given by Equation B.1, where N is Avogadro's number ($6.022 \times 10^{23}\ \frac{molecules}{mol}$).

$$area = wt.molecules \times \frac{1}{avg\ MW} \times N \times \frac{area}{molecule} \quad \text{(B.1)}$$

For the lipids, we used the average molecular weight (avg MW) of asolectin, 800 g/mol and avg area/lipid ≈ 70 Å^2 [7]. Then the total area of lipids is $6{,}250 \times 10^{-6} g \times \frac{1\ mol}{800\ g} \times 6.022 \times 10^{23}\ \frac{molecules}{mol} \times 70\ \frac{Å^2}{molecule} \times (\frac{10^{-10}\ m}{Å})^2$, for a total area of all lipids of $3.3\ m^2$. But the lipids orient themselves into bilayers, so the area of the lipid membrane is half the total area, or $1.6\ m^2$.

Non-glycosylated P-gp has an average MW of about 140 kDa, or 140 kg/mol. We estimated the area of P-gp based on the dimensions determined by its crystal structure as ~(70 Å)^2, or ~4900 Å^2 [8]. The area of all expected active P-gp in small proteoliposomes is $17.5 \times 10^{-6}\ g \times \frac{1\ mol}{140{,}000\ g} \times 6.022 \times 10^{23}\ \frac{molecules}{mol} \times 4900\ \frac{Å^2}{molec} \times (\frac{10^{-10}\ m}{Å})^2$ (= total area of all active P-gp is $3.7 \times 10^{-3}\ m^2$). Thus, the ratio of the area of all P-gp to the area all lipid bilayers is $3.7 \times 10^{-3}\ m^2 : 1.6\ m^2$ ≈ 1:430. This ratio is in agreement with previously published findings.[6]

The surface area of a GUV was calculated by the formula for the surface area of a sphere, $area = 4\pi r^2$, where r is the radius. Thus, a 20 µm diameter GUV has a surface area of $4\pi(10 \times 10^{-6} m)^2 \approx 1.25 \times 10^{-9}\ m^2$.

The area of a 20 µm diameter GUV occupied by P-gp, if reconstituted at same ratio is $\frac{1}{430} \times area\ of\ GUV$, or $2.9 \times 10^{-12}\ m^2$. The number of P-gp in a 20 µm diameter

GUV is the area occupied by P-gp divided by the area of 1 P-gp, calculated as 2.9× $10^{-12}\ m^2\ \div [4{,}900\ \frac{\text{Å}^2}{molecule\ P-gp} \times (10^{-10}\ \frac{\text{m}}{\text{Å}})^2]$ ≈ 59,000 molecules of P-gp, or 9.8×10^{-20} moles of P-gp.

The surface density of P-gp, Γ_{P-gp}, is the moles of P-gp divided by the surface area. From the surface area and the number of moles of P-gp in a 20 µm diameter GUV, $\Gamma_{P-gp} = \frac{9.8 \times 10^{-20} mol\ P-gp}{1.3 \times 10^{-9}\ m^2} = 7.6 \times 10^{-11}\ \frac{mol}{m^2}$. We assume this surface density to be constant and independent of the liposome size.

B.3.2 Theoretical transport rate

P-gp is reported to have an average transport rate of 1 molecule per second per protein [(9)]. Theoretical transport rate (molecules/s/µm^2) is the number of P-gp divided by the area of the GUV times the transport rate, calculated as $\frac{59{,}000\ P-gp}{1.3 \times 10^{-9} m^2} \times \frac{1\ molecule}{P-gp\ \ s} \approx 4.5 \times 10^{13}\ \frac{molecules}{m^2 s}$.

B.3.3 Experimentally determined transport rate

We calculated the active transport-related flux as the number of molecules per elapsed time using Equation B.2 (the transport portion of Equation 3.2 in Chapter III), where k_T is the transport rate $\left(\frac{m^3}{mol_{Pgp}\ s}\right)$, Γ_{Pgp} is the surface density of P-gp $\left(\frac{mol_{Pgp}}{m^2}\right)$, C_{out} is the concentration of Rho123 in the external solution $\left(1\ \mu M, or\ 10^{-3}\ \frac{mol}{m^3}\right)$, A is the area of the membrane (m^2), and N is Avogadro's Number $(6.022 \times 10^{23}\ \frac{molecules}{mol})$.

$$Transport\ Flux\ \left(\frac{molecules}{s}\right) = k_T \times \Gamma_{Pgp} \times C_{out} \times A \times N \qquad \text{(B.2)}$$

Using the median k_T value determined from the fits to Equation 3.2 of Chapter III, under the conditions of active transport (assayed with ATP without inhibitor), we determined the transport flux per area, *Transport Flux/A*, to be $1.7 \times 10^{16} \frac{molecules}{m^2\ s}$.

B.4 Comparison of Giant Liposomes Formed by Two Different Methods

To assess the ease of forming giant proteoliposomes from a film of dried agarose, we followed a previously described protocol[(10)] and compared the liposomes generated by each method. We found that either method could produce a good yield of giant liposomes (see Figure B.4). When formed from a film of dried agarose, fewer of the giant liposomes were filled with smaller vesicles in comparison to giant liposomes formed from bare glass. We also found that formation from a film of dried agarose consistently produced a good yield of giant liposomes (i.e., every trial generated a good yield of free-floating liposomes), whereas the previously established protocol did not always yield many free-floating liposomes.

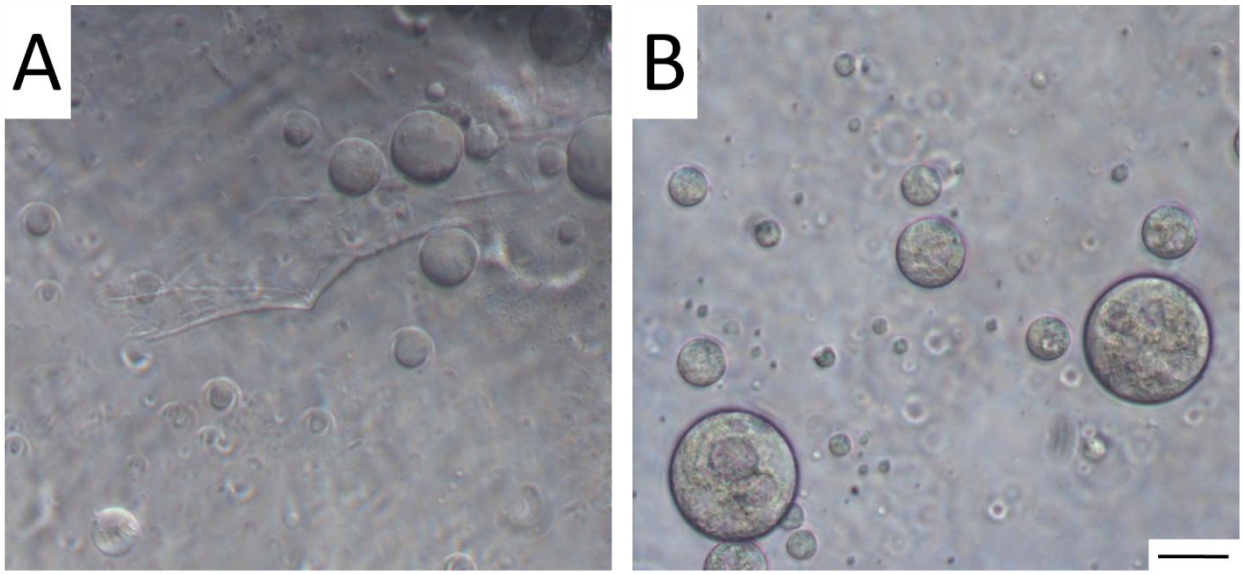

Figure B.4. Phase contrast images of giant liposomes formed from small proteoliposomes. A) Small proteoliposomes were dehydrated on a dried film of ultra-low melting agarose before reconstitution in an aqueous solution of 10 mM Tris (pH 7.0), 190 mM sucrose, 1 mM dithiothreitol, and 1× protease inhibitor. B) Small proteliposomes were partially dehydrated on bare glass in the presence of 5% (v/v) ethylene glycol.[(10)] Dehydration of small proteoliposomes was followed by overnight reconstitution in the aqueous solution used in (A). Scale bar = 50 μm.

B.5 Calibration Curves of Osmolarity and Density for Solutions of Sucrose and Sorbitol

We analyzed aqueous solutions of sucrose, glucose, and sorbitol with an osmometer (Advanced Instruments Inc., Norwood, MA) to establish calibration curves for the osmolarity of these substances at varying concentrations. We measured each sample at least three times, plotted the osmolarity against concentration, and established a linear fit to the data for each substance (see Figure B.5).

We also determined the density of sucrose, glucose, and sorbitol solutions as a function of concentration. We used three pre-weighed centrifuge tubes for each sample, weighed each tube with 10 mL of solution, and calculated the density from the data. We then plotted the density against concentration and established a linear fit to the data for each substance (see Figure B.5).

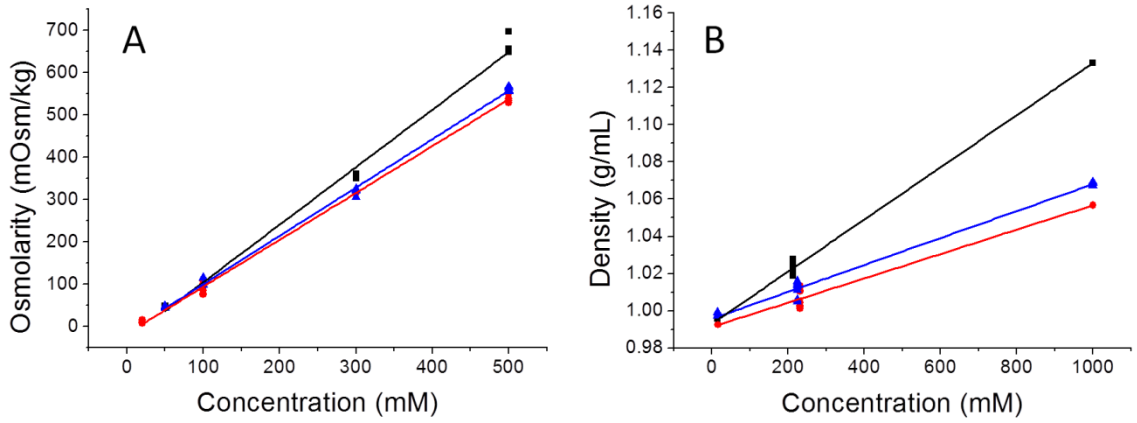

Figure B.5. Dependence of osmolarity and density on concentration for (■) sucrose, (▲) glucose, and (●) sorbitol. A) Calibration curve of osmolarity vs. concentration. B) Calibration curve of density vs. concentration. Solid lines show the linear fit to the data.

B.6 Calibration Curve of Concentration to Fluorescence Intensity

To assess the relationship between the concentration of rhodamine 123 (Rho123) and fluorescence intensity, we used a confocal microscope to collect images of samples of Rho123 with known concentrations in 50 mM Tris-HCl, pH 7.0, and determined the fluorescence intensity of the images. We found that the fluorescence intensity had a linear dependence on concentration of Rho123 (see Figure B.6).

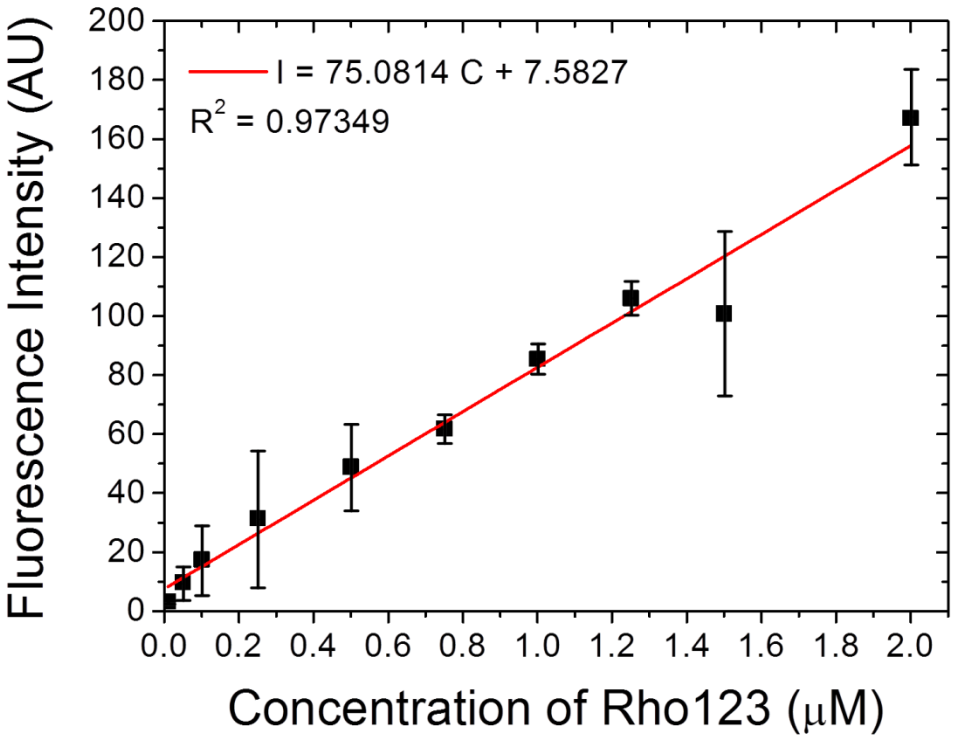

Figure B.6. Dependence of fluorescence intensity on concentration of rhodamine 123 (Rho123). Images of samples of Rho123 at known concentrations in 50 mM Tris-HCl, pH 7.0, were collected using confocal microscopy and analyzed for fluorescence concentration.

References

1. Ambudkar, S. V. (1998) Drug-stimulatable ATPase activity in crude membranes of human MDR1-transfected mammalian cells, *Methods Enzymol. 292*, 504-514.

2. Ramachandran, C., and Melnick, S. J. (1999) Multidrug resistance review in human tumors - Molecular diagnosis and clinical significance, *Molecular Diagnosis 4*, 81-94.

3. Sharom, F. J. (2011) The P-glycoprotein multidrug transporter, In *Essays in Biochemistry: Abc Transporters* (Sharom, F. J., Ed.), pp 161-178, Portland Press Ltd, London.

4. Ambudkar, S. V., Lelong, I. H., Zhang, J. P., Cardarelli, C. O., Gottesman, M. M., and Pastan, I. (1992) Partial-purification and reconstitution of the human multidrug-resistance pump - characterization of the drug-stimulatable ATP hydrolysis, *Proceedings of the National Academy of Sciences of the United States of America 89*, 8472-8476.

5. Shukla, S., Wu, C. P., and Ambudkar, S. V. (2008) Development of inhibitors of ATP-binding cassette drug transporters - present status and challenges, *Expert Opin. Drug Metab. Toxicol. 4*, 205-223.

6. Ambudkar, S. V. (1995) PURIFICATION AND RECONSTITUTION OF FUNCTIONAL HUMAN P-GLYCOPROTEIN, *Journal of Bioenergetics and Biomembranes 27*, 23-29.

7. Browning, J. L. (1981) MOTIONS AND INTERACTIONS OF PHOSPHOLIPID HEAD GROUPS AT THE MEMBRANE-SURFACE .1. SIMPLE ALKYL HEAD GROUPS, *Biochemistry 20*, 7123-7133.

8. Aller, S. G., Yu, J., Ward, A., Weng, Y., Chittaboina, S., Zhuo, R. P., Harrell, P. M., Trinh, Y. T., Zhang, Q. H., Urbatsch, I. L., and Chang, G. (2009) Structure of P-Glycoprotein Reveals a Molecular Basis for Poly-Specific Drug Binding, *Science 323*, 1718-1722.

9. Ambudkar, S. V., Cardarelli, C. O., Pashinsky, I., and Stein, W. D. (1997) Relation between the turnover number for vinblastine transport and for vinblastine-stimulated ATP hydrolysis by human P-glycoprotein, *Journal of Biological Chemistry 272*, 21160-21166.

10. Riquelme, G., Lopez, E., Garciasegura, L. M., Ferragut, J. A., and Gonzalezros, J. M. (1990) Giant Liposomes - a Model System in Which to Obtain Patch-Clamp Recordings of Ionic Channels, *Biochemistry 29*, 11215-11222.